Robustness Analysis for Identification and Control of Nonlinear Systems

by

Mark M. Tobenkin

B.S., Computer Science, MIT, 2009
M. Eng., Electrical Engineering and Computer Science, MIT, 2009

Submitted to the Department of Electrical Engineering and Computer Science
in partial fulfillment of the requirements for the degree of
Doctor of Philosophy in Electrical Engineering and Computer Science
at the Massachusetts Institute of Technology

February 2014

Signature of Author: _____

Department of Electrical Engineering and Computer Science
January 10, 2014

Certified by: _____

Russ Tedrake
Professor of Electrical Engineering and Computer Science
Thesis Co-supervisor

Certified by: _____

Alexandre Megretski
Professor of Electrical Engineering and Computer Science
Thesis Co-supervisor

Accepted by: _____

Leslie A. Kolodziejski
Professor of Electrical Engineering
Chair, Committee for Graduate Students

Robustness Analysis for Identification and Control of Nonlinear Systems

by

Mark M. Tobenkin

Submitted to the Department of Electrical Engineering
and Computer Science on January 10th, 2014 in partial fulfillment
of the requirements for the degree of Doctor of Philosophy

Abstract

This thesis concerns two problems of robustness in the modeling and control of nonlinear dynamical systems. First, I examine the problem of selecting a stable nonlinear state-space model whose open-loop simulations are to match experimental data. I provide a family of techniques for addressing this problem based on minimizing convex upper bounds for simulation error over convex sets of stable nonlinear models. I unify and extend existing convex parameterizations of stable models and convex upper bounds. I then provide a detailed analysis which demonstrates that existing methods based on these principles lead to significantly biased model estimates in the presence of output noise. This thesis contains two algorithmic advances to overcome these difficulties. First, I propose a bias removal algorithm based on techniques from the instrumental-variables literature. Second, for the class of state-affine dynamical models, I introduce a family of tighter convex upper bounds for simulation error which naturally lead to an iterative identification scheme. The performance of this scheme is demonstrated on several benchmark experimental data sets from the system identification literature.

The second portion of this thesis addresses robustness analysis for trajectory-tracking feedback control applied to nonlinear systems. I introduce a family of numerical methods for computing regions of finite-time invariance (funnels) around solutions of polynomial differential equations. These methods naturally apply to non-autonomous differential equations that arise in closed-loop trajectory-tracking control. The performance of these techniques is analyzed through simulated examples.

Thesis Co-Supervisor: Russ Tedrake
Title: Professor of Electrical Engineering and Computer Science

Thesis Co-Supervisor: Alexandre Megretski
Title: Professor of Electrical Engineering and Computer Science

Contents

Acknowledgments **9**

1 Introduction and Motivation **11**
1.1 State-of-the-Art in Stable System Identification 12
1.1.1 Model Identification Criteria 12
Maximum-Likelihood and Prediction-Error Methods 12
Simulation Error Minimization 13
Subspace Identification Methods 14
Set-Membership Identification 14
1.1.2 Identification of Stable Models 15
1.1.3 Relationship to [88] and [13] 16
1.2 Existing Approaches to Reachability Analysis 16
1.3 Chapter Outline 18
1.3.1 Part I: Robust Convex Optimization for Nonlinear System Identification 18
1.3.2 Part II: Robustness Analysis of Dynamic Trajectories . . . 19
1.4 Notation and Terminology 19

I: Robust Convex Optimization for Nonlinear System Identification **21**

2 Stability and Robust Identification Error **23**
2.1 Preliminaries 23
2.1.1 State Space Models 23
2.1.2 Observed Data 24
2.1.3 Stability 24
2.1.4 Objectives, Contribution, and Discussion 25
2.2 Implicit State-Space Models 26
2.2.1 Terminology and Motivations for the Use of Implicit Functions 27
2.2.2 Invertibility of Implicit Models 29

Solution via the Ellipsoid Method 31
2.3 Model Stability 31
2.3.1 Conditions For Guaranteeing Model Stability 31
2.3.2 Existing Convex Parameterizations of Stable State-Space Models 32
Parameterization of Stable LTI Models ([70]) 32
Parameterization of Stable Nonlinear Models ([88] and [13]) 33
2.3.3 New Convex Parameterizations of Stable Nonlinear Models 34
Relationship to [70] 35
Relationship to [88] 36
2.4 Robust Identification Error 37
2.4.1 A Preliminary Upper Bound for LTI Systems 37
2.4.2 Upper Bounds for Nonlinear Models 39
2.4.3 Analysis for the LTI Case 40
2.5 Proofs 42

3 Bias Elimination for Robust Identification Error Methods 45
3.1 Additional Notation 45
3.2 The Effects of Noise on Equation Error Minimizers 46
3.2.1 Analysis of the RIE in the First Order LTI Case 47
3.3 Problem Setup 49
3.3.1 Observed Data and Noiseless Process 52
3.3.2 Properties of the Noiseless Process 52
3.3.3 Relation Between the Observed Data and the Noiseless Process 53
3.3.4 System Identification Procedures and Loss Functions . . . 54
3.3.5 Contributions 54
3.4 Regression Algorithm 55
3.4.1 Convex Model Parameterization and Loss Function 55
Notation For Dissipation Inequalities 56
Model Class Definition 56
Optimization Problem 57
3.4.2 Correctness 59
3.5 Identification Algorithm 60
3.5.1 Empirical Moment Approximation 60
3.5.2 Proposed Algorithm 60
3.5.3 Asymptotic Optimality of Estimates 61
3.5.4 Consistency Analysis 61
3.6 Simulated Example 62
3.6.1 Data Set Generation 62

3.6.2 Model Structure . . . 63
3.6.3 Alternative Methods Compared . . . 63
Proposed Method . . . 63
Least Squares Method . . . 64
Simulation Error Minimization . . . 64
3.6.4 Results . . . 64
3.7 Proofs . . . 65
3.7.1 Proof of Lemma 3.10 . . . 65
3.7.2 Proof of Lemma 3.12 . . . 67
3.7.3 Proof of Lemma 3.13 . . . 69
3.7.4 Proof of Theorem 3.14 . . . 69

4 Robust Simulation Error **71**
4.1 Preliminaries . . . 71
4.1.1 State-Affine Models . . . 71
4.1.2 Error Dynamics . . . 72
4.2 A Family of Upper Bounds on Weighted Simulation Error . . . 73
4.2.1 Analysis of the RWSE . . . 73
4.2.2 A Simple Example . . . 75
4.3 Frequency Domain Analysis . . . 76
4.3.1 Notation . . . 76
4.3.2 Analysis . . . 78
Upper Bound and Stability . . . 79
4.4 An Iterative Identification Scheme . . . 81
4.5 Examples . . . 82
4.5.1 Heat Exchanger Example . . . 82
4.5.2 Wiener-Hammerstein Benchmark Example . . . 83
Proposed Method . . . 85
Alternative Methods . . . 85
Results . . . 85
4.6 Proofs . . . 86

II: Robustness Analysis of Dynamic Trajectories **91**

5 Introduction **93**
5.1 Constructing Funnels with Lyapunov Functions . . . 94
5.1.1 Rational Parameterizations . . . 96
5.1.2 A Simple Example . . . 96
5.1.3 Composition and Piecewise Functions . . . 98

6 Optimization of Funnels **99**
6.1 Time-Varying Quadratic Candidate Lyapunov Functions 99
6.1.1 Quantifying Size 100
6.1.2 Linearized Analysis 100
6.1.3 Parameterizations of Quadratic Lyapunov Functions 101
6.2 Optimization Approach 102
6.2.1 The L-Step: Finding Multipliers 103
6.2.2 The V-Step: Improving $\rho(t)$. 103
6.2.3 Variations 104
6.2.4 Time Sampled Relaxation 104
General Quadratic Lyapunov Functions 105

7 Examples and Applications **107**
7.1 A One-Dimensional Example 107
7.2 Trajectory Stabilization of Satellite Dynamics 109

8 Conclusion **113**
8.1 Robust Convex Optimization for Nonlinear System Identification . 113
8.1.1 Extensions and Future Work 114
Alternative Identification Objectives 114
Continuous Time Identification 114
Incremental Passivity and ℓ_2-Gain Bounds 115
Limit Cycle Stability 115
8.2 Robustness Analysis of Dynamic Trajectories 116
8.2.1 Extensions and Future Work 116

References **119**

Acknowledgments

I would first like to thank Russ Tedrake for his generosity, instruction, and encouragement over the course of the past five years. He gave me a tremendous amount of freedom to pursue my interests and time and time again showed an earnest concern for my happiness and success, both professionally and personally. He also fostered a comfortable, collaborative atmosphere at the Robot Locomotion Group. I know I'm not alone in feeling incredibly lucky to have known Russ as an advisor and a friend.

I would also like to thank Alexandre Megretski. Alex has been a patient guide on my journey through system identification and control theory. He went to great lengths to help further me professionally: he arranged collaborations with national laboratories and other groups at MIT, spent countless hours revising papers, and once caught a cross-country flight to a conference he could only attend for 6 hours in order to introduce me to fellow researchers. Alex has deeply influenced the way I solve problems and communicate my ideas, and for this I am very grateful.

I want to thank the other members of my committee, Pablo Parrilo and Gerald Jay Sussman for their influence of the course of my graduate school years. I would also like to thank Gerry for his impact on me as an undergraduate and MEng student. Gerry helped me bring down my vapor pressure, learn to apply myself, and discover my passion for teaching. I am sincerely thankful for his steadfast friendship and support for all these years.

I have been fortunate to be part of two wonderful communities while pursuing my PhD. The Robot Locomotion Group has been my home at MIT for the last five years. I would especially like to thank Andy Barry for helping me get this document submitted and for the hours spent on our skill exchange. I will always wonder if he found that last snake. I want to thank Hongkai Dai for helping me burn the midnight-oil and understanding the long-distance grind; Anirudha Majumdar for tolerating my distracting banter in exchange for snippets of code ; Ian Manchester for the wonderful opportunities we had to work together and his efforts to show me the ropes at my first few conferences; Frank Permenter

for giving me a window into what it really means to love Free Software; Mike Posa for those moments when I came over with something to say, but instead ended up snickering for five minutes straight; and the rest of the RLG for their patience with my invitations to discuss some trifling technical question or go grab lunch at the food trucks. I also want to thank Kathy Bates and Mieke Moran for making the RLG the functional place that it is and also tolerating my "academic" desk style. LIDS has been my home away from home. Thank you to Amir Ali Ahmadi, Giancarlo Baldan, Hamza Fawzi, Mitra Osqui, Hajir Roozbehani, Mardavij Roozbehani, James Saunderson, and Omer Tanovic for their friendship. Thanks also to Piotr Mitros, Stefie Tellex, Jaybug, Yehuda Avniel, Gabriel Bousquet, Jennifer Wang, Ashwin Vishwanathan, Vladimir Stojanovic, Yan Li, and Zhipeng Li.

I am forever indebted to my friends at PTZ, Evilcorp, and, of course, the Purple Palace that is tEp. Its hard to put in words what tEp has done for me for the last ten years. Staying in Boston I've been able to meet generations of wonderful, quirky people. I've watched them make the place I called home their own, then head off to their next adventure. I'm filled with the bittersweet longing to somehow cram them all back in one place — I guess San Francisco will have to do. I am truly grateful that, in spite of the all-consuming nature of grad-school, I have received such unwavering friendship from so many of you.

With all these homes, what to call Cruft? And will they pick up? Thank you for being my belay partners, my dates at the movies, my card-game companions, my excuse to eat KRB, and a patient audience for the monotonous tune of the Grad School Blues. And while I'm sure I'll see you all fairly soon, I will miss the comfort of the red couch, the sunlight in the shower, and the howl of the train whistle followed by the inevitable roar of the compressor.

I want to thank my family for their support. I especially want to thank my parents for their support during the rough spots during this whole process and my brother Billy for his friendship. Most importantly, thank you to Yang for her love, understanding, perspective, and endless support.

Chapter 1

Introduction and Motivation

Nonlinear dynamics are at the heart of a number of engineering and scientific endeavors such as the design and analysis of robotic systems [29, 94], experimental and theoretical electro-physiology [58], and computer-aided design for high-speed electronics [115]. The explosive growth of computing power over the last 50 years has revolutionized the role that simulation models of dynamical systems play in these disciplines. For nonlinear dynamical systems, however, there remains a strong demand for computational techniques to effectively identify models from experimental data and describe their behavior in a sense that is more informative than examining individual solutions.

This thesis looks at two problems dealing with summarizing the behavior of nonlinear dynamical systems and their robustness to variations in initial condition. The first three chapters of this thesis study a fundamental problem in system identification which is easy to state, but surprisingly challenging to address: find a simple dynamical model whose simulations match, as closely as possible, available experimental data. Several issues contribute to the difficulty of this task. First, when a model is to be used for open-loop simulations it is crucial to ensure that the identified dynamics are insensitive to small changes in initial conditions, but for nonlinear models general techniques do not exist for testing this form of stability, [76, 119]. Second, while it is natural to desire a model whose open-loop simulations match the experimental data, minimization of such simulation errors leads to challenging nonlinear programming problems for both linear and nonlinear models. The second problem addressed in the remainder of this thesis is quantifying the effectiveness of trajectory-tracking feedback controllers for nonlinear systems. This task is cast in terms of reachability analysis of closed loop systems, i.e. identifying a set of initial conditions which are guaranteed to reach a goal region. This thesis uses a common set of computational tools based on Lyapunov analysis and convex optimization to make algorithmic progress on these two challenging topics.

1.1 State-of-the-Art in Stable System Identification

System identification concerns transforming experimental data into models of dynamical systems suitable for control design, prediction, and simulation. The breadth of system-identification applications can hardly be overstated, yet a core set of theories and algorithms has been successfully applied to diverse fields such as parameter estimation for flight vehicles ([57]) and robotic manipulators ([64]), and approximate modeling in process control [35].

The existing literature on nonlinear system identification is extremely broad (see, for example, [75] Chapter 4, [96], [73], [53] Chapter 2, [119], [35]), owing both to the diversity of systems that nonlinear dynamics encompasses and the wide range of applications for which models need to be identified. This section, however briefly, provides a summary of the most popular modern approaches for nonlinear system identification followed by an overview of existing techniques for providing stability guarantees when performing system identification.

1.1.1 Model Identification Criteria

Maximum-Likelihood and Prediction-Error Methods

Maximum-likelihood (ML) estimators are extremely popular for addressing a broad range of statistical parameter identification problems (see, for example, [21] Chapter 7). Applying the ML principle involves first positing a parametric probabilistic model for how the observed data was generated, and then selecting the model parameters that maximize the likelihood of the actual observations. Identifying global maxima can be a difficult task and is frequently approached through local gradient-based search methods (assuming the likelihood is differentiable) or the EM algorithm (see [21] for discussion). Under the simplifying assumption that the model class is *correctly specified*, i.e. that the experimental data observed is generated by a model in the given model class, a number of desirable properties can be established for the maximum likelihood estimate (MLE), including asymptotic normality and strong consistency (see [75]).

The assumption of a correctly specified model is generally unrealistic. This, in part, inspired the development of the prediction error method (PEM) in the seminal papers [74], [18], and [79]. In the PEM, again a parametric family of probabilistic models is specified. A sequence of "one-step-prediction" errors are then formed. Each such error is the difference between an actual observation and the expected value for that observation conditioned on all past data. A weighted cost function is then constructed from these errors and minimized. Under relatively weak assumptions on the mechanism that generates the experimental data, it has been shown that the models arrived at using the PEM provide nearly optimal

one-step-ahead predictions as the amount of available data tends to infinity (see [74]). Such a framework can naturally be extended to k-step-ahead predictions as well. While these results are encouraging, *finding* the model which minimizes the prediction error is challenging for the same reasons that complicate ML estimation. For correctly specified linear time-invariant (LTI) models, recently published work has examined how careful design of inputs can improve the convergence of local optimization of the PEM to the true model parameters (see [37]).

In the dynamical systems context, probabilistic models as above are naturally parameterized implicitly in terms of dynamical equations by specifying distributions for measurement and process noises (see [75], Chapter 5). When working with nonlinear dynamical models, this creates additional challenges for both the ML method and the PEM. For linear-Gaussian models, computation of likelihood function and/or one-step ahead predictions can often be reduced to a Kalman-filtering problem (see [75]). In the nonlinear setting, however, even evaluating likelihood function or computing one-step ahead prediction densities can be challenging in the presence of process noise, leading several authors to consider approximation techniques based on extended Kalman filters and particle filters (e.g. [44, 116, 140]).

Simulation Error Minimization

Identifying models for which open-loop simulations accurately predict the experimental system's long-term behavior is often approached by minimizing the mean square simulation error (MSSE) (i.e. the difference between open loop simulations and recorded data). See, for example: [75] Chapter 5, [96] Chapter 17, [11] Chapter 5, or [137]. Under the assumption of i.i.d. Gaussian output noise with a fixed covariance, minimization of the MSSE corresponds to ML identification and is a familiar topic in texts on numerical optimization and parameter identification (e.g. [137] or [11] Chapter 5). Similarly, assuming i.i.d. output noise and a quadratic cost on one-step-ahead prediction errors, minimization of the MSSE corresponds to the prediction error method associated with nonlinear output error problems (see [75] or [96]). For nonlinear models, simulation error minimization has the computational advantage of not requiring approximation of prediction densities. This comes at at a cost as simulation error models do not directly account for possible process noise.

If the true system agrees with the model and noise assumptions, the global minimizers of the MSSE often have desirable properties associated with ML and PEM techniques, such as consistency, statistical efficiency, and asymptotic normality ([18, 74, 79]). When the model is not correctly specified, one can still connect the asymptotic performance of these minimizers to the best approximate

model in the model class for the system being studied (see, for example, Section V of [74]). Exploiting these results in practice can be difficult, however, as the MSSE generally has many local minima (as noted in [121] and [75]) and minimization is usually pursued via direct search or gradient descent methods.

The model-order reduction (MOR) community has also examined the problem of identifying low order dynamical models to match simulation or experimental data. The MOR methods proposed in [88], [13], and [123] are closely related to the approach proposed in this work (in referencing [123], I specifically mean Algorithm 2 contained in that work). Each of these works proposes a convex parameterization of a set of stable systems and an upper bound for simulation error which is convex in these parameters. Specifically, [88] and [13] propose parameterizations of stable nonlinear systems with [13] providing an upper bound for an approximation of simulation error. The reference [123] proposes an iterative method for discrete-time frequency domain fitting technique for stable LTI models. The relationship of this thesis to these papers is discussed further below.

Subspace Identification Methods

Subspace identification methods (see [54] and [98]) provide a notable alternative to the ML and PEM approaches given above. These methods exploit basic facts from LTI realization theory to find state-space model estimates from input-output data using only basic numerical linear algebra. Easily interpreted model-order estimates are generated as an additional benefit. These methods are most fully developed for identifying LTI models, though some progress has been made on modeling bilinear systems (see [33, 39]) and other nonlinear systems (as in [46] or [107]).

Set-Membership Identification

Set-membership (SM) identification refers to a family of system identification techniques whose development began in the robust control community during the 1980s and 1990s (see [25, 26, 90]). The object of study for these methods is the set of "unfalsified models", i.e. those models which are consistent with the given observations and certain *a-priori* assumptions on model structure and, usually, bounded-noise assumptions. In [77], Ljung provides an interesting discussion relating these approaches to classical statistical "model quality" tests. These techniques are generally interested in both a "nominal model" as well as outer approximations of the entire set of unfalsified models. The majority of the SM literature has been focused on LTI systems, [23, 25], with extensions to nonlinear models with "block-oriented" structure, [24, 127], and models whose simulation response is linear in the parameters (see [8]). The works [23] and [24]

address errors-in-variables problems with bounded noise assumption for LTI and Hammerstein systems with stability assumptions.

1.1.2 Identification of Stable Models

Identification of stable LTI models has been studied in the system identification community for many decades. Early work was focused on conditions required of the data to guarantee that least-squares (or equation error) fitting would generate stable models, despite potential under-modeling, (as in [109, 110, 120, 135]). Other work was aimed at ensuring model stability irrespective of the nature of the input data. In [95], stability guarantees for ARX identification are enforced via Jury's criterion. This constraint is necessary and sufficient for stability of scalar LTI difference equations, but is non-convex and requires careful handling to allow for efficient optimization. In [22], Jury's criterion was used to tighten *a-posteriori* parameter bounds in set-membership identification using moment-relaxation techniques. Conditions that are merely sufficient for stability but *convex* with respect to a difference equation's coefficients have been pursued in filter design (for example, in [28, 36]), and model-order reduction (see [123]). For linear state-space models, stability issues have repeatedly been addressed in the subspace identification literature: [136] uses regularization to ensure model stability at the cost of biasing estimates, whereas [70] provides a convex parameterization of all stable linear state-space models.

The results on identification of stable *nonlinear* models are substantially more limited. The most common way to guarantee model stability is to approximate the output response of a system via linear combinations of a fixed basis of stable system responses, as in Volterra series methods (see, for example, [15, 35]). A common challenge for these methods is that accurately approximating systems with a "long memory" can require an intractable number of basis elements or information about the system that is generally unavailable, as discussed in [40] and [7]. This has motivated the development of non-parametric approaches including kernel-based methods, [40], and output-interpolation schemes, [6, 67, 114]. One complication in employing these methods is that the complexity of evaluating the resulting models generally scales with the amount of available data (for example, see [40]). Accuracy of the resulting models can also depend heavily on the choice of kernel parameters, as in [40], or measures of distance between regressors, as in [67] and [6].

Methods guaranteeing stability for general nonlinear models with state include [89]. That work combined a fixed LTI system approximation with a non-parametric nonlinear function estimation scheme based on considerations from set-membership identification. Stability of the resulting models was guaranteed

by constraining the gradient of the nonlinearity based on bounds specific to the given LTI approximation. The present work is closely related to [88], and [13], which constructed large classes of stable nonlinear models and will be discussed below.

1.1.3 Relationship to [88] and [13]

This work takes as its starting point an approach to system identification suggested in [88]. In that paper, a convex parameterization of stable nonlinear difference equations was provided and several convex upper bounds for simulation error were suggested based on passivity analysis. An approach in a similar spirit was presented in [13], which provided an alternative parameterization of stable nonlinear models and upper bounds for a linearized approximation of simulation error. This second paper then provided a number of example applications drawn from model-order reduction of nonlinear circuits.

This thesis begins by unifying and extended the model classes presented in these previous works with an eye toward applications in system identification. Through a detailed analysis, it is shown that serious limitations arise when these previous approaches are applied to noisy data or systems which are "lightly damped" (i.e. nearly marginally stable). The main contribution of the system identification portion of this thesis is in addressing these issues through noise-removal algorithms and new upper bounds for simulation error.

1.2 Existing Approaches to Reachability Analysis

Reachability analysis refers to the dual problems of characterizing the flow of solutions starting from a fixed initial condition set (forward reachability) and the problem of identifying which initial conditions lead to solutions which flow through a fixed set (backwards reachability). Using this terminology, the trajectory robustness problem we consider is a problem of backwards reachability. This section briefly reviews some of the most popular computational techniques for approximating *backwards reachable sets* (a recent overview of more general reachability problems and computational methods can be found in [69]).

For linear dynamical systems, a large number of techniques are available which exploit the fact that certain families of sets are closed under linear maps (e.g. polytopes [71], ellipsoids [68], parallelotopes [65], zonotopes [45]). The review below, however, will focus exclusively on techniques applicable to nonlinear dynamical systems. The most popular techniques can be grouped as level-set methods, barrier-certificate methods, discretization methods, and trajectory-sampling techniques. The algorithms proposed in Chapter 6 combine barrier certificates with

trajectory-sampling techniques.

Level-set methods approximate backwards reachable sets as sub-level sets of a scalar valued function, usually an approximate solution to a Hamilton-Jacobi-Isaacs (HJI) partial differential equation (PDE), [66, 91]. This concept has been extended to hybrid systems in papers such as [83] and [91]. These techniques have fairly weak requirements of the underlying vector-field and, in certain cases, generate candidate state-feedback control laws. However the scalability of these approaches is limited as approximate solution of the HJI equations is generally accomplished through discretization of the state-space (see, for example, the discussion in [92]).

Barrier certificates solve a similar, though in some ways simpler, problem by replacing partial differential equations with partial differential inequalities ([104, 106]), and have close connections to Lyapunov analysis (an introduction to Lyapunov analysis can be found in many texts on nonlinear systems, such as [63]). Modern optimization tools such as sums-of-squares (SOS) programming have, in many situations, made the computational search for Lyapunov functions satisfying such differential inequalities tractable (for examples, see [101]). Finding functions satisfying such inequalities generally leads to computation of *inner approximations* of backwards reachable sets. These techniques have been applied to both deterministic and stochastic safety analysis (e.g. [105]). In [105], the guarantees referenced above are computed via SOS programming, and are extended to probabilistic guarantees for stochastic models of a disturbance.

The most popular alternatives to level-set and barrier-certificate methods involve, to varying degrees, approximating the continuous dynamics of a system through a discrete graph structure. Explicitly partitioning the state-space into "cells" and examining the cell-to-cell mapping induced by the dynamics was proposed in [56]. The set of publications based on similar state-space partitions is quite large (e.g. [1, 2, 100, 112, 128, 141]). These methods primarily differ in terms of how approximate the resulting reachability and safety analysis is, ranging from formal equivalence, as in [2], to asymptotic guarantees as the partition grows arbitrarily fine (for example, [1]).

Trajectory-based methods, that is methods based on iterative simulation of a system, are a popular alternative to "gridding" or other state-space decompositions. Notable amongst these methods is the Rapidly-Exploring Random Tree (RRT) algorithm of LaValle and Kuffner [72], which incrementally fills the backwards reachable set with an interconnected tree of trajectories. This algorithm has been extended both to address hybrid dynamics in [16] and to asymptotically recover optimal control laws on the backwards reachable set in [62]. These algorithms have the disadvantage that their approximation of the backwards reachable set has no volume. In particular, the set of trajectories that lie on the tree is

measure zero, and for any initial condition off the tree it is unclear what control strategy to use. Several recent works have attempted to address this deficiency through additional robustness analysis. The works [60] and [61] propose bounding the rate at which solutions of an autonomous dynamical system diverge from one another on a fixed domain by identifying Lyapunov-like functions using SOS optimization. By contrast, the work in [129] and [130], which this thesis extends, derives time-varying barrier certificates, initialized through a linearized analysis about a sample trajectory. This barrier certificate is then iteratively optimized to enclose more solutions. The key distinctions between these approaches are that this latter method requires no *a-priori* domain to design the barrier certificate and searches over time-varying Lyapunov functions. These two features can potentially greatly reduce the conservatism of the resulting approximations of the backwards reachable set.

1.3 Chapter Outline

1.3.1 Part I: Robust Convex Optimization for Nonlinear System Identification

The next three chapters of this thesis are dedicated to system identification with robustness guarantees. Chapter 2 introduces the notion of stability, formal definition of simulation error, and class of models that is studied throughout this portion of the thesis. This is followed by an overview of existing convex parameterizations of stable nonlinear models, as well as the introduction of several novel parameterizations provided by this work. A family of convex upper bounds for simulation error, referred to as *robust identification error* (RIE), is then reviewed, followed by a detailed analysis of these upper bounds when applied to LTI models.

Chapter 3 discusses a limitation of these existing upper bounds on simulation error that leads to biased estimates in the presence of measurement noise. These difficulties are explained in terms of the errors-in-variables problem from classical regression and statistics. A scheme is proposed for eliminating this bias when a pair of repeated experiments is available. The scheme is demonstrated on a simulated example.

Chapter 4 next introduces *robust simulation error* (RSE), a family of tighter convex upper bounds for the simulation error of state-affine systems. A simple example is given to demonstrate how these tighter upper bounds aid in overcoming the bias of the previously proposed approaches, at the cost of additional computational complexity. A frequency domain interpretation of this upper bound is given for single-input single-output (SISO) LTI models. Finally, a new iterative scheme is suggested for identifying state-affine models. The improvement

achieved by applying this scheme is demonstrated on several benchmark system identification data sets.

1.3.2 Part II: Robustness Analysis of Dynamic Trajectories

Part II of this thesis considers the problem of evaluating the robustness of local feedback controllers applied to nonlinear dynamical systems. Chapter 5 describes the general problem setting and how Lyapunov functions can be used to construct "funnels" — approximate geometric descriptions of the flow of solutions of a differential equation. Chapter 6 then introduces a methodology for searching for Lyapunov functions which define funnels and optimizing their size. Finally, Chapter 7 provides a pair of simulated examples demonstrating the effectiveness of the proposed optimization scheme.

1.4 Notation and Terminology

For an arbitrary complex matrix $A \in \mathbb{C}^{k\times n}$, denote by $[A]_{ab}$ the scalar element in the a-th row and b-th column of A. Let $[A; B]$ denote vertical concatenation of matrices. When dimensions are unambiguous, I and 0 will denote the identity matrix and the zero matrix of appropriate size. Table 1.1 lists frequently used symbols specified for an arbitrary matrix $A \in \mathbb{C}^{k\times n}$, vector $v \in \mathbb{C}^n$, and pair of matrices $P, Q \in \mathbb{C}^{n\times n}$ that are Hermitian (i.e. $P = P'$ and $Q = Q'$). For derivatives of functions we at times use the notation of [124], which indicates the derivative of a function f with respect to its k-th argument by $\partial_k f$. The *spectral radius* of a matrix $A \in \mathbb{C}^{n\times n}$ will refer the magnitude of the largest eigenvalue of A.

Table 1.1. Frequently Used Symbols

$\mathbb{C}$	The set of complex numbers.
$\mathbb{T}$	The unit circle in $\mathbb{C}$ (i.e. $z \in \mathbb{C}$ such that $\|z\| = 1$).
$\mathbb{R}$	The set of real numbers.
$\mathbb{Z}$	The integers.
$\mathbb{Z}_+$	The non-negative integers, $\{0, 1, 2, \ldots\}$.
$\mathbb{N}$	The positive integers, $\{1, 2, 3, \ldots\}$.
$\ell(\mathbb{R}^n)$	The space of functions $x : \mathbb{Z}_+ \to \mathbb{R}^n$.
$\ell_T(\mathbb{R}^n)$	The space of functions $x : \{0, 1, \ldots, T\} \to \mathbb{R}^n$, for $T \in \mathbb{N}$.
$x^{(T)}$	The restriction of $x \in \ell(\mathbb{R}^n)$ to $\{0, 1, \ldots, T\}$ for $T \in \mathbb{N}$.
I_n	The n-by-n identity matrix.
$0_{k\times n}$	The all zeros matrix of dimension k-by-n.
A'	The complex conjugate transpose of A.
$A^\dagger$	Moore-Penrose pseudo-inverse of A.
$\mathrm{tr}(A)$	The trace of A, $\mathrm{tr}(A) = \sum_{i=1}^n [A]_{ii}$ (assuming $k = n$).
$\|A\|_2$	The largest singular value of A.
$\|A\|_F$	The Frobenius norm of A, $\|A\|_F = \sqrt{\mathrm{tr}(A'A)}$.
$\|v\|_1$	The ℓ_1 norm of v, $\|v\|_1 = \sum_{i=1}^n \|v_i\|$.
$\|v\|$	The ℓ_2 norm of v, $\|v\| = \sqrt{\sum_{i=1}^n \|v_i\|^2}$.
$\|v\|_P^2$	$\|v\|_P^2 = v'Pv$.
$P \geq Q$	$P - Q$ positive semidefinite.
$P > Q$	$P - Q$ positive definite.

Part I:
Robust Convex Optimization for Nonlinear System Identification

Chapter 2

Stability and Robust Identification Error

This chapter describes a family of regression techniques for identifying stable nonlinear state-space models. Section 2.1 provides the basic problem setup and terminology. Section 2.2 contains relevant facts about state-space models defined by implicit equations. This is followed by Section 2.3 which reviews methods for guaranteeing model stability and presents several new parameterizations of stable nonlinear models. Finally, Section 2.4 presents and analyzes a family of convex upper bounds for simulation error. Unless otherwise noted, proofs that do not immediately follow the statement of a proposition, lemma or theorem are contained in Section 2.5.

2.1 Preliminaries

The following general definitions will be used throughout this chapter and the two that follow.

2.1.1 State Space Models

Definition 2.1. *A state-space model is determined by a function* $a : \mathbb{R}^{n_x} \times \mathbb{R}^{n_w} \to \mathbb{R}^{n_x}$ *via*

$$x(t) = a(x(t-1), w(t)) \tag{2.1}$$

where $x(t)$ *and* $x(t-1)$ *denote the next and current state of the system and* $w(t)$ *denotes the input. By* $G_a : \mathbb{R}^{n_x} \times \ell(\mathbb{R}^{n_w}) \to \ell(\mathbb{R}^{n_x})$ *we denote the solution map which takes an initial condition* $\xi \in \mathbb{R}^{n_x}$ *and an input signal* $\hat{w} \in \ell(\mathbb{R}^{n_w})$ *to the solution* $x = G_a(\xi, \hat{w})$ *of* (2.1) *which satisfies* $x(0) = \xi$ *and* $w(t) \equiv \hat{w}(t)$.

2.1.2 Observed Data

In this chapter, the observed data is assumed to be a pair of signals $(\tilde{w}, \tilde{x}) \in \ell_T(\mathbb{R}^{n_w}) \times \ell_T(\mathbb{R}^{n_x})$ for some positive integer T. The signal $\tilde{w}$ represents a recorded excitation applied to the experimental system whereas $\tilde{x}$ is assumed to be an approximation of the state of the system. One choice of $\tilde{x}$ which will be examined throughout the paper is constructed from an initial data set consisting of an input signal $\tilde{u}$ and an output signal $\tilde{y}$ as follows. For a given $k \in \mathbb{Z}_+$ and $(\tilde{u}, \tilde{y}) \in \ell_{T+k}(\mathbb{R}^{n_u}) \times \ell_{T+k}(\mathbb{R}^{n_y})$ take

$$\tilde{w}(t) = \begin{bmatrix} \tilde{u}(t+k) \\ \vdots \\ \tilde{u}(t) \end{bmatrix}, \quad \tilde{x}(t) = \begin{bmatrix} \tilde{y}(t+k) \\ \vdots \\ \tilde{y}(t) \end{bmatrix}, \quad (t \in \{0, \dots, T\}) \tag{2.2}$$

so that $n_w = (k+1)n_u$, and $n_x = (k+1)n_y$.

The following loss function will serve as an important measure of how well a state-space model agrees with the observed data.

Definition 2.2. *Let $Q \in \mathbb{R}^{n_x \times n_x}$ be a fixed, symmetric positive-semidefinite weight matrix. For every function $a : \mathbb{R}^{n_x} \times \mathbb{R}^{n_w} \to \mathbb{R}^{n_x}$ defining a state-space model* (2.1) *and pair of signals $(\tilde{w}, \tilde{x}) \in \ell_T(\mathbb{R}^{n_w}) \times \ell_T(\mathbb{R}^{n_x})$, define the mean-square simulation error (MSSE) J_Q^{SE} to be*

$$J_Q^{\mathrm{SE}}(a, \tilde{w}, \tilde{x}) := \frac{1}{T} \sum_{t=0}^{T-1} |\tilde{x}(t) - x(t)|_Q^2,$$

where x is the solution of (2.1) *with $w(t) \equiv \tilde{w}(t)$ and $x(0) = \tilde{x}(0)$.*

The role of the matrix Q above is to select particular components of the state-signal which are to be accurately reproduced. It should also be noted that more general definitions of simulation error treat the initial condition, $x(0)$, as an additional decision parameter. As an alternative, which is explained below, we require models to be stable in a sense that ensures solutions "forget" initial conditions asymptotically.

2.1.3 Stability

The notion of stability considered in this work is that of "ℓ_2-incremental stability" which is sketched by Figure 2.1, and defined below.

Definition 2.3. *We say a state-space model* (2.1) *is ℓ_2-incrementally stable (hereafter stable) if for all input signals $w \in \ell(\mathbb{R}^{n_w})$ and pairs of initial conditions*

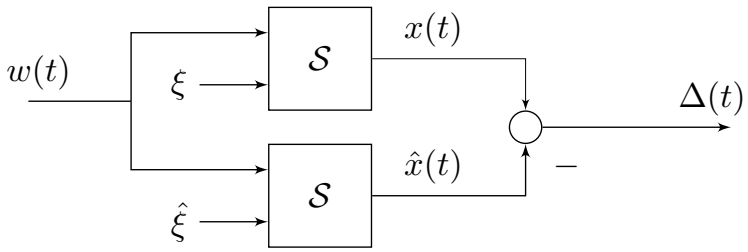

Figure 2.1. A schematic diagram describing incremental stability. Two copies of a system are subjected to the same input, but differing initial conditions. The difference in the state, $\Delta(t)$, is required to be square summable (thus tend to zero).

$\xi, \hat{\xi} \in \mathbb{R}^{n_x}$,

$$\sum_{t=1}^{\infty} |x(t) - \hat{x}(t)|^2 < \infty,$$

where $x = G_a(\xi, w)$ *and* $\hat{x} = G_a(\hat{\xi}, w)$.

Example 2.1.1. Consider an LTI state-space model defined by (2.1) with

$$a(x, w) \equiv Ax + Bw, \tag{2.3}$$

for some pair of matrices $A \in \mathbb{R}^{n_x \times n_x}$ and $B \in \mathbb{R}^{n_x \times n_w}$. It is easy to see that such a model is ℓ_2-incrementally stable if and only if spectral radius of A is less than one.

■ 2.1.4 Objectives, Contribution, and Discussion

The nominal objective of this chapter is selection of a stable nonlinear state-space model (of limited complexity) which minimizes the MSSE. This task is challenging both due to the complexity of representing stable nonlinear systems and the difficulty of minimizing simulation error. To partially address these issues, we take an approach which has been adopted in works such as [88], [13], and [123]. These works provide convex parameterizations of stable models combined with a convex upper bound for simulation error (or approximations of simulation error). This chapter reviews and extends those parameterizations and upper bounds.

Our choice to require ℓ_2-incremental stability is to ensure that models asymptotically "forget" their initial conditions in a sense that is compatible with minimizing mean square simulation error. Alternative conditions encoding such forgetting of initial conditions or "fading memory" appear frequently in the system

identification literature, both as a desirable property for models (e.g. [38, 74, 89]), and as an assumption on the theoretical system generating observations, (e.g. [6, 15, 30, 74, 142]). Incremental input-output stability and passivity are covered in detail in classic texts such as [32], and have seen a recent resurgence in interest (e.g. [3, 10, 42, 43, 80, 111, 122]). Physical systems that are ℓ_2-incrementally stable arise, for example, from the feedback interconnection of passive LTI systems and strictly monotone memoryless nonlinearities. Such systems occur frequently in structural dynamics and circuit modeling, a fact which has recently been exploited for model-order reduction in [111] and [10].

2.2 Implicit State-Space Models

This work generally examines *implicit state-space models*. The most general such systems considered are defined by a pair of functions $h : \mathbb{R}^{n_v} \times \mathbb{R}^{n_x} \times \mathbb{R}^{n_w} \to \mathbb{R}^{n_v}$ and $\bar{a} : \mathbb{R}^{n_x} \times \mathbb{R}^{n_w} \to \mathbb{R}^{n_x - n_v}$ according to

$$\begin{aligned} 0 &= h(v(t), x(t-1), w(t)), \\ x(t) &= \begin{bmatrix} v(t) \\ \bar{a}(x(t-1), w(t)) \end{bmatrix}, \end{aligned} \tag{2.4}$$

where it is required that $v \mapsto h(v, x, w)$ be a *bijection* for every $x \in \mathbb{R}^{n_x}$ and $w \in \mathbb{R}^{n_w}$. In applications, the function $\bar{a}$ will represent some portion of dynamical equations which are fixed *a-priori*, whereas the function h is to be identified through optimization. This additional fixed structure will exploited in subsequent sections of this chapter to simplify certain optimization problems. The following matrix will be used to simplify notation:

$$\Pi_{n_v} = \begin{bmatrix} I_{n_v \times n_v} & 0_{n_v \times n_x - n_v} \end{bmatrix}.$$

When such structure is not present (or ignored), we will examine implicit state-space models of the form

$$0 = h(x(t), x(t-1), w(t)), \tag{2.5}$$

where h is defined as above with $n_v = n_x$.

A natural example of when the structure (2.4) might arise is given below.

Example 2.2.1. Consider a nonlinear difference equation of the form

$$0 = q(y(t), y(t-1), \ldots, y(t-n), u(t), u(t-1), \ldots, u(t-n)), \tag{2.6}$$

with $u(t) \in \mathbb{R}$ representing an input signal, $y(t) \in \mathbb{R}$ representing an output signal, and $v \mapsto q(v, y_1, \ldots, y_n, u_0, u_1, \ldots, u_n)$ being a bijection for all $y_1, \ldots, y_n \in \mathbb{R}$ and

$u_0, u_1, \ldots, u_n \in \mathbb{R}$. The above system can naturally be associated with a model of the form (2.4) by taking $n_v = 1, n_x = n$, $n_w = n + 1$,

$$h(v, x, w) = q(v, x_1, \ldots, x_n, w_1, \ldots, w_{n+1}),$$

and

$$\bar{a}(x, w) = \begin{bmatrix} x_1 \\ x_2 \\ \vdots \\ x_{n_x-1} \end{bmatrix}.$$

The interpretation here is that

$$x(t-1) \equiv \begin{bmatrix} y(t-1) \\ \vdots \\ y(t-n) \end{bmatrix}, \quad w(t) \equiv \begin{bmatrix} u(t) \\ u(t-1) \\ \vdots \\ u(t-n) \end{bmatrix}.$$

A similar correspondence can be made when the signals $y(t)$ and $u(t)$ are vector-valued.

Another subclass of implicit state-space models which are in some ways simpler to work with are *separable implicit state-space models*. These are models of the form

$$e(x(t)) = f(x(t-1), w(t)) \tag{2.7}$$

defined by a bijection $e : \mathbb{R}^{n_x} \to \mathbb{R}^{n_x}$ and a function $f : \mathbb{R}^{n_x} \times \mathbb{R}^{n_w} \to \mathbb{R}^{n_x}$. Such systems can always be put in the form of (2.5) by taking $h(v, x, w) = e(v) - f(x, w)$. Clearly (2.7) is equivalent to (2.1) with $a = e^{-1} \circ f$.

■ 2.2.1 Terminology and Motivations for the Use of Implicit Functions

First, we define some additional terminology. We say the equations (2.4) or (2.5) are *well-posed* when h satisfies the previously mentioned invertibility requirement (similarly we say (2.7) is well posed if e is invertible). When (2.4) is well-posed, we will denote by use the notation a_h to denote the unique function satisfying

$$0 = h(a_h(x, w), x, w), \quad \forall\, x \in \mathbb{R}^{n_x}, w \in \mathbb{R}^{n_w}. \tag{2.8}$$

When working with implicit dynamics we will frequently have need to talk about *equivalence* of models. We say a well-posed implicit state-space model (2.4) is equivalent a state-space model (2.1) when

$$a(x, w) \equiv \begin{bmatrix} a_h(x, w) \\ \bar{a}(x, w) \end{bmatrix}.$$

Similarly, two well-posed implicit state-space models, say defined by $(h, \bar{a}) = (h_1, \bar{a}_1)$ and $(h, \bar{a}) = (h_2, \bar{a}_2)$ respectively, are equivalent when $a_{h_1} \equiv a_{h_2}$ and $\bar{a}_1 \equiv \bar{a}_2$. In practice, it is also important that a_h can be evaluated with limited computational effort (this topic will be discussed below).

Example 2.2.2. Consider the linear function

$$h(v, x, w) = Ev - Fx - Kw \tag{2.9}$$

with $E, F \in \mathbb{R}^{n_x \times n_x}$ and $K \in \mathbb{R}^{n_x \times n_w}$ For such a function, (2.5) is well-posed iff E is invertible. When E is invertible, (2.9) defines a model that is equivalent to a state-space model defined by (2.3) if and only if[1]

$$F = EA, \quad K = EB.$$

The choice to use implicit equations has several motivations related to the optimization strategies detailed later in this chapter. One such motivation regards the representation of stable systems. It is well known that the set

$$\mathcal{S} = \{A \in \mathbb{R}^{n_x \times n_x} \ : \ \text{the spectral radius of } A \text{ is less than one}\}$$

is not convex. For example, both of the following matrices,

$$A_0 = \begin{bmatrix} 0 & 10 \\ 0 & 0 \end{bmatrix}, \quad \text{and} \quad A_1 = \begin{bmatrix} 0 & 0 \\ 10 & 0 \end{bmatrix},$$

have repeated eigenvalues at zero, but the eigenvalues of their average, $\frac{1}{2}(A_0 + A_1)$, are 5 and -5. Despite this fact, there is a convex set $C \subset \mathbb{R}^{n_x \times n_x} \times \mathbb{R}^{n_x \times n_x}$ of matrix pairs such that

$$\mathcal{S} = \{E^{-1}F \ : \ (E, F) \in C\}.$$

— the construction of this parameterization will be given in Section 2.3.2. Thus, by examining implicit dynamics such as (2.9), one can conveniently represent all stable LTI models (this topic is discussed in more detail in Section 2.3).

A second motivation for implicit equations regards nonlinear models. To apply certain convex optimization techniques, it will be important to select h from an *affinely parameterized* family of functions. Such a family is described in terms of a basis, $\{\phi_i\}_{i=0}^{n_\theta}$, of vector-valued functions, $\phi_i : \mathbb{R}^{n_v} \times \mathbb{R}^{n_x} \times \mathbb{R}^{n_w} \to \mathbb{R}^{n_v}$ by means of

$$h_\theta(v, x, w) \equiv \phi_0(v, x, w) + \sum_{i=1}^{n_\theta} \theta_i \phi_i(v, x, w), \quad (\theta \in \mathbb{R}^{n_\theta}). \tag{2.10}$$

[1]Recall that equivalence is stated in terms of *state* signals. Issues of minimality or input/output equivalence are not part of this definition.

Here θ is a parameter vector to be identified. The use of implicit functions allows for an affine parameterization as above to represent general *rational polynomial* functions which are known to have significant advantages over polynomial functions in performing function approximation (see, for example, [97] or [81], Chapter 6). The following example makes the construction of such rational functions more explicit.

Example 2.2.3. Fixing $n_x = 1$, let $\{\psi_i\}_{i=1}^{n_\psi}$ be a collection of continuous functions $\psi_i : \mathbb{R} \times \mathbb{R}^{n_w} \to \mathbb{R}$. Taking $n_\theta = 2n_\psi$, define as above via

$$\begin{aligned}
&\phi_0(v, x, w) = 0,\\
&\phi_i(v, x, w) = \psi_i(x, w)v, \quad (i \in \{1, \dots, n_\psi\}),\\
&\phi_i(v, x, w) = \psi_i(x, w), \quad (i \in \{1 + n_\psi, \dots, 2n_\psi\}).
\end{aligned}$$

Then

$$h_\theta(v, x, w) = q_\theta(x, w)v - p_\theta(x, w) \quad (\theta \in \mathbb{R}^{n_\theta})$$

where

$$q_\theta(x, w) := \sum_{i=1}^{n_\psi} \theta_i \psi_i(x, w), \qquad \text{and} \qquad p_\theta(x, w) := -\sum_{i=1}^{n_\psi} \theta_{i+n_\psi} \psi_i(x, w).$$

If q_θ is bounded away from zero, (2.5) with $h = h_\theta$ defined by (2.10) is well-posed and

$$a_h(x, w) = \frac{p_\theta(x, w)}{q_\theta(x, w)}.$$

■ 2.2.2 Invertibility of Implicit Models

We next discuss convex conditions for ensuring a continuous function $c : \mathbb{R}^n \to \mathbb{R}^n$ is invertible and that an efficient method for approximating its inverse is available. For separable implicit state-space models, i.e. models of the form (2.7), requiring any of these conditions to hold for the function $e : \mathbb{R}^{n_x} \to \mathbb{R}^{n_x}$ ensures well-posedness. For an implicit state-space model of the form (2.4) showing these conditions hold for $c(\cdot) = h(\cdot, x, w)$ for every $(x, w) \in \mathbb{R}^{n_x} \times \mathbb{R}^{n_w}$ is sufficient to guarantee well-posedness.

We make use of the following definitions and results from the study of monotone operators.

Definition 2.4. *A function $c : \mathbb{R}^n \to \mathbb{R}^n$ is said to be strictly monotone if there exists a $\delta > 0$ such that*

$$(v - \hat{v})'(c(v) - c(\hat{v})) \geq \delta |v - \hat{v}|^2, \qquad \forall\, v, \hat{v} \in \mathbb{R}^n. \tag{2.11}$$

Theorem 2.5. *Let $c : \mathbb{R}^n \to \mathbb{R}^n$ be a function that is continuous and strictly monotone. Then c is a bijection.*

A proof can be found in [103], Theorem 18.15. The following simple proposition will also be used below.

Proposition 2.6. *A continuously differentiable function $c : \mathbb{R}^n \to \mathbb{R}^n$ satisfies* (2.11) *iff*

$$\frac{1}{2}(C(v) + C(v)') \geq \delta I, \quad \forall v \in \mathbb{R}^n \tag{2.12}$$

where $C(v) = \partial_1 c(v)$.

This claim can be easily verified by analyzing the following relationship:

$$2\Delta'(c(v+\Delta) - c(v)) = \int_0^1 2\Delta' C(v+\theta\Delta)\Delta \, d\theta \quad \forall \Delta, v \in \mathbb{R}^n. \tag{2.13}$$

The following proposition provides a family of convex sets of invertible nonlinear functions.

Proposition 2.7. *Let e and e_0 be continuous functions such that e_0 is a bijection. Then e is a bijection if either of the following two conditions holds:*

(i)

$$2(e_0(x) - e_0(\hat{x}))'(e(x) - e(\hat{x})) \geq |e_0(x) - e_0(\hat{x})|^2, \quad \forall\, x, \hat{x} \in \mathbb{R}^n. \tag{2.14}$$

(ii) e and e_0 are continuously differentiable, $E_0(x) = \partial_1 e_0(x)$ is invertible for all $x \in \mathbb{R}^{n_x}$, and

$$E_0(x)'E(x) + E(x)'E_0(x) \geq E_0(x)'E_0(x), \quad \forall x \in \mathbb{R}^n, \tag{2.15}$$

where $E(x) = \partial_1 e(x)$.

Furthermore if (ii) holds e^{-1} is continuously differentiable.

Note that both (2.14) and (2.15) are families of linear inequalities in e. Clearly (2.14) holds whenever $e \equiv e_0$ and similarly (2.15) holds when $e \equiv e_0$ and e is continuously differentiable. In this sense, the above proposition parameterizes convex sets of invertible nonlinear functions "centered" on e_0.

Solution via the Ellipsoid Method

We briefly point out the results of [82] which establish that equations of the form $c(v) = z$ can be efficiently solved via the ellipsoid method when c is a strictly monotone function. Given an initial guess $v_0 \in \mathbb{R}^n$ the initial ellipse for the method can be taken to be

$$\{v \ : \ \delta|v - v_0|^2 \leq |c(v_0) - z|\},$$

as, by Cauchy Schwarz, (2.11) implies

$$|c(v + \Delta) - c(v)| \geq \delta|\Delta| \quad \forall \, v, \Delta \in \mathbb{R}^n.$$

■ 2.3 Model Stability

This section details methods for ensuring a nonlinear state-space model (2.1) is stable beginning with a review of conditions for verifying incremental stability of a model determined by a fixed function a. This is followed by a review of joint parameterizations of model dynamics and stability certificates which are amenable to convex optimization and the presentation of a new convex parameterization of stable models.

■ 2.3.1 Conditions For Guaranteeing Model Stability

The following lemma closely follows the developments of [3].

Lemma 2.8. *For any function $a : \mathbb{R}^{n_x} \times \mathbb{R}^{n_w} \to \mathbb{R}^{n_x}$, if there exists a positive constant δ and a non-negative function $V : \mathbb{R}^{n_x} \times \mathbb{R}^{n_x} \to \mathbb{R}$ such that*

$$V(x, \hat{x}) \geq V(a(x, w), a(\hat{x}, w)) + \delta|x - \hat{x}|^2 \quad \forall \, x, \hat{x} \in \mathbb{R}^{n_x}, w \in \mathbb{R}^{n_w}, \tag{2.16}$$

then the state-space model (2.1) *is ℓ_2-incrementally stable.*

The function V in this context is known as an *incremental Lyapunov function.*

When a is continuously differentiable, the principle of contraction analysis can be applied to enforce ℓ_2-incremental stability (for variations of this result, see [80] or [43]).

Lemma 2.9. *For any continuously differentiable function $a : \mathbb{R}^{n_x} \times \mathbb{R}^{n_w} \to \mathbb{R}^{n_x}$, if there exists a positive constant δ and a function $M : \mathbb{R}^{n_x} \to \mathbb{R}^{n_x \times n_x}$ such that*

$$M(x) = M(x)' \geq 0, \quad \forall \, x \in \mathbb{R}^{n_x}, \tag{2.17}$$

and

$$|\Delta|^2_{M(x)} \geq |A(x,w)\Delta|^2_{M(a(x,w))} + \delta|\Delta|^2 \qquad \forall\, \Delta, x \in \mathbb{R}^{n_x}, w \in \mathbb{R}^{n_w}, \tag{2.18}$$

where $A(x,w) = \partial_1 a(x,w)$*, then the state-space model* (2.1) *is* ℓ_2*-incrementally stable.*

The function $(\Delta, x) \mapsto |\Delta|^2_{M(x)}$ will be referred to as a *contraction metric.*

The inequalities (2.17), (2.16), and (2.18) are linear in V and M respectively. As a result, the above lemmas can be combined with convex optimization techniques to analyze the stability of a system (2.1) determined by a fixed function a. The added challenge addressed in the next two sections is applying these lemmas to the identification of stable models by jointly optimizing over the function a and either an incremental Lyapunov function or a contraction metric.

■ 2.3.2 Existing Convex Parameterizations of Stable State-Space Models

This section recalls several existing convex parameterizations of stable models in greater detail than given in the Section 1.1 to facilitate comparison with the results to be presented in Section 2.3.3.

Parameterization of Stable LTI Models ([70])

In [70] it was noted that a standard technique for jointly searching over Lyapunov functions and observer / state-feedback-controller gains (attributed to [9]) could be applied to provide a convex parameterization of stable LTI systems. The parameterization is given in terms of a separable, linear implicit dynamics as in (2.9):

$$e(v) = Ev, \quad f(x,w) = Fx + Kw,$$

where $E, F \in \mathbb{R}^{n_x \times n_x}$ and $K \in \mathbb{R}^{n_x \times n_w}$. These matrices are constrained to satisfy

$$E = E' > 0$$

and

$$E \geq F' E^{-1} F + I. \tag{2.19}$$

Defining $A = E^{-1}F$ one sees this latter inequality immediately implies that

$$E \geq A' E A + I$$

which is a standard Lyapunov inequality for demonstrating stability of a LTI system. By Lyapunov's Theorem (for example, [143] Lemma 21.6), for any stable matrix A (i.e. with spectral radius less than one) there exists an $E = E' > 0$ such that $E - A'EA = I$. Thus this parameterization includes all stable LTI models.

Parameterization of Stable Nonlinear Models ([88] and [13])

The next parameterization is based on the work in [88] and provides a family of stable nonlinear state-space models.

Lemma 2.10. *Let $h : \mathbb{R}^{n_v} \times \mathbb{R}^{n_x} \times \mathbb{R}^{n_w} \to \mathbb{R}^{n_v}$ and $\bar{a} : \mathbb{R}^{n_x} \times \mathbb{R}^{n_w} \to \mathbb{R}^{n_x - n_v}$ be continuous functions. If there exists a positive constant δ and a non-negative function $V : \mathbb{R}^{n_x} \times \mathbb{R}^{n_x} \to \mathbb{R}$ such that $V(x,x) = 0$ for all $x \in \mathbb{R}^{n_x}$ and*

$$\begin{aligned} 2(v-\hat{v})'(h(v,x,w) - h(\hat{v},\hat{x},w)) + V(x,\hat{x}) \\ -V\left(\begin{bmatrix} v \\ \bar{a}(x,w) \end{bmatrix}, \begin{bmatrix} \hat{v} \\ \bar{a}(\hat{x},w) \end{bmatrix}\right) - \delta|x-\hat{x}|^2 \geq 0 \end{aligned} \tag{2.20}$$

holds for all $v, \hat{v} \in \mathbb{R}^{n_v}, x, \hat{x} \in \mathbb{R}^{n_x}$, and $w \in \mathbb{R}^{n_w}$, then the implicit state-space model (2.4) is well-posed and ℓ_2-incrementally stable.

The next lemma is based on ideas contained in [13] which provided a convex parameterization of stable nonlinear models based on contraction analysis.

Lemma 2.11. *Let $h : \mathbb{R}^{n_v} \times \mathbb{R}^{n_x} \times \mathbb{R}^{n_w} \to \mathbb{R}^{n_v}$ and $\bar{a} : \mathbb{R}^{n_x} \times \mathbb{R}^{n_w} \to \mathbb{R}^{n_x - n_v}$ be continuously differentiable functions and let $H_1(v,x,w) = \partial_1 h(v,x,w)$, $H_2(v,x,w) = \partial_2 h(v,x,w)$, and $\bar{A}(x,w) = \partial_1 \bar{a}(x,w)$. If there exists a positive constant δ and a function $M : \mathbb{R}^{n_x} \to \mathbb{R}^{n_x \times n_x}$ such that*

$$M(x) = M(x)' \geq 0 \quad \forall\, x \in \mathbb{R}^{n_x} \tag{2.21}$$

holds and

$$\begin{aligned} 2\nu'(H_1(v,x,w)\nu + H_2(v,x,w)\Delta) + |\Delta|^2_{M(x)} \\ - \left|\left|\begin{bmatrix} \nu \\ \bar{A}(x,w)\Delta \end{bmatrix}\right|^2_{M([v;\bar{a}(x,w)])} - \delta|\Delta|^2 \geq 0, \end{aligned} \tag{2.22}$$

holds for all $\nu, v \in \mathbb{R}^{n_v}$, $\Delta, x \in \mathbb{R}^{n_x}$, and $w \in \mathbb{R}^{n_w}$, then (2.4) is well-posed and ℓ_2-incrementally stable.

Note that Lemma 2.10 involves a system of inequalities that guarantee model stability and are linear in h and V. Similarly, Lemma 2.11 involves inequalities which are linear in h and M. Thus, these lemmas define convex sets of stable implicit models. The above lemmas generalize the presentations given in [88] and [13] to allow for a more flexible notion of "fixed structure" determined by $\bar{a}$.

2.3.3 New Convex Parameterizations of Stable Nonlinear Models

This section presents two families of alternative convex parameterizations of stable nonlinear models related to those above. These parameterizations of stable nonlinear models rely on the fact that, for every symmetric positive definite matrix $Q \in \mathbb{R}^{n\times n}$,

$$|c|^2_{Q^{-1}} \geq 2c'd - |d|^2_Q \qquad \forall\, c, d, \in \mathbb{R}^n. \tag{2.23}$$

This holds due to the trivial inequality $|c - Qd|^2_{Q^{-1}} \geq 0$.

Lemma 2.12. *For any pair of continuous functions $e : \mathbb{R}^{n_x} \to \mathbb{R}^{n_x}$ and $f : \mathbb{R}^{n_x} \times \mathbb{R}^{n_w} \to \mathbb{R}^{n_x}$, if there exists a positive constant δ and a positive definite matrix $P = P' \in \mathbb{R}^{n_x\times n_x}$ such that*

$$2(x - \hat{x})'(e(x) - e(\hat{x})) - |x - \hat{x}|^2_P \geq |f(x, w) - f(\hat{x}, w)|^2_{P^{-1}} + \delta|x - \hat{x}|^2 \tag{2.24}$$

holds for all $x, \hat{x} \in \mathbb{R}^{n_x}$ and $w \in \mathbb{R}^{n_w}$, then the state-space model (2.7) is well-posed and ℓ_2-incrementally stable.

Proof. Clearly e satisfies the conditions for invertibility described in Theorem 2.5 so that (2.7) is well-posed. Examining (2.23) with $d = x - \hat{x}$, $c = e(x) - e(\hat{x})$ and $Q = P$ yields

$$|e(x) - e(\hat{x})|^2_{P^{-1}} \geq 2(x - \hat{x})'(e(x) - e(x)) - |x - \hat{x}|^2_P.$$

Thus (2.24) implies the hypothesis of Lemma 2.8 with $V(x, \hat{x}) = |e(x) - e(\hat{x})|^2_{P^{-1}}$ and $a = e^{-1} \circ f$. □

Lemma 2.13. *For any pair of continuously differentiable functions $e : \mathbb{R}^{n_x} \to \mathbb{R}^{n_x}$ and $f : \mathbb{R}^{n_x} \times \mathbb{R}^{n_w} \to \mathbb{R}^{n_x}$, if there exists a positive constant δ and a positive definite matrix $P = P' \in \mathbb{R}^{n_x\times n_x}$ such that*

$$2\Delta' E(x)\Delta - |\Delta|^2_P \geq |F(x, w)\Delta|^2_{P^{-1}} + \delta|\Delta|^2, \quad \forall\, x, \Delta \in \mathbb{R}^{n_x}, w \in \mathbb{R}^{n_w}, \tag{2.25}$$

where $E(x) = \partial_1 e(x)$ and $F(x, w) = \partial_1 f(x, w)$, then the state-space model (2.7) is ℓ_2-incrementally stable.

Proof. Combining Theorem 2.5 with Proposition 2.6 and the fact that $E(x) + E(x)' \geq \delta I$ ensures that e is invertible. Examining (2.23) with $d = \Delta$, $c = E(x)\Delta$ and $Q = P$ yields

$$|\Delta|^2_{E(x)'P^{-1}E(x)} \geq 2\Delta' E(x)\Delta - |\Delta|^2_P.$$

Thus (2.25) implies the hypothesis of Lemma 2.9 with $a = e^{-1} \circ f$ and $M(x) = E(x)'P^{-1}E(x)$, as $\partial_1 a(x, w) = E(x)^{-1}F(x)$. □

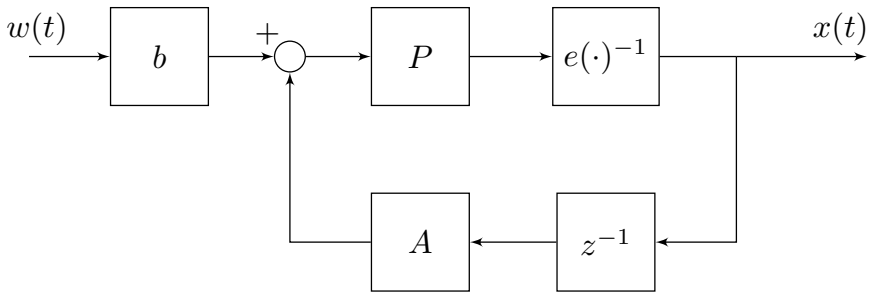

Figure 2.2. A schematic diagram of the models described by Proposition 2.14 (here z^{-1} denotes a unit delay).

The inequalities described in both of these lemmas define convex sets of function pairs (e, f) defining stable nonlinear models. When e and f are continuously differentiable functions, then (2.24) implies (2.25) (this can be seen by taking limits with x approaching $\hat{x}$). For the remainder of this section we will therefore focus on Lemma 2.13.

It is interesting to note that the parameterization defined by Lemma 2.13 contains models whose incremental stability cannot be verified using contraction metrics where M (as defined in Lemma 2.9) is a constant function. The following example demonstrates this fact.

Example 2.3.1. Consider Lemma 2.9 in the case where $n_x = 1$. In this setting all choices of M which are constant functions imply that

$$1 > |\partial_1 a(x, w)|^2 \quad \forall\, x \in \mathbb{R}, w \in \mathbb{R}^{n_w},$$

i.e. each $a(\cdot, w)$ must be a contraction map. Consider the pair of functions $e : \mathbb{R} \to \mathbb{R}$ and $f : \mathbb{R} \to \mathbb{R}$ given by

$$e(v) = v + \frac{1}{5}v^5, \quad f(x, w) = \frac{1}{3}x^3.$$

One can verify that with $P = 1$ and $\delta \leq 1$ these functions satisfy (2.25). However, $|\partial_1 a(5/4)|^2 > 1$, where $a = e^{-1} \circ f$.

Relationship to [70]

The following proposition demonstrates how the model class defined by Lemma 2.13 is a strict generalization of the stable model class proposed in [70].

Proposition 2.14. *Let $A \in \mathbb{R}^{n_x \times n_x}$ be a matrix with spectral radius less than one, $b : \mathbb{R}^{n_w} \to \mathbb{R}^{n_x}$ be an arbitrary continuous function, and $P \in \mathbb{R}^{n_x \times n_x}$ be a positive-definite matrix satisfying the Lyapunov inequality*

$$P - A'PA > 0.$$

Then for any continuously differentiable function $e : \mathbb{R}^{n_x} \to \mathbb{R}^{n_x}$ whose Jacobian, $E(x) = \partial_1 e(x)$, satisfies

$$E(x) + E(x)' \geq 2P \quad \forall\, x \in \mathbb{R}^{n_x},$$

(2.25) *holds with*

$$f(x, w) = PAx + Pb(w).$$

The proof is straightforward and omitted. The model described in the above proposition is diagrammed in Figure 2.2. Examining the case where $e(v) \equiv Pv$ on sees that the above proposition generalizes the fact that for every stable LTI state-space model there is an equivalent model of the form (2.7) which satisfies (2.25).

Relationship to [88]

Next we show that (2.25) is actually a special case of (2.22) with $n_v = n_x$. For any (e, f) in the hypothesis of Lemma 2.12, let

$$h(v, x, w) = e(v) - f(x, w), \quad M(x) = E(x) + E(x)' - P.$$

Then

$$\begin{gathered}
2\nu'(H_1(v,x,w)\nu + H_2(v,x,w)\Delta) + |\Delta|^2_{M(x)} - |\nu|^2_{M(v)} - \delta|\Delta|^2 \\
= \\
2\nu'(E(v)\nu - F(x,w)\Delta) + |\Delta|^2_{E(x)+E(x)'-P} - |\nu|^2_{E(v)+E(v)'-P} - \delta|\Delta|^2 \\
= \\
-2\nu' F(x,w)\Delta + |\Delta|^2_{E(x)+E(x)'-P} + |\nu|^2_P - \delta|\Delta|^2.
\end{gathered}$$

When $P = P' > 0$, this last expression can be minimized explicitly w.r.t ν, which yields the lower bound

$$|\Delta|^2_{E(x)+E(x)'-P} - |F(x,w)\Delta|^2_{P^{-1}} + \delta|\Delta|^2.$$

Thus if (2.22) holds globally for this choice of δ, h, and M, then (2.25) holds.

While the parameterization provided by Lemma 2.10 is apparently more flexible, Lemma 2.12 provides some advantage in terms of simplicity. In particular, the result of Lemma 2.12 replaces the need to parameterize a general matrix valued function $M(x)$ with the need to parameterize a single additional positive definite matrix P without sacrificing representing systems with highly nonlinear behavior (e.g. functions which are not contraction maps).

2.4 Robust Identification Error

In this section we introduce the *robust identification error* (RIE), a convex upper bound for simulation error based on dissipation inequalities. This upper can be viewed as, in some sense, bounding the amount which errors in one-step predictions are amplified by the system dynamics. To provide some intuition for later results, we first present a related upper bound specifically for LTI systems. Next the RIE is presented, and some analysis is provided for the quality of this upper bound.

2.4.1 A Preliminary Upper Bound for LTI Systems

The following section describes in detail a simple and easily interpreted scheme for upper bounding the simulation error of implicit LTI state-space models by a convex function. This scheme will provide some intuition as to the behavior of upper bounds for nonlinear systems presented in the remainder of this chapter.

Consider the *error dynamics* defined by

$$E\Delta(t) = F\Delta(t-1) + \epsilon(t), \quad \Delta(0) = 0, \tag{2.26}$$

where $E, F \in \mathbb{R}^{n_x \times n_x}$ are fixed matrices such that E is invertible and $\epsilon(t)$ is a perturbation signal. Our interest in these dynamics is due to the following observation. Fix a pair of signals $\tilde{w} \in \ell(\mathbb{R}^{n_w})$, $\tilde{x} \in \ell(\mathbb{R}^{n_x})$ and let

$$h(v, x, w) = Ev - Fx - Gw$$

for some matrix $G \in \mathbb{R}^{n_x \times n_w}$. The solution of (2.26) with

$$\epsilon(t) \equiv E\tilde{x}(t) - F\tilde{x}(t-1) - G\tilde{w}(t),$$

satisfies

$$\Delta(t) = x(t) - \tilde{x}(t),$$

where $x = G_{a_h}(\tilde{x}(0), \tilde{w})$ is the result of simulating the system (2.5) with the input $\tilde{w}(\cdot)$. Thus,

$$\frac{1}{T}\sum_{t=0}^{T-1} |\Delta(t)|_Q^2 = J_Q^{\mathrm{SE}}(a_h, \tilde{w}^{(T)}, \tilde{x}^{(T)}), \quad \forall\, T \in \mathbb{N},$$

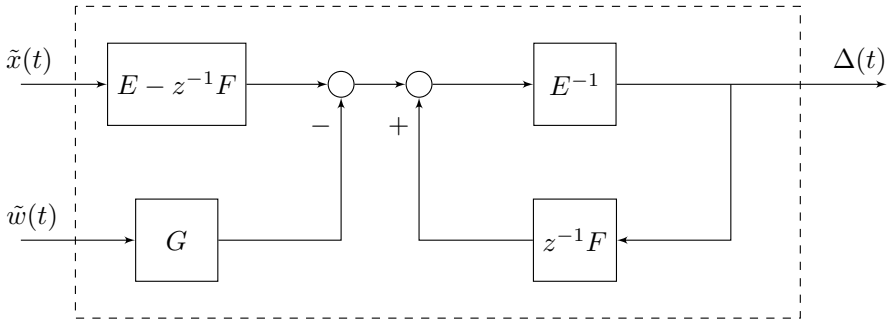

Figure 2.3. A block diagram of the error dynamics analyzed in Proposition 2.15 (here z^{-1} denotes a unit delay).

where, again, J_Q^{SE} is the mean square simulation error defined on page 24. The next proposition describes a convex upper bound for J_Q^{SE} derived from this observation.

Proposition 2.15. *Let $R \in \mathbb{R}^{(2n_x+n_w)\times(2n_x+n_w)}$, $E, F, Q \in \mathbb{R}^{n_x\times n_x}$ and $G \in \mathbb{R}^{n_x\times n_w}$ be matrices such that $E = E' > 0, Q = Q' \geq 0$ and $R = R'$. If*

$$\left|\begin{bmatrix}\xi^+\\ \xi\\ w\end{bmatrix}\right|_R^2 + |\Delta|_E^2 \geq |F\Delta + E\xi^+ - F\xi - Gw|_{E^{-1}}^2 + |\Delta|_Q^2 \tag{2.27}$$

holds for every $\xi, \xi^+, \Delta \in \mathbb{R}^{n_x}$ and $w \in \mathbb{R}^{n_w}$, then (2.5) with $h(v, x, w) = Ev - Fx - Gw$ is well-posed and

$$\frac{1}{T}\sum_{t=1}^{T}\left|\begin{bmatrix}\tilde{x}(t)\\ \tilde{x}(t-1)\\ \tilde{w}(t)\end{bmatrix}\right|_R^2 \geq J_Q^{\mathrm{SE}}(a_h, \tilde{w}, \tilde{x}), \quad \forall\, T \in \mathbb{N}, \tilde{w} \in \ell_T(\mathbb{R}^{n_w}),\ \tilde{x} \in \ell_T(\mathbb{R}^{n_x}).$$

The proof of this proposition is based on standard techniques from the study of dissipation inequalities (see [139]) and is omitted (a more general result is provided in the next section). Note that the constraint (2.27) is jointly convex in E, F, G, and R. This proposition can be interpreted in terms of the block diagram in Figure 2.3. The error dynamics are viewed as a system transforming the input data signals into the error signal $\Delta(t)$. In the above proposition, a dissipation inequality is used to establish a generalized "gain bound" from these input signals to the simulation error.

2.4.2 Upper Bounds for Nonlinear Models

This section presents a family of upper bounds for simulation error, based on [88], which are convex in the function h and an auxiliary function V. For any functions $\bar{a}$ and h as in (2.4) and $V : \mathbb{R}^{n_x} \times \mathbb{R}^{n_x} \to \mathbb{R}$ define

$$q_{(h,V)}(x, v, \xi, \xi^+, w) = |x - \xi|_Q^2 - 2(v - \Pi_{n_v}\xi^+)' h(v, x, w) + V\left(\xi^+, \begin{bmatrix} v \\ \bar{a}(x, w) \end{bmatrix}\right) - V(\xi, x), \tag{2.28}$$

where Π_{n_v} is defined as on page 26. Additionally, define

$$\mathcal{E}_Q(h, V, \xi, \xi^+, w) = \sup_{x \in \mathbb{R}^{n_x}, v \in \mathbb{R}^{n_v}} \Big\{ q_{(h,V)}(x, v, \xi, \xi^+, w) \Big\},$$

and

$$J_Q^{\mathrm{RIE}}(h, V, \tilde{w}, \tilde{x}) = V(\tilde{x}(0), \tilde{x}(0)) + \sum_{t=1}^{T} \mathcal{E}_Q(h, V, \tilde{x}(t-1), \tilde{x}(t), \tilde{w}(t)).$$

where $(\tilde{w}, \tilde{x}) \in \ell_T(\mathbb{R}^{n_w}) \times \ell_T(\mathbb{R}^{n_x})$ for an arbitrary positive integer T.

Lemma 2.16. *Let h, V, be functions defined as above. If (2.4) is well-posed and V is non-negative then*

$$(1/T) J_Q^{\mathrm{RIE}}(h, V, \tilde{w}, \tilde{x}) \geq J_Q^{\mathrm{SE}}(a, \tilde{w}, \tilde{x}), \quad \forall\, T \in \mathbb{N}, \tilde{w} \in \ell_T(\mathbb{R}^{n_w}), \tilde{x} \in \ell_T(\mathbb{R}^{n_x}),$$

where $a(x, w) \equiv [a_h(x, w); \bar{a}(x, w)]$.

Proof. Fix $T \in \mathbb{N}$ and $(\tilde{w}, \tilde{x}) \in \ell_T(\mathbb{R}^{n_w}) \times \ell_T(\mathbb{R}^{n_x})$. Letting $x(t)$ and $v(t)$ be the solutions of (2.4) with $x(0) = \tilde{x}(0)$ and $w(t) \equiv \tilde{w}(t)$,

$$\begin{aligned} \mathcal{E}_Q(h, V, \tilde{x}(t-1), \tilde{x}(t), \tilde{w}(t)) &\geq q_{(h,V)}(x(t-1), v(t), \tilde{x}(t-1), \tilde{x}(t), \tilde{w}(t)) \\ &= |x(t-1) - \tilde{x}(t-1)|_Q^2 \\ &\quad + V(\tilde{x}(t), x(t)) - V(\tilde{x}(t-1), x(t-1)), \end{aligned}$$

for $t \in \{1, \ldots, T\}$. Summing these inequalities over t yields

$$V(\tilde{x}(0), \tilde{x}(0)) + \sum_{t=1}^{T} \mathcal{E}_Q(h, V, \tilde{x}(t-1), \tilde{x}(t), \tilde{w}(t)) \geq \sum_{t=1}^{T} |x(t-1) - \tilde{x}(t-1)|_Q^2,$$

as $V(\tilde{x}(T), x(T))$ is non-negative. □

■ 2.4.3 Analysis for the LTI Case

This section provides new analysis of the upper bound suggested by Lemma 2.16 for the case of LTI models. In particular, we examine models of the form (2.4) with

$$h(v, x, w) = Ev - Fx - Gw,$$

for fixed matrices $E, F \in \mathbb{R}^{n_x \times n_x}$ and $G \in \mathbb{R}^{n_x \times n_w}$ such that E is invertible. The behavior of the upper bound for such models will be related back to the *explicit* model (2.1) defined by

$$a(x, w) = Ax + Bw.$$

where $A = E^{-1}F$ and $B = E^{-1}G$. We will also specialize to the case where the function $V : \mathbb{R}^{n_x} \times \mathbb{R}^{n_x} \to \mathbb{R}$ is of the form

$$V(x, \hat{x}) = |x - \hat{x}|_P^2$$

for some symmetric positive-semidefinite matrix $P \in \mathbb{R}^{n_x \times n_x}$.

For an arbitrary constant $r \in \mathbb{R}$,

$$r \geq q_{(h,V)}(x, v, \xi, \xi^+, w) \quad \forall\, x, v \in \mathbb{R}^{n_x}$$

is equivalent to the linear matrix inequality

$$\begin{bmatrix} r & h(\xi^+, \xi, w)' & 0_n' \\ h(\xi^+, \xi, w) & E + E' - P & -F \\ 0_n & -F' & P - Q \end{bmatrix} \geq 0.$$

This observation has the following consequences.

Claim 2.17. *If the matrix*

$$S_Q(E, F, P) := \begin{bmatrix} E + E' - P & -F \\ -F' & P - Q \end{bmatrix}$$

has any negative eigenvalues then $\mathcal{E}_Q(h, V, \xi, \xi^+, w) = +\infty$ for all $\xi, \xi^+ \in \mathbb{R}^{n_x}$ and $w \in \mathbb{R}^{n_w}$. Otherwise, if (A, Q) is observable then $A = E^{-1}F$ has spectral radius less than one.

Proof. Substituting $x = \xi + \Delta$ and $v = \xi^+ + \nu$,

$$\begin{aligned} \mathcal{E}_Q(h, V, \xi, \xi^+, w) &= \sup_{\Delta, \nu \in \mathbb{R}^{n_x}} \left\{ |\Delta|_Q^2 - 2\nu'(E\nu - F\Delta + h(\xi^+, \xi, w)) + |\nu|_P^2 - |\Delta|_P^2 \right\} \\ &= \sup_{\Delta, \nu \in \mathbb{R}^{n_x}} \left\{ -2\nu' h(\xi^+, \xi, w) - \left| \begin{bmatrix} \Delta \\ \nu \end{bmatrix} \right|_{S_Q(E,F,P)}^2 \right\}. \end{aligned}$$

This establishes that $S_Q(E, F, P) \geq 0$ is required for $\mathcal{E}_Q$ to be finite. Next,

$$\begin{bmatrix} A \\ I_{n_x} \end{bmatrix}' S_Q(E, F, P) \begin{bmatrix} A \\ I_{n_x} \end{bmatrix} = P - A'PA - Q.$$

Thus $S_Q(E, F, P) \geq 0$ implies a Lyapunov inequality which establishes the stability of A when (A, Q) is observable (for example, [143] Lemma 21.6). □

The next claim and proposition establish a partial relationship between $\mathcal{E}_Q$ and the *equation errors*. Given a pair of data signals, $\tilde{x} \in \ell_T(\mathbb{R}^{n_x})$ and $\tilde{w} \in \ell_T(\mathbb{R}^{n_w})$, the equation errors are defined by

$$\epsilon(t) = \tilde{x}(t) - A\tilde{x}(t-1) - B\tilde{w}(t),$$

and can be viewed as the error of a "one-step-ahead" prediction (i.e. predicting $\tilde{x}(t)$ from $\tilde{x}(t-1)$ and $\tilde{w}(t)$).

Claim 2.18. *Let E, F, and P be matrices as above for which $S_Q(E, F, P)$ is positive semidefinite. If the vector*

$$\begin{bmatrix} h(\xi^+, \xi, w) \\ 0_n \end{bmatrix}$$

does not lie in the range of $S_Q(E, F, P)$, then $\mathcal{E}_Q(h, V, \xi, \xi^+, w) = +\infty$. Otherwise,

$$\mathcal{E}_Q(h, V, \xi, \xi^+, w) = |\xi^+ - A\xi - Bw|^2_{E'\Gamma E}$$

where $A = E^{-1}F$, $B = E^{-1}G$ and Γ is equal to

$$(E + E' - P)^\dagger \left(E + E' - P + F(P - Q - F'(E + E' - P)^\dagger F)^\dagger F'\right)(E + E' - P)^\dagger.$$

Recall that $(\cdot)^\dagger$ denotes the Moore-Penrose pseudoinverse. This second claim, whose proof is also omitted, follows from first-order optimality criteria and the formula for block pseudo-inverses of Hermitian positive semidefinite matrices (see [113]).

The next proposition suggests that the upper bound derived from $\mathcal{E}_Q$ can be particularly conservative to situations where the matrix A has eigenvalues near the unit circle in the complex plane, $\mathbb{T}$.

Proposition 2.19. *Let E, F, and G be matrices as above such that the spectral radius of $A = E^{-1}F$ is less than one. Then for any symmetric positive semidefinite matrix $P \in \mathbb{R}^{n_x \times n_x}$ one has*

$$\mathcal{E}_Q(h, V, \xi, \xi^+, w) \geq \sup\left\{|(zI - A)^{-1}(\xi^+ - A\xi - Bw)|^2_Q \ : \ z \in \mathbb{T}\right\},$$

where $B = E^{-1}G$, and h and V are defined as above.

Proof. We briefly recall the fact that a quadratic function

$$g(\Delta) = \Delta' H \Delta + 2b'\Delta \quad (\Delta \in \mathbb{R}^{n_x})$$

with $H = H' \in \mathbb{R}^{n_x \times n_x}$ and $b \in \mathbb{R}^{n_x}$ can be naturally extended to a real-valued function of complex arguments by taking

$$g(\Delta) = \Delta' H \Delta + 2\mathrm{Re}\{b'\Delta\} \quad (\Delta \in \mathbb{C}^{n_x}).$$

Furthermore,

$$\sup\{g(\Delta) \ : \ \Delta \in \mathbb{R}^{n_x}\} = \sup\{g(\Delta) \ : \ \Delta \in \mathbb{C}^{n_x}\}.$$

Thus, for every $z \in \mathbb{T}$ and $\Delta \in \mathbb{C}^{n_x}$,

$$\begin{aligned}\mathcal{E}_Q(h, V, \xi, \xi^+, w) &\geq q_{(h,V)}(\xi + \Delta, \xi^+ + z\Delta, \xi, \xi^+, w) \\ &= |\Delta|_Q^2 - 2\mathrm{Re}\{(z\Delta)'((zE - F)\Delta - h(\xi^+, \xi, w))\},\end{aligned}$$

where the equality holds as $V(\xi, \xi + \Delta) = |\Delta|_P^2 = |z\Delta|_P^2 = V(\xi^+, \xi^+ + z\Delta)$. Letting $\bar{\Delta} = (zE - F)^{-1}h(\xi^+, \xi, w)$,

$$\begin{aligned}q_{(h,V)}(\xi + \bar{\Delta}, \xi^+ + z\bar{\Delta}, \xi, \xi^+, w) &= |(zE - F)^{-1}h(\xi^+, \xi, w)|_Q^2 \\ &= |(zI - A)^{-1}E^{-1}(E\xi^+ - F\xi - G)|_Q^2 \\ &= |(zI - A)^{-1}(\xi^+ - A\xi - Bw)|_Q^2.\end{aligned}$$

□

■ 2.5 Proofs

.

Proof of Proposition 2.7. The proof follows from Theorem 2.5 with $c = e \circ e_0^{-1}$ and $\delta = 1/2$. If (2.14) holds, then for any $v, \hat{v} \in \mathbb{R}^n$ taking $x = e_0^{-1}(v)$ and $\hat{x} = e_0^{-1}(\hat{v})$ implies that (2.11) holds. Thus c and e_0 are both bijections, implying e is a bijection. Assuming (2.15) holds, note that $C(v) = \partial_1 c(v) = E(x)E_0(x)^{-1}$, where $e_0(x) = v$. Multiplying (2.15) on the left and right by $E_0(x)'^{-1}$ and $E_0(x)^{-1}$ respectively yields (2.12) with $\delta = 1/2$. Proposition 2.6 then implies that (2.11) holds. □

Proof of Lemma 2.8. For any $w \in \ell(\mathbb{R}^{n_w})$ and $\xi, \hat{\xi} \in \mathbb{R}^{n_x}$, let $x = G_a(\xi, w)$ and $\hat{x} = G_a(\hat{\xi}, w)$. Then (2.16) implies

$$V(x(t), \hat{x}(t)) \geq V(x(t+1), \hat{x}(t+1)) + \delta|x(t) - \hat{x}(t)|^2, \ \forall \ t \in \mathbb{Z}_+.$$

Summing these inequalities w.r.t. t yields

$$V(x(0),\hat{x}(0)) \geq V(x(T+1),\hat{x}(T+1)) + \delta \sum_{t=0}^{T} |x(t)-\hat{x}(t)|^2,\ \forall\, T \in \mathbb{Z}_+.$$

As $V(x(T+1),\hat{x}(T+1))$ is non-negative this yields the result. □

Proof of Lemma 2.9. For any $w \in \ell(\mathbb{R}^{n_w})$ and $\xi_0, \xi_1 \in \mathbb{R}^{n_x}$ let $x(\theta,\cdot) = G_a(\theta\xi_1 + (1-\theta)\xi_0, w)$ for all $\theta \in [0,1]$. Then each $x(\theta,t)$ is a continuously differentiable function of θ and $\Delta_\theta(t) = \partial_1 x(\theta,t)$ satisfies

$$\Delta_\theta(0) = \xi_1 - \xi_0, \quad \Delta_\theta(t) = A(x(\theta,t-1),w(t))\Delta_\theta(t-1).$$

Applying (2.18) one has

$$|\Delta_\theta(t)|^2_{M(x(\theta,t))} \geq |\Delta_\theta(t+1)|^2_{M(x(\theta,t+1))} + \delta|\Delta_\theta(t)|^2, \quad \forall\, \theta \in [0,1], t \in \mathbb{Z}_+.$$

Summing these inequalities over t yields

$$|\xi_1 - \xi_0|^2_{M(x(\theta,0))} \geq \delta \sum_{t=0}^{T} |\Delta_\theta(t)|^2, \quad \forall\, \theta \in [0,1], T \in \mathbb{Z}_+,$$

as each $M(x(\theta,T+1))$ is positive definite. Finally, integrating both sides w.r.t. θ yields the result as

$$\int_0^1 |\Delta_\theta(t)|^2 d\theta \geq \left| \int_0^1 \Delta_\theta(t) d\theta \right|^2 = |x(1,t) - x(0,t)|^2$$

due to Jensen's inequality and the Fundamental Theorem of Calculus. □

Proof of Lemma 2.10. Assume that (2.20) holds globally. Examining (2.20) for $v = \hat{v} = 0$ yields

$$V(x,\hat{x}) \geq \delta|x-\hat{x}|^2.$$

Next, for any $x \in \mathbb{R}^{n_x}$, examining (2.20) with $x = \hat{x}$ leads to

$$2(v-\hat{v})'(h(v,x,w)-h(\hat{v},x,w)) \geq V\left(\begin{bmatrix} v \\ \bar{a}_h(x,w) \end{bmatrix}, \begin{bmatrix} \hat{v} \\ \bar{a}_h(x,w) \end{bmatrix}\right) \geq \delta|v-\hat{v}|^2. \quad (2.29)$$

By Theorem 2.5, the map $v \to h(v,x,w)$ is invertible for every $(x,w) \in \mathbb{R}^{n_x} \times \mathbb{R}^{n_w}$ so that (2.5) is well-posed.

Next, examine (2.20) with $v = a_h(x,w)$ and $\hat{v} = a_h(\hat{x},w)$, where a_h is again the unique function satisfying

$$0 = h(a_h(x,w),x,w) \quad \forall x, \in \mathbb{R}^{n_x}, w \in \mathbb{R}^{n_w}.$$

One sees that, with $a(x,w) = [a_h(x,w); \bar{a}(x,w)]$, the conditions of Lemma 2.8 are implied guaranteeing ℓ_2-incremental stability of (2.5). □

Proof of Lemma 2.11. First we show that for every $(x, w) \in \mathbb{R}^{n_x} \times \mathbb{R}^{n_w}$ the function $h(\cdot, x, w)$ is a bijection. Examining (2.22) with $\nu = 0$ yields $M(x) \geq \delta I$. Instead taking $\Delta = 0$ yields

$$2\nu' H_1(v, x, w)\nu \geq \delta|\nu|^2,$$

which implies that $h(\cdot, x, w)$ is invertible in light of Theorem 2.5 and Proposition 2.6. The implicit function theorem implies

$$\partial_1 a_h(x, w) = -H_1(a_h(x, w), x, w)^{-1} H_2(a_h(x, w), x, w).$$

Examining (2.22) with

$$v = a_h(x, w) \text{ and } \nu = -H_1(a_h(x, w), x, w)^{-1} H_2(a_h(x, w), x, w)\Delta$$

demonstrates that δ, M, and a_h meet the hypothesis required by Lemma 2.9 to ensure ℓ_2-incremental stability. □

Chapter 3

Bias Elimination for Robust Identification Error Methods

This chapter analyzes the effects of measurement noise on model estimates obtained by minimizing the robust identification error (RIE). It is shown that significant bias can result when attempting to identify systems which are nearly marginally stable, even for a moderately low signal-to-noise ratio (SNR). This observation is explained in terms of the concept of errors-in-variables (EIV) in detail in Section 3.2. The remainder of the chapter provides a method for eliminating the bias due to measurement noise, assuming access to a pair of repeated experiments with suitably independent measurement noise. Section 3.4 provides an upper bound on the RIE that depends on the data through *empirical moments*, i.e. time-averages of polynomial functions. This then allows us to apply results from the nonlinear instrumental variables (IV) literature, specifically [50], to remove the effect of noise on the RIE in Section 3.5. A simulated example is examined in Section 3.6.

■ 3.1 Additional Notation

For $\alpha, \beta \in \mathbb{Z}_+^n$, the relation $\beta \leq \alpha$ holds iff $\beta_k \leq \alpha_k$ for each k. For $v \in \mathbb{C}^n$ and $\alpha \in \mathbb{Z}_+^n$,

$$v^\alpha := \prod_{d=1}^{n} v_d^{\alpha_d}$$

is the monomial function of v with *vector degree* α, and *total degree* $\|\alpha\|_1$. For any $v \in \ell(\mathbb{R}^n)$ and $\alpha \in \mathbb{Z}_+^n$, let $v^\alpha : \mathbb{Z}_+ \to \mathbb{R}$ be defined by

$$v^\alpha(t) := v(t)^\alpha.$$

For any $v \in \ell(\mathbb{R}^n)$ and positive integer T define

$$\mathbf{S}_T[v] := \frac{1}{T}\sum_{t=1}^{T} v(t).$$

■ 3.2 The Effects of Noise on Equation Error Minimizers

At the end of the previous chapter it was shown that, when identifying LTI models, the robust identification error amounts to a *weighted equation error* (see Claim 2.18 on page 41). For this reason, we recall the difficulties associated with identifying LTI models via minimizing equation error when output noise is present. Consider the problem of choosing $A \in \mathbb{R}^{n_x \times n_x}$ and $B \in \mathbb{R}^{n_x \times n_w}$ to minimize

$$J_T^{\mathrm{EE}} = (1/T)\sum_{t=1}^{T} |\tilde{x}(t) - A\tilde{x}(t-1) - B\tilde{w}(t)|^2$$

where the signals $\tilde{x}(t) \in \mathbb{R}^{n_x}$ and $\tilde{w}(t) \in \mathbb{R}^{n_w}$ satisfy

$$\tilde{x}(t) = \bar{x}(t) + \eta(t), \quad \bar{x}(t) = A_\star \bar{x}(t-1) + B_\star \tilde{w}(t), \quad \bar{x}(0) = 0,$$

for some $A_\star \in \mathbb{R}^{n_x \times n_x}$ with spectral radius less than one, $B_\star \in \mathbb{R}^{n_x \times n_w}$, and noise signal $\eta(t)$. Here $\bar{x}(t)$ denotes some underlying process driven by $\tilde{w}(t)$, whereas the measurements $\tilde{x}(t)$ are corrupted by the output noise $\eta(t)$.

For simplicity, assume that $\tilde{w}(t)$ is a realization of an i.i.d., zero mean normal stochastic process with covariance I. Similarly, assume that $\eta(t)$ is an i.i.d. normal stochastic process with zero mean and covariance $\sigma_\eta^2 I$ and is independent of $\tilde{w}(t)$. Then

$$\lim_{T\to\infty} J_T^{\mathrm{EE}} = \sigma_\eta^2(I + \|A\|_F^2) + \|B_\star - B\|_F^2 + \mathrm{tr}((A_\star - A)'\Sigma(A_\star - A)),$$

almost surely, where Σ is the positive semidefinite solution of the Lyapunov equation

$$\Sigma = A\Sigma A' + BB'$$

(see, for example, [19]). This expression is minimized by $B = B_\star$ and the minimizing choice of A,

$$A = (\sigma_\eta^2 I + \Sigma)^{-1}\Sigma A_\star,$$

can be found by completing the squares. Thus, one only expects minimization of J_T^{EE} to result in an *unbiased* estimate of $A_\star$ when the output noise variance σ_η^2 is identically zero. Furthermore, as σ_η^2 tends to ∞, the minimizing choice for A tends to zero. This result is known as an *attenuation bias* in the statistics

literature, and the term *errors-in-variables* is used to refer to the situation of regressors (here specifically $\tilde{x}(t-1)$) themselves being noise corrupted (see [21], Chapter 12).

3.2.1 Analysis of the RIE in the First Order LTI Case

We next demonstrate that minimization of the RIE for LTI models leads to biased estimates in the presence of output noise. This is unsurprising in light of the discussion above and the previously mentioned observation that the RIE is a weighted form equation error. This section establishes that the bias incurred by minimizing the RIE can be much more severe than that which occurs for equation error minimization when the true system is nearly marginally stable.

We examine first order LTI models of the form

$$ex(t) = fx(t-1) + gw(t) \tag{3.1}$$

with $e, f, g \in \mathbb{R}$ and $e > 0$. This corresponds to (2.5) with

$$h(v, x, w) = ev - fx - gw$$

in the notation of the previous chapter. We begin by analyzing the robust identification error, $\mathcal{E}_Q(h, V, \xi, \xi^+, w)$, when $Q = 1$ and $V(x, \xi) = p|x - \xi|^2$ for some $p \geq 0$. We assume that

$$S_Q(e, f, p) = \begin{bmatrix} 2e - p & -f \\ -f & p - 1 \end{bmatrix} > 0$$

which guarantees that $\mathcal{E}_Q$ is finite (see Claim 2.17 of the previous chapter). From Claim 2.18 on page 41 it can be seen that

$$\mathcal{E}_Q(h, V, \xi, \xi^+, w) = \frac{|e\xi^+ - f\xi - gw|^2}{2e - p - f^2/(p-1)}.$$

The following proposition relates the above cost function back to explicit LTI state-space models of the form

$$x(t) = \hat{a}x(t-1) + \hat{b}w(t).$$

Proposition 3.1. *Fix $\hat{a} \in (-1, 1)$ and $\hat{b} \in \mathbb{R}$. Then,*

$$\min \left\{ \frac{|e\xi^+ - e\hat{a}\xi - e\hat{b}w|^2}{2e - p - (e\hat{a})^2/(p-1)} \ : \ e, p \in \mathbb{R} \text{ s.t. } S_Q(e, e\hat{a}, p) \geq 0 \right\}$$

$$= \frac{|\xi^+ - \hat{a}\xi - \hat{b}w|^2}{(1 - |\hat{a}|)^2}.$$

Proof. We demonstrate that the optimizing (e, p) are $e = p = \frac{1}{1-|\hat{a}|}$. For an arbitrary $e > 0$, the choice of $p \geq 1$ that maximizes $2e - p - (e\hat{a})^2/(p-1)$ is $p = |e\hat{a}| + 1$ (this can be concluded from first and second order optimality conditions). For this choice of p,

$$\frac{|e\xi^+ - e\hat{a}\xi - e\hat{b}w|^2}{2e - p - (e\hat{a})^2/(p-1)} = \frac{e^2}{2e(1-|\hat{a}|) - 1}|\xi^+ - \hat{a}\xi - \hat{b}w|^2.$$

The minimum of this expression over all $e > 0$ is attained by $e = \frac{1}{1-|\hat{a}|}$, and the minimum is the desired expression (for this choice $e = p$).

Finally, we show that $S_Q(e, e\hat{a}, p) \geq 0$. The diagonal entries of this matrix are non-negative as $2e - p = p \geq 1$. The determinant can then be computed to be

$$(2e-p)(p-1) - e^2\hat{a}^2 = e(e-1) - e^2\hat{a}^2 = e(e(1-\hat{a}^2) - 1) = e|\hat{a}|^2.$$

□

Let $\tilde{w}(t)$, $\tilde{x}(t)$, and $\eta(t)$ be as in the previous section with $n_x = n_w = 1$, $A_\star = a \in (-1, 1)$ and $B_\star = b \in \mathbb{R}$. Then

$$\begin{aligned}\lim_{T\to\infty} \frac{1}{T}\sum_{t=1}^{T} \mathcal{E}_Q(h, V, \tilde{x}(t-1), \tilde{x}(t), \tilde{w}(t)) &= \frac{1}{(1-|\hat{a}|)^2} \lim_{T\to\infty} J_T^{EE} \\ &= \frac{\sigma_\eta^2(1+\hat{a}^2) + (a-\hat{a})^2\Sigma}{(1-|\hat{a}|^2)}.\end{aligned}$$

Proposition 3.2. *The quantity*

$$\frac{\sigma_\eta^2(1+\hat{a}^2) + (a-\hat{a})^2\Sigma}{(1-|\hat{a}|)^2}$$

is minimized by

$$\hat{a} = \begin{cases} \operatorname{sign}(a)\frac{|a|\sigma^2(1-|a|)-1}{1+\sigma^2(1-|a|)} & \sigma^2 \geq \frac{1}{|a|(1-|a|)} \\ 0 & \text{o.w.} \end{cases}$$

where σ^2 is the signal to noise ratio, Σ/σ_η^2.

The proof requires tedious calculations and is omitted. Figure 3.1 plots the relationship between a (the true pole) and $\hat{a}$ (the estimated pole) for various SNRs. Two features of the graph are particularly noteworthy, both having to do with the bias of the estimate $\hat{a}$ toward zero. First, note for low SNRs $\hat{a}$ is zero irrespective of the true dynamics. In particular, as the function $\frac{1}{|a|(1-|a|)}$ achieves

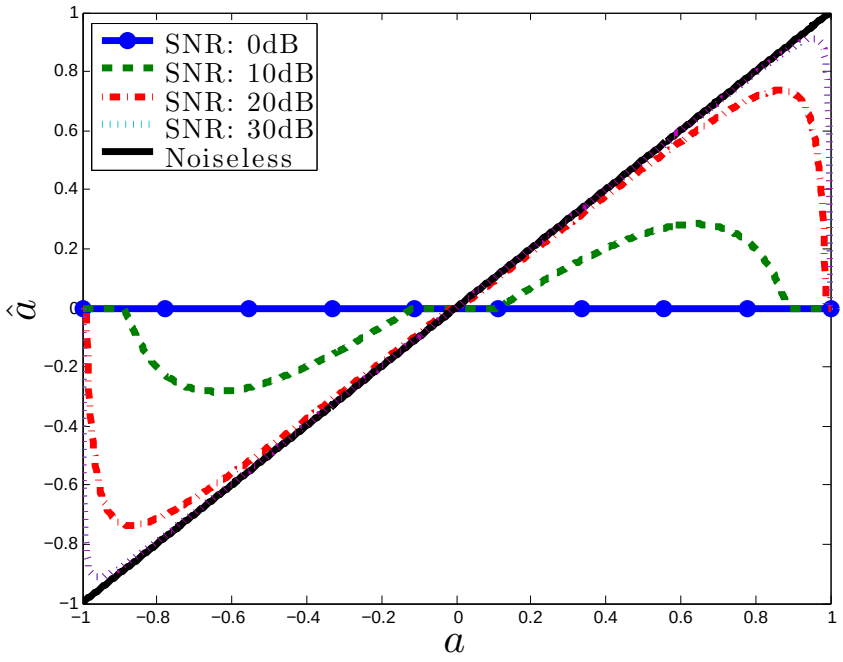

Figure 3.1. A comparison of the true system pole, a, to the pole $\hat{a}$ of the model found by minimizing the RIE for various SNRs. For low SNRs (specifically less than approximately 6 dB) the estimate is zero irrespective of the true pole location. Even for high SNRs the estimate is zero if the true pole location is near ± 1 (i.e. the true system is nearly marginally stable).

a minimum of 4 for $a \in [-1, 1] \setminus \{-1, 0, 1\}$, the estimate is zero whenever σ is less than 2 (an SNR of 6 dB). Second, note that even for a high SNR, $\hat{a}$ is nearly zero when $|a|$ approaches 1 (that is, when the dynamics are nearly marginally stable).

The bias for robust identification error minimization can be much more severe than for equation error minimization, especially for values of a near ± 1. This is illustrated in Figures 3.2 and 3.3 which fix $a = 0.9$ and plot both the simulation error, equation error, RIE and associated estimates for varying SNRs.

3.3 Problem Setup

The remainder of this chapter examines the following problem setup.

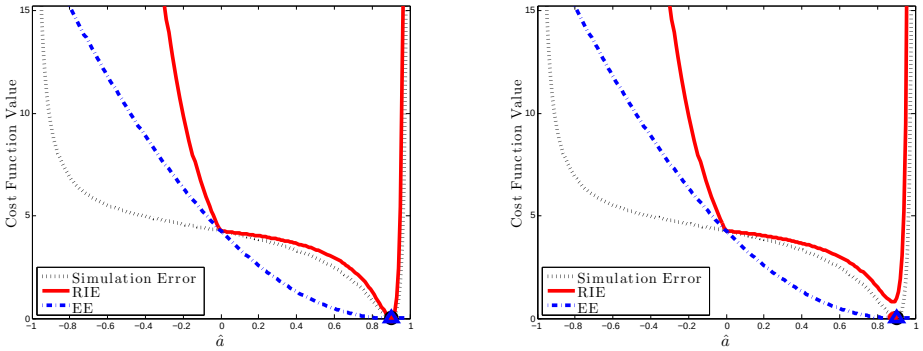

(a) SNR= ∞ (b) SNR= 30dB

(c) SNR= 20dB (d) SNR= 10dB

Figure 3.2. Comparison of the asymptotic values of simulation error, equation error, and RIE when fitting a first order linear model (3.1) to data from a first order system with output noise and a pole at 0.9. Figures (a)-(d) plot the cost functions for increasing noise levels. The optimizers of the RIE and equation error shift toward zero as noise levels increase, whereas the simulation error optimum remains at the true value of a. While the RIE is a reasonable approximation of the simulation error for high SNRs, the bias at low SNRs is considerably worse that that of equation error.

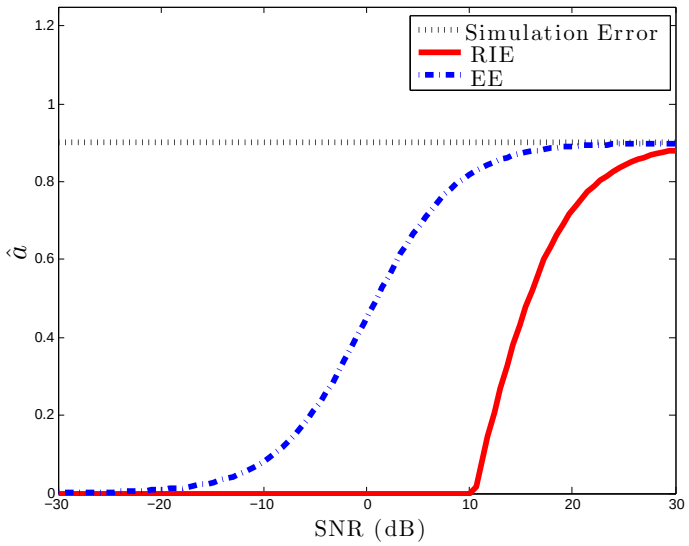

Figure 3.3. Comparison of bias that results from fitting a first order linear model (3.1) to data from a first order system with output noise and a pole at 0.9. The above plot provides the values of $\hat{a}$ which minimize the simulation error, equation error and RIE for varying SNRs. Note that $\hat{a} = 0$ minimizes the RIE for a large range of SNRs, indicating severe bias.

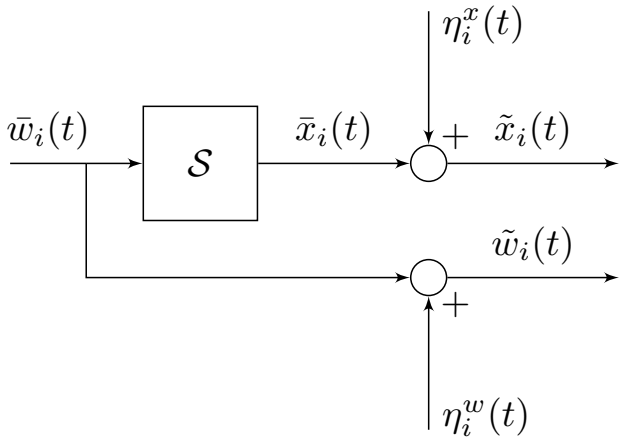

Figure 3.4. A schematic diagram of the manner in which the observed data is assumed to be generated. Here $i \in \{1, 2\}$ is the experiment number, $\bar{w}_i(t)$ is the unobserved noiseless excitation and $\bar{x}_i(t)$ is the corresponding noiseless response. The signals $\eta_i^x(t)$ and $\eta_i^w(t)$ are additive noise which corrupts the actual recorded signals.

3.3.1 Observed Data and Noiseless Process

An input/state signal pair will refer to a tuple $(\tilde{w}, \tilde{x}) \in \ell(\mathbb{R}^{n_w}) \times \ell(\mathbb{R}^{n_x})$, where $\tilde{w}$ represents an excitation signal and $\tilde{x}$ represents a system response. While system identification is always performed on finite data sets, our definitions are given in terms of signals of infinite duration to facilitate asymptotic analysis of the system identification procedures proposed in Section 3.5.

The *observed data* consists of two input/state signal pairs, $(\tilde{w}_i, \tilde{x}_i) \in \ell(\mathbb{R}^{n_w}) \times \ell(\mathbb{R}^{n_x})$ for $i \in \{1, 2\}$. It is assumed there exists another two unmeasurable input/state signal pairs, $(\bar{w}_i, \bar{x}_i) \in \ell(\mathbb{R}^{n_w}) \times \ell(\mathbb{R}^{n_x})$, which will be referred to as the *noiseless process*. The meaning here is that the observed data is a noise corrupted measurement of the underlying noiseless process. Figure 3.4 provides a diagram describing these signals in terms of additive noise processes, $\eta_i^x(t)$ and $\eta_i^w(t)$.

For convenience, we additionally define

$$\bar{z}_i(t) = \begin{bmatrix} \bar{x}_i(t) \\ \bar{x}_i(t-1) \\ \bar{w}_i(t) \end{bmatrix}, \quad \text{and} \quad \tilde{z}_i(t) = \begin{bmatrix} \tilde{x}_i(t) \\ \tilde{x}_i(t-1) \\ \tilde{w}_i(t) \end{bmatrix} = \bar{z}_i(t) + \begin{bmatrix} \eta_i^x(t) \\ \eta_i^x(t-1) \\ \eta_i^w(t) \end{bmatrix} \tag{3.2}$$

for $t \geq 1$ and $i \in \{1, 2\}$. Naturally, $n_z = 2n_x + n_w$.

3.3.2 Properties of the Noiseless Process

The following condition is assumed to hold.

(A1) The signals $\bar{w}_1, \bar{w}_2, \bar{x}_1, \bar{x}_2$, are bounded and satisfy

$$\lim_{t\to\infty} \bar{w}_1(t) - \bar{w}_2(t) = 0, \text{ and } \lim_{t\to\infty} \bar{x}_1(t) - \bar{x}_2(t) = 0.$$

That is, the two underlying noiseless processes are bounded and identical except for some initial transients. This assumption is motivated by the scenario where the observed signals are the response of a stable system to some other excitation the experimenter controls.

The following definition will be used to describe the persistence of excitation of the signals $(\bar{x}_1, \bar{w}_1)$ in the sequel.

Definition 3.3. *Let $\Omega \subset \mathbb{R}^{n_x} \times \mathbb{R}^{n_w}$ denote those pairs $(\hat{x}, \hat{w})$ for which there exists a compact neighborhood, K, and a positive constant c satisfying*

$$\liminf_{T\to\infty} \frac{1}{T} \sum_{t=1}^{T} \rho(\bar{x}_1(t), \bar{w}_1(t)) \geq c \int \int_K \rho(x, w)\, dx\, dw$$

for all non-negative continuous functions $\rho : \mathbb{R}^{n_x} \times \mathbb{R}^{n_w} \to \mathbb{R}$.

■ 3.3.3 Relation Between the Observed Data and the Noiseless Process

The following additional assumptions are made:

(A2) The signals $\tilde{z}_1, \tilde{z}_2$ are bounded.

(A3) For all $\alpha, \beta, \gamma \in \mathbb{Z}_+^{n_z}$,

$$\lim_{T\to\infty} \mathbf{S}_T\left[\bar{z}_1^{\alpha}\zeta_1^{\beta}\zeta_2^{\gamma}\right] - \mathbf{S}_T\left[\bar{z}_1^{\alpha}\right]\mathbf{S}_T\left[\zeta_1^{\beta}\right]\mathbf{S}_T\left[\zeta_2^{\gamma}\right] = 0,$$

and

$$\lim_{T\to\infty} \mathbf{S}_T[\zeta_1] = \lim_{T\to\infty} \mathbf{S}_T[\zeta_2] = 0,$$

where

$$\zeta_i = \tilde{z}_i - \bar{z}_i = \begin{bmatrix} \eta_i^x(t) \\ \eta_i^x(t-1) \\ \eta_i^w(t) \end{bmatrix} \quad (i \in \{1, 2\}).$$

This condition holds almost surely, for example, if $\bar{z}_1(t)$, $\zeta_1(t)$, and $\zeta_2(t)$ are independent, bounded vector random processes such that: (i) ζ_1 and ζ_2 are zero mean, (ii) the processes are ergodic in the sense that

$$\mathbf{S}_T[\rho(\bar{z}_1(\cdot), \zeta_1(\cdot), \zeta_2(\cdot))],$$

converges to the mean of $\rho(\bar{z}_1(0), \zeta_1(0), \zeta_2(0))$ almost surely for any continuous function ρ.

3.3.4 System Identification Procedures and Loss Functions

In this chapter a *system identification procedure* will refer to a function mapping elements of

$$\mathcal{D} = \{(w_1, x_1, w_2, x_2) : w_i \in \ell_T(\mathbb{R}^{n_w}),\ x_i \in \ell_T(\mathbb{R}^{n_x}), i \in \{1, 2\},\ T \in \mathbb{N}\}$$

to functions $a : \mathbb{R}^{n_x} \times \mathbb{R}^{n_w} \to \mathbb{R}^{n_x}$ defining state-space models (2.1).

The following definition will be used to characterize classes of approximations of the MSSE J_Q^{SE} (see Definition 2.2 on page 24).

Definition 3.4. *For a given set $\mathbf{A} = \{a\}$ of functions defining state-space models as in* (2.1)*, we say a real-valued function J is a correct upper bound for J_Q^{SE} on $\mathbf{A}$ if it satisfies*

$$J(a, \tilde{w}, \tilde{x}) \geq J_Q^{\mathrm{SE}}(a, \tilde{w}, \tilde{x})$$

for all $a \in \mathbf{A}$, positive integers T, and $(\tilde{x}, \tilde{w}) \in \ell_T(\mathbb{R}^{n_x}) \times \ell_T(\mathbb{R}^{n_w})$ and

$$J(a, \tilde{w}, \tilde{x}) = 0$$

whenever $\tilde{x}(t) = a(\tilde{x}(t-1), \tilde{w}(t))$ for all $t \in \{1, \ldots, T\}$.

3.3.5 Contributions

We provide a sequence of system identification procedures $\{\mathcal{A}_\kappa\}_{\kappa=1}^{\infty}$ and sets $\{\bar{\mathbf{A}}_\kappa\}_{\kappa=1}^{\infty}$, with $\bar{\mathbf{A}}_\kappa \subset \mathcal{A}_\kappa(\mathcal{D})$, which have the following properties:

(a) every $a \in \mathcal{A}_\kappa(\mathcal{D})$ defines a stable state-space model;

(b) $\bar{\mathbf{A}}_\kappa \subset \bar{\mathbf{A}}_{\kappa+1}$ for each $\kappa \geq 1$ and $\bar{\mathbf{A}} = \bigcup_{\kappa=1}^{\infty} \bar{\mathbf{A}}_\kappa$ is sufficiently broad in that every linear function a such that (2.1) is stable belongs to $\bar{\mathbf{A}}$, as well as some non-linear functions.

Furthermore, fixing κ and taking

$$a_T := \mathcal{A}_\kappa(\tilde{w}_1^{(T)}, \tilde{x}_1^{(T)}, \tilde{w}_2^{(T)}, \tilde{x}_2^{(T)}) \quad \forall\, T \in \mathbb{N}$$

we show that:

(c) when conditions (A1), (A2), and (A3) hold and there exists a $a^\star \in \bar{\mathbf{A}}_\kappa$ such that

$$\bar{x}_1 = G_{a^\star}(\bar{x}_1(0), \bar{w}_1)$$

then

$$\lim_{T \to \infty} a_T(x, w) = a^\star(x, w)$$

for each $(x, w) \in \Omega$ (as defined in Definition 3.3).

We also provide a function J_κ that is an upper bound for J_Q^{SE} on $\mathcal{A}_\kappa(\mathcal{D})$ and show that:

(d) J_κ is a correct upper bound for J_Q^{SE} on $\bar{\mathbf{A}}_\kappa$;

(e) when conditions (A1), (A2) and (A3) hold,

$$\liminf_{T\to\infty} J_\kappa(a, \bar{w}_1^{(T)}, \bar{x}_1^{(T)}) - J_\kappa(a_T, \bar{w}_1^{(T)}, \bar{x}_1^{(T)}) \geq 0$$

for each $a \in \mathcal{A}_\kappa(\mathcal{D})$.

Furthermore, computing the estimates a_T is computationally tractable. It consists of a calculation whose complexity grows linearly with T, followed by solution of a semidefinite program (SDP) whose size is independent of T and κ.

Property (c) is a statement about consistency of the generated estimates, whereas property (e) can be interpreted as saying that the above algorithms generate estimates which asymptotically optimize the upper bound J_κ as if one had access to the unobserved noiseless process.

3.4 Regression Algorithm

This section presents a regression algorithm based on the stability constraints and upper bounds for simulation error presented in the previous chapter. As mentioned, a similar strategy for fitting nonlinear dynamical models is pursued in [88], [13], and [132]. By construction, the upper bound presented here depends on data sets only through empirical moments. This provides two advantages compared to these related works. First, the complexity of solving the regression problem scales linearly with the amount of available data. Second, this property of the upper bound enables the bias removal schemes used in later sections of this paper to mitigate the effects of measurement noise.

3.4.1 Convex Model Parameterization and Loss Function

In this section we describe a convex parameterization of stable state-space models of the form (2.7), where e and f are affinely parameterized vector polynomial functions. Additionally, an upper bound on the MSSE is provided that is convex in the model parameters. These constructions combine Lemmas 2.10 and 2.16 with the semidefinite representation of sum-of-squares (SOS) polynomials, [101]. A polynomial (with real coefficients) is said to be SOS if it is equal to a sum of squares of other polynomials (such polynomials are obviously non-negative for real-valued arguments). For an affinely parameterized family of polynomials, the

set of coefficients that correspond to SOS polynomials can be represented via a linear matrix inequality (LMI).

For notational simplicity, we make use separable implicit state-space models, i.e. models of the form

$$e(x(t)) = f(x(t-1), w(t)), \tag{3.3}$$

where $e : \mathbb{R}^{n_x} \to \mathbb{R}^{n_x}$ is required to be a continuous bijection. For any fixed function pair (e, f), this is equivalent to (2.1) taking $a \equiv e^{-1} \circ f$.

Notation For Dissipation Inequalities

The following two definitions will help simplify the presentation of the regression technique. For any $\delta > 0$, pair of functions (e, f) as in (3.3), and function $V : \mathbb{R}^{n_x} \times \mathbb{R}^{n_x} \to \mathbb{R}$, let

$$\begin{aligned} &p_{(\delta,e,f,V)}(x_1, x_1^+, x_2, x_2^+, w) \\ &\quad = V(x_1, x_2) - V(x_1^+, x_2^+) - \delta|x_1 - x_2|^2 \\ &\qquad +2(x_1^+ - x_1^+)'(e(x_1^+) - f(x_1, w)) \\ &\qquad -2(x_1^+ - x_2^+)'(e(x_2^+) - f(x_2, w)). \end{aligned}$$

Note that $p_{(\delta,e,f,V)}$ is an affine function of e, f, and V. This definition should be compared to Lemma 2.10. Non-negativity of p will be used to guarantee model stability and well-posedness.

For any triple (e, f, V) as above and any function $r : \mathbb{R}^{n_z} \to \mathbb{R}$ define

$$\begin{aligned} q_{(e,f,V,r)}(x, x^+, \xi, \xi^+, w) = r([\xi^+; \xi; w]) - |x - \xi|_Q^2 \\ + V(x, \xi) - V(x^+, \xi^+) \\ + 2(x^+ - \xi^+)'(e(x^+) - f(x, w)). \end{aligned}$$

Note that $q_{(e,f,V,r)}$ is an affine function of e, f, V, and r. This definition should be compared to Lemma 2.16. In particular, global non-negativity of q will imply that

$$r([\xi^+; \xi; w]) \geq \mathcal{E}_Q(h, V, \xi^+, \xi, w) \quad \forall\, \xi, \xi^+ \in \mathbb{R}^{n_x}, w \in \mathbb{R}^{n_w},$$

with $h(v, x, w) = e(v) - f(x, w)$.

Model Class Definition

Let $\Psi = \{\psi_i\}_{i=0}^{n_\psi}$ and $\Phi = \{\phi_i\}_{i=0}^{n_\phi}$ be two sequences of vector polynomial functions $\psi_i : \mathbb{R}^{n_x} \to \mathbb{R}^{n_x}$, $\phi_i : \mathbb{R}^{n_x} \times \mathbb{R}^{n_w} \to \mathbb{R}^{n_x}$, and take $n_\theta = n_\psi + n_\phi$. For each $\theta \in \mathbb{R}^{n_\theta}$,

define

$$e_\theta(x) = \psi_0(x) + \sum_{i=1}^{n_\psi} \theta_i \psi_i(x), \tag{3.4}$$

$$f_\theta(x,w) = \phi_0(x,w) + \sum_{i=1}^{n_\phi} \theta_{(i+n_\psi)} \phi_i(x,w). \tag{3.5}$$

Additionally, for every $\omega \in \mathbb{R}^{n_\psi}$, define $V_\omega : \mathbb{R}^{n_x} \times \mathbb{R}^{n_x} \to \mathbb{R}$ via

$$V_\omega(x_1,x_2) = (x_1 - x_2)' \sum_{i=1}^{n_\psi} \omega_i \left(\psi_i(x_1) - \psi_i(x_2)\right).$$

Optimization Problem

Let $\lambda : \mathbb{R}^{n_z} \to \mathbb{R}^{n_\lambda}$ be any vector polynomial function whose components:

$$\{\lambda_k([x^+; x; w])\}_{k=1}^{n_\lambda}$$

form a maximal linearly independent subset of the polynomials

$$\{[e_\theta(x^+) - f_\theta(x,w)]_{j1} \mid \theta \in \mathbb{R}^{n_\theta}, j \in \{1,\dots,n_x\}\}.$$

Fix $\delta > 0$ and $\kappa \in (0,\infty]$, and consider the optimization problem:

$$\begin{aligned}
\underset{\theta,\omega,R}{\text{minimize}} \quad & \operatorname{tr}(RM) && (3.6)\\
\text{subj. to} \quad & R = R' \geq 0, \quad \|R\|_F \leq \kappa, && (3.7)\\
& p_{(\delta,e_\theta,f_\theta,V_\omega)} \text{ is SOS}, && (3.8)\\
& q_{(e_\theta,f_\theta,V_\omega,|\lambda(\cdot)|_R^2)} \text{ is SOS}, && (3.9)
\end{aligned}$$

where the decision variables are $\theta \in \mathbb{R}^{n_\theta}, \omega \in \mathbb{R}^{n_\psi}$ and $R \in \mathbb{R}^{n_\lambda \times n_\lambda}$, and the symmetric positive definite matrix $M \in \mathbb{R}^{n_\lambda \times n_\lambda}$ is problem data. The small, positive constant δ will be considered fixed for the remainder of the paper. Define $F_\kappa \subset \mathbb{R}^{n_\theta} \times \mathbb{R}^{n_\psi} \times \mathbb{R}^{n_\lambda \times n_\lambda}$ to be

$$F_\kappa = \{(\theta,\omega,R) \ : \ (3.7), (3.8), \text{and } (3.9) \text{ hold.}\},$$

i.e. the feasible set of the above optimization problem. Lemma 2.10 immediately implies the following.

Claim 3.5. *For each $(\theta,\omega,R) \in F_\kappa$, e_θ is a bijection and the system (2.1) with $a = e_\theta^{-1} \circ f_\theta$ is stable.*

The next several definitions relate the optimization problem above to the explicit state-space models, (2.1), which can be obtained as model estimates. Define $\mathbf{A}_\kappa$ via

$$\mathbf{A}_\kappa = \{e_\theta^{-1} \circ f_\theta \ : \ (\theta, \omega, R) \in F_\kappa\}$$

and define $\hat{J}_\kappa : \mathbf{A}_\kappa \times \mathbb{R}^{n_\lambda \times n_\lambda} \to \mathbb{R}$ by

$$\hat{J}_\kappa(a, M) := \inf\{\mathrm{tr}(RM) \ : \exists \ (\theta, \omega, R) \in F_\kappa \text{ s.t. } a = e_\theta^{-1} \circ f_\theta\}.$$

Finally, for each $a \in \mathbf{A}_\kappa$, $T \in \mathbb{N}$, and $(\tilde{w}, \tilde{x}) \in \ell_T(\mathbb{R}^{n_w}) \times \ell_T(\mathbb{R}^{n_x})$ let

$$J_\kappa(a, \tilde{w}, \tilde{x}) = \hat{J}_\kappa(a, M)$$

where

$$M = \frac{1}{T} \sum_{t=1}^{T} \lambda(\tilde{z}(t)) \lambda(\tilde{z}(t))' \tag{3.10}$$

with $\tilde{z}(t) = [\tilde{x}(t); \tilde{x}(t-1); \tilde{w}(t)]$.

Claim 3.6. *$J_\kappa \geq J_Q^{\mathrm{SE}}$ on $\mathbf{A}_\kappa$.*

This follows from Lemmas 2.10 and 2.16, and the observation that, for all symmetric matrices $R \in \mathbb{R}^{n_\lambda \times n_\lambda}$,

$$\mathrm{tr}(RM) \equiv \frac{1}{T} \sum_{t=1}^{T} r([\tilde{x}(t); \tilde{x}(t-1); \tilde{w}(t)])$$

where $r(\cdot) \equiv |\lambda(\cdot)|_R^2$.

The role of κ is explained by the following simple proposition.

Proposition 3.7. *For any $\kappa \in (0, \infty)$, and $a \in \mathbf{A}_\kappa$, the function $\hat{J}_\kappa(a, \cdot)$ is Lipschitz with constant κ.*

Proof. For any symmetric matrices $R, N, M \in \mathbb{R}^{n_\lambda \times n_\lambda}$ one has

$$|\mathrm{tr}(RM) - \mathrm{tr}(RN)| \leq \|R\|_F \|N - M\|_F$$

by Cauchy-Schwarz. Each $\hat{J}_\kappa(a, \cdot)$ thus has a Lipschitz constant of κ as it is the infimum of a family of functions with Lipschitz constant κ. □

Remark 3.4.1. For fixed bases, Φ and Ψ, computation of the matrix M in (3.10) requires time time linear in T. Minimization of $\hat{J}_\kappa(\cdot, M)$ can then be accomplished by solving an SDP whose size is independent of κ.

3.4.2 Correctness

The following definition is used to characterize the set of models for which the upper bound J_κ is correct (see Definition 3.4 on page 54).

Definition 3.8. *For $\kappa \in (0, \infty]$ define $\bar{\mathbf{A}}_\kappa$ to be those functions $a : \mathbb{R}^{n_x} \times \mathbb{R}^{n_w} \to \mathbb{R}^{n_x}$ for which there exists a tuple $(\theta, \omega, R) \in F_\kappa$ satisfying $a = e_\theta^{-1} \circ f_\theta$ and*

$$|\lambda([a(x,w);x;w])|_R^2 = 0 \qquad \forall\, (x,w) \in \mathbb{R}^{n_x} \times \mathbb{R}^{n_w}. \tag{3.11}$$

The functions $a \in \bar{\mathbf{A}}_\kappa$ are those for which $J(a, \tilde{w}, \tilde{x}) = 0$ whenever the data signals $\tilde{w} \in \ell_T(\mathbb{R}^{n_w})$ and $\tilde{x} \in \ell_T(\mathbb{R}^{n_w})$ satisfy

$$\tilde{x}(t) = a(\tilde{x}(t-1), \tilde{w}(t)), \quad \forall t \in \{1, 2, \ldots, T\}.$$

Claim 3.9. *For $0 < \kappa \leq \hat{\kappa} \leq \infty$ one has $\bar{\mathbf{A}}_\kappa \subset \bar{\mathbf{A}}_{\hat{\kappa}}$, and J_κ is a correct upper bound for each $a \in \bar{\mathbf{A}}_\kappa$.*

The next lemma partially describes the behavior of the upper bound J_κ and the sets $\bar{\mathbf{A}}_\kappa$ when the bases Φ and Ψ each span all linear functions.

Lemma 3.10. *Let $A \in \mathbb{R}^{n_x \times n_x}$ and $B \in \mathbb{R}^{n_x \times n_w}$ be matrices such that the spectral radius of A is less than one. Additionally, assume that Ψ and Φ span all linear functions and let $\kappa \in (0, \infty)$, $\Gamma = \Gamma' \in \mathbb{R}^{n_x \times n_x}$ be such that*

$$\kappa \geq \| \begin{bmatrix} I & -A & -B \end{bmatrix}' \Gamma \begin{bmatrix} I & -A & -B \end{bmatrix} \|_F$$

and

$$|\epsilon|_\Gamma \geq |(zI - A)^{-1}\epsilon|_{\delta I + Q} \qquad \forall\, \epsilon \in \mathbb{C}^{n_x}, z \in \mathbb{T}. \tag{3.12}$$

Then the function $a(x,w) = Ax + Bw$ belongs to $\bar{\mathbf{A}}_\kappa$ and

$$J_\kappa(a, \tilde{w}, \tilde{x}) \leq \frac{1}{T} \sum_{t=1}^{T} |\tilde{x}(t) - A\tilde{x}(t-1) - B\tilde{w}(t)|_\Gamma^2.$$

for all positive integers T and $(\tilde{w}, \tilde{x}) \in \ell_T(\mathbb{R}^{n_w}) \times \ell_T(\mathbb{R}^{n_x})$.

The proof of this lemma is in the Section 3.7. The following corollary is immediate.

Corollary 3.11. *For every pair of matrices $(A, B) \in \mathbb{R}^{n_x \times n_x} \times \mathbb{R}^{n_x \times n_w}$ such that A has spectral radius less than one, there exists a $\kappa \in (0, \infty)$ such that such that the function $a(x,w) = Ax + Bw$ belongs to $\bar{\mathbf{A}}_{\hat{\kappa}}$ for all $\hat{\kappa} \geq \kappa$.*

3.5 Identification Algorithm

In this section, we propose a system identification algorithm based on the regression technique described in Section 3.4 and a method for estimating empirical moments derived from the work of Hausman et al. [50]. We consider the choice of bases Φ,Ψ, the function $\lambda : \mathbb{R}^{n_z} \to \mathbb{R}^{n_\lambda}$, and the constant $\kappa \in (0, \infty]$ to be fixed.

3.5.1 Empirical Moment Approximation

For each positive integer T define the function $\tilde{\mu}_T : \mathbb{Z}_+^{n_z} \times \mathbb{Z}_+^{n_z} \to \mathbb{R}$ via

$$\tilde{\mu}_T(\beta, \iota) := \mathbf{S}_T\left[\tilde{z}_1^\beta \tilde{z}_2^\iota\right]$$

and for $k \in \{1, \ldots, n_z\}$ let ι_k be the k-th column of the identity matrix, I_{n_z}. For each $\alpha \in \mathbb{Z}_+^{n_z}$ let

$$\mathcal{B}_\alpha = \{\beta \in \mathbb{Z}_+^{n_z} \ : \ \beta \leq \alpha\} \times \{0, \iota_1, \ldots, \iota_{n_z}\} \subset \mathbb{Z}_+^{n_z} \times \mathbb{Z}_+^{n_z}.$$

and let $\tilde{\mu}_T|_{\mathcal{B}_\alpha}$ denote the restriction of $\tilde{\mu}_T$ to $\mathcal{B}_\alpha$.

Lemma 3.12. *For every $\alpha \in \mathbb{Z}_+^{n_z}$ there exists a continuous real-valued function $m_\alpha : \mathcal{B}_\alpha \to \mathbb{R}$ such that*

$$\lim_{T\to\infty} \mathbf{S}_T\left[\tilde{z}_1^\alpha\right] - m_\alpha(\tilde{\mu}_T|_{\mathcal{B}_\alpha}) = 0$$

whenever conditions (A1), (A2), and (A3) hold.

The proof of this lemma, and an explicit construction of the functions m_α is given in Section 3.7.

3.5.2 Proposed Algorithm

(i) Let $\mathcal{B}$ be the minimal subset of $\mathbb{Z}_+^{n_z}$ such that for each $k \in \{1, \ldots, n_\lambda\}$ there exist real coefficients $\{\Lambda_{k\alpha}\}_{\alpha\in\mathcal{B}}$ satisfying $\lambda_k(z) = \sum_{\alpha\in\mathcal{B}} \Lambda_{k\alpha} z^\alpha$. Compute

$$\tilde{\mu}_T(\gamma, \iota) = \mathbf{S}_T\left[\tilde{z}_1^\gamma \tilde{z}_2^\iota\right]$$

for all $(\gamma, \iota) \in \{\gamma \in \mathbb{Z}_+^{n_z} \ : \ \gamma \leq \alpha + \beta, \ \alpha, \beta \in \mathcal{B}\} \times \{0, \iota_1, \ldots, \iota_{n_z}\}$.

(ii) Compute an approximate moment matrix $\tilde{M}_T \in \mathbb{R}^{n_\lambda \times n_\lambda}$ with coefficients

$$[\tilde{M}_T]_{jk} = \sum_{\alpha\in\mathcal{B}} \sum_{\beta\in\mathcal{B}} \Lambda_{j\alpha}\Lambda_{k\beta} m_{\alpha+\beta}(\tilde{\mu}_T|_{\mathcal{B}_{\alpha+\beta}}),$$

where each $m_{\alpha+\beta}(\cdot)$ is defined as in Lemma 3.12.

(iii) Let $\hat{M}_T$ be the projection of $\tilde{M}_T$ onto the closed convex cone of symmetric positive semidefinite matrices.

(iv) Take $a_T = e_\theta^{-1} \circ f_\theta$ where (θ, ω, R) is an optimal solution of (3.6) with $M = \hat{M}_T$. Note that is equivalent to taking $a_T \in \operatorname{argmin}_{a \in \mathbf{A}_\kappa} \{\hat{J}_\kappa(a, \hat{M}_T)\}$.

The remainder of this section analyses this algorithm.

3.5.3 Asymptotic Optimality of Estimates

The following lemma provides a general statement about the effectiveness of the proposed bias elimination scheme.

Lemma 3.13. *Assume that $\kappa \in (0, \infty)$, and conditions (A1), (A2), and (A3) hold. Let a_T be a sequence of estimates generated by applying the algorithm defined above. Then, for all $a \in \mathbf{A}_\kappa$,*

$$\liminf_{T \to \infty} J_\kappa(a, \bar{w}_1^{(T)}, \bar{x}_1^{(T)}) - J_\kappa(a_T, \bar{w}_1^{(T)}, \bar{x}_1^{(T)}) \geq 0.$$

That is to say, as T grows, the estimates a_T generated by the above algorithm are nearly optimal for minimizing the upper bound on simulation error that is described by Proposition 3.6 evaluated on the unmeasurable noiseless data. The proof of this lemma is in the Section 3.7.

3.5.4 Consistency Analysis

The following theorem provides a consistency result for the estimates provided by the above algorithm.

Theorem 3.14. *Assume that $\kappa \in (0, \infty)$, conditions (A1), (A2), and (A3) hold, and that there exists a function $a^\star \in \bar{\mathbf{A}}_\kappa$ such that*

$$\bar{x}_1 = G_{a^\star}(\bar{x}_1(0), \bar{w}_1).$$

Then for every $(x, w) \in \Omega$ (defined in Definition 3.3 on page 53)

$$\lim_{T \to \infty} a_T(x, w) = a^\star(x, w).$$

The proof of this result is contained in Section 3.7..

The additional assumption for applying this theorem is that there exist a function $a^\star$ such that the underlying noiseless process should exactly satisfies $\bar{x}_1(t) = a(\bar{x}_1(t-1), \bar{w}_1(t))$ for every $t \in \{1, 2, \ldots\}$. When this condition is satisfied, the estimates a_T converge point-wise to $a^\star$ on the set Ω.

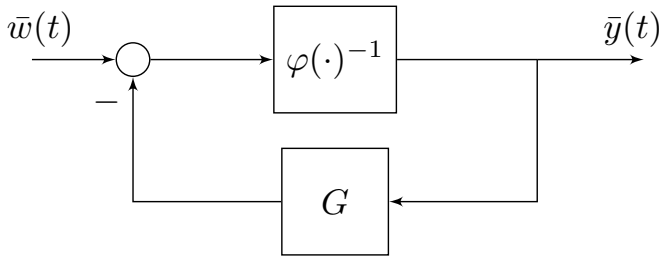

Figure 3.5. Schematic of the noiseless dynamics for the simulated example.

3.6 Simulated Example

This section compares the proposed method to two natural alternatives, one based on least squares and the other based on minimization of simulation error. Simulations were conducted on a computer with 24 GB of RAM and two six-core Intel Xeon 3.33 GHz CPUs. Computational times are reported in CPU seconds, rather than real-time. Programs were run in MATLAB R2012b, and semidefinite programs were solved using the commercial solver MOSEK 7.0.0.70. SOS programs were prepared using a custom software toolbox.

3.6.1 Data Set Generation

Consider the nonlinear dynamical system defined by the feedback interconnection pictured in Figure 3.5. Here φ is a monotone nonlinearity in feedback with a single-input single-output, finite impulse response LTI system, G, leading to the overall dynamics

$$\varphi(\bar{y}(t)) = \bar{w}(t) - \sum_{k=0}^{\infty} g(k)\bar{y}(t-k). \tag{3.13}$$

In our example, $\varphi(y) = \frac{3}{2}y + \frac{3}{2}y^2 + y^3$ and $g(\cdot)$ is defined by

$$g(0) = \frac{5}{4}, \quad g(1) = -\frac{4}{5}, \quad g(8) = g(15) = -\frac{1}{10},$$

and $g(t) = 0$ otherwise. This defines a 15 state nonlinear system. Strict passivity of this LTI system and the strict monotonicity of φ^{-1} ensure this system is incrementally stable.

Two input sequences were computed, $\bar{w}_{\text{train}} : \{1, \ldots, 50000\} \to [-1, 1]$ and $\bar{w}_{\text{test}} : \{1, \ldots, 50000\} \to [-1, 1]$, to be realizations of i.i.d random variables, uniformly distributed on $[-1, 1]$. Next, $\bar{y}_{\text{test}}(t) = \bar{y}(t)$ was taken to be the solution of (3.13) with $\bar{w}(t) \equiv \bar{w}_{\text{test}}(t)$ and zero initial conditions. To examine the statistical

performance of the compared methods, we produced 100 Monte Carlo simulations using the following specification.

For $i \in \{1, 2\}$, the solution $\bar{y}_i(t) = \bar{y}(t)$ of (3.13) was computed with $\bar{w}(t) \equiv \bar{w}_{\text{train}}(t)$ and random initial conditions $[\bar{y}(-1); \ldots; \bar{y}(-15)]$ chosen according to a zero mean normal distribution with covariance $\sigma^2_{\text{noise}} I$ (here $\sigma_{\text{noise}} = 0.05$). Next, we defined $\tilde{y}_i(t) = \bar{y}_i(t) + v_i(t)$, where $v_i(\cdot)$ were realizations of i.i.d. zero mean normal random variables with variance σ^2_{noise}, and $\tilde{w}_i(t) = \bar{w}_{\text{train}}(t)$. Finally, we took $\tilde{x}_i(t) = \big[\tilde{y}_i(t); \tilde{y}_i(t-1); \ldots; \tilde{y}_i(t-n_x+1)\big]$, where the choice of n_x is explained below.

3.6.2 Model Structure

We examined a family of related model classes designed to cover both the misspecified and correctly specified modeling scenarios, and to explore how well the proposed method scales. For each fixed model order n_x, the identified models were of the form

$$\bar{e}_\theta(y(t)) = \bar{f}_\theta([y(t-1); \ldots; y(t-n_x)], w(t)). \tag{3.14}$$

We took $\bar{e}_\theta$ to be an arbitrary cubic polynomial with root at zero, i.e.

$$\bar{e}_\theta(y) = \sum_{k=1}^{3} \theta_k y^k.$$

The function $\bar{f}_\theta$ was parameterized as an arbitrary affine function (this yields $n_\theta = 5 + n_x$).

When applying alternatives to the proposed method, additional constraints were imposed to ensure that the above equations are well-posed (i.e. that $\bar{e}_\theta$ is invertible). We required $\frac{\partial \bar{e}_\theta}{\partial y}$ to be positive so that $\bar{e}_\theta$ is strictly monotone. Note that the constraint that $\frac{\partial \bar{e}_\theta}{\partial y} \geq c$ can be represented by the LMI

$$W_c(\theta) := \begin{bmatrix} \theta_1 - c & \theta_2 \\ \theta_2 & 3\theta_3 \end{bmatrix} \geq 0,$$

via a straightforward application of the SOS representation of non-negative univariate polynomials. The equation (3.14) can then be solved via by bisection accelerated by Newton's method.

3.6.3 Alternative Methods Compared

Proposed Method

When identifying models using the proposed method, we took $\kappa = \infty$ and $\delta = 1 \times 10^{-3}$. The weight matrix Q used in the definition of MSSE is taken to have

$[Q]_{11} = 1$ an $[Q]_{ij} = 0$ otherwise.

Least Squares Method

The *least squares* methods will refer to minimization of

$$\sum_{i=1}^{2}\sum_{t=0}^{T-1} |\bar{e}_\theta(\tilde{y}_i(t+n_x)) - \bar{f}_\theta([\tilde{y}_i(t+n_x-1);\ldots;\tilde{y}_i(t)], \tilde{w}_i(t+n_x))|^2$$

subject to $W_{1/2}(\theta) \geq 0$. This constrained least squares problem can be posed as an SDP.

Simulation Error Minimization

Minimization of the simulation error J_Q^{SE} is attempted using MATLAB's `fmincon` function, in particular its interior point algorithm. The model parameterization is normalized by fixing $\theta_1 = 1$. The condition that $W_{1/2}(\theta) \geq 0$ is represented by a constraint function taking the value ∞ when $W_{1/2}(\theta)$ is indefinite and $-\det(W_{1/2}(\theta))$ otherwise. Cost function and cost gradient evaluations were implemented in C to provide a more relevant comparison of execution times. Zero initial conditions were used for each simulation.

We make use of two initial parameter choices:

(i) $\theta_1 = \theta_3 = 1$ and $\theta_2 = 0$ otherwise.

(ii) The model derived from the least squares method, appropriately normalized.

The first choice corresponds to a system that lies in the interior of the feasible set (i.e. $W_{1/2}(\theta) > 0$) and has zero output response, whereas the second choice is a commonly adopted heuristic for multi-stage optimization of models [75].

3.6.4 Results

For each method and model order $n_x \in \{1, 8, 15, 22\}$ a model was fit based on the first 500, 5000 and 50000 data points of the given experiments. The quality of the models was judged by the *validation error*, i.e. the simulation error on a held-out data set, computed as

$$\cdot \frac{\sqrt{\frac{1}{50{,}000}\sum_{t=1}^{50{,}000} |\bar{y}_{\mathrm{test}}(t) - \hat{y}(t)|^2}}{\sqrt{\frac{1}{50{,}000}\sum_{t=1}^{50{,}000} |\bar{y}_{\mathrm{test}}(t) - \bar{\mu}_{\mathrm{test}}|^2}},$$

where $\bar{\mu}_{\mathrm{test}} := \frac{1}{50{,}000}\sum_{t=1}^{50{,}000} \bar{y}_{\mathrm{test}}(t)$, and $\hat{y}$ corresponds to the model simulation given zero initial conditions and input $\bar{w}_{\mathrm{test}}$.

Table 3.1. Mean % Validation Error (Standard Deviation) for $T = 5 \times 10^4$

	Model Order (n_x)			
Method	1	8	15	22
Proposed	6.9 (0.3)	5.0 (0.5)	1.3 (0.94)	1.4 (1.1)
SEM	10.9 (0.02)	10.1 (0.01)	9.0 (0.01)	9.1 (0.1)
LS	51.8 (0.02)	51.8 (0.02)	51.9 (0.02)	52.2 (0.1)
SEM (LS Init.)	13.3 (0.01)	12.5 (0.01)	11.7 (0.01)	11.6 (0.08)

Figure 3.6 contains a plot of the run time and validation error for all methods and 100 trials when $T = 50,000$ and $n_x = 8$. Note that the scales are $\log - \log$. One sees that the least squares approach produces a model with very large validation error ($\sim 52\%$), which is anticipated due to the presence of output noise. Two sets of errors are reported for simulation error minimization: the first corresponds to minimization initialized from a zero model and achieves an error of approximately 10% but generally takes about 8 seconds to compute. The second set of models are initialized with the least squares fit and terminate very quickly at a local minimum (the validation error is approximately 12.5%). The proposed method generates models with $\sim 5\%$ validation error, generally in under a second. Table 3.1 presents a similar comparison of the mean validation errors for each method and model order when $T = 50,000$.

Table 3.2 presents the performance of the proposed method in terms of both convergence of the validation error and computation time. For reference, a single fit is computed given access to a noiseless data set ($\sigma_{\text{noise}} = 0$) of duration $T = 50,000$. For each model order one sees the gradual convergence of the validation error toward the performance achieved based on fits to noiseless data. The time in CPU seconds required to compute these examples is reported in Table 3.2(b), and demonstrates the scalability of the algorithm as T grows.

3.7 Proofs

3.7.1 Proof of Lemma 3.10

As A has spectral radius less than one and (A, I) is trivially controllable, the inequality (3.12) implies the existence of a positive semidefinite matrix $P = P' \in \mathbb{R}^{n_x \times n_x}$ such that

$$|\epsilon|_\Gamma^2 + |\Delta|_P^2 \geq |A\Delta + \epsilon|_P^2 + |\Delta|_{Q+\delta I}^2 \quad \forall \Delta, \epsilon \in \mathbb{C}^{n_x} \tag{3.15}$$

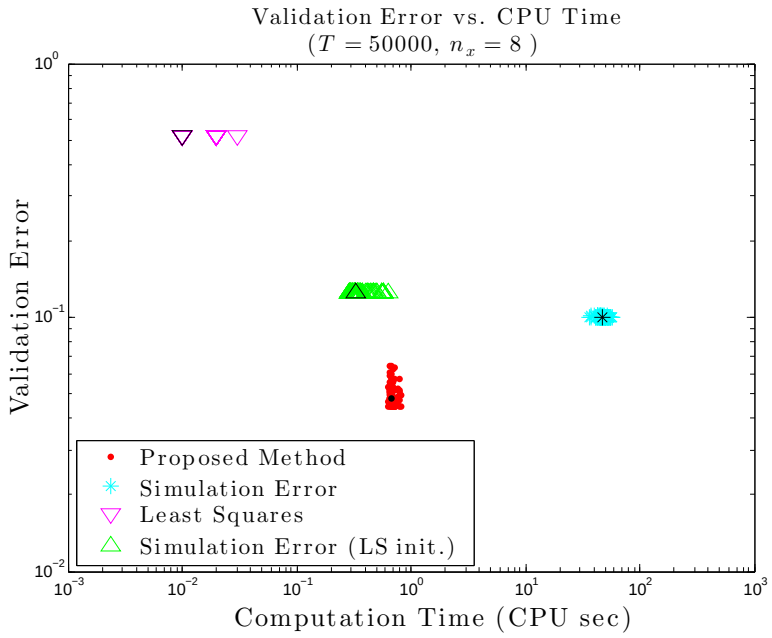

Figure 3.6. Comparison of the proposed method to the alternative methods. Points indicate the simulation error on a validation data set and computation time on log scales. Black markers indicate medians of the distributions. The true system does not belong to the model class.

Table 3.2. Performance of the Proposed Method for Varying Model Order and Experiment Length

(a) Mean % Validation Error (Standard Deviation)

		Model Order (n_x)			
T	σ_{noise}	1	8	15	22
5×10^2	0.05	9.1 (3)	8.0 (3)	6.7 (2)	7.7 (2.5)
5×10^3	0.05	7.3 (1)	5.9 (1)	3.0 (2)	3.5 (1.9)
5×10^4	0.05	6.9 (0.3)	5.0 (0.5)	1.3 (1)	1.4 (1.1)
5×10^4	**0.0**	**6.7**	**4.5**	**0.0**	**0.0**

(b) Mean CPU Time in seconds (Standard Deviation)

	Model Order (n_x)			
T	1	8	15	22
5×10^2	0.05 (0.009)	0.23 (0.03)	2.4 (0.3)	11.8 (1.7)
5×10^3	0.05 (0.008)	0.25 (0.02)	2.5 (0.3)	11.9 (1.7)
5×10^4	0.08 (0.009)	0.69 (0.04)	4.0 (0.3)	15.0 (0.6)

by the the Kalman-Yakubovich-Popov Lemma (see, for example, [108] Theorem 2). Let

$$e(x) = Px,\ f(x,w) = PAx + PBw, V(x_1,x_2) = |x_1 - x_2|_P^2,$$

$$r([\xi_+;\xi;w]) = |\xi_+ - A\xi - Bw|_\Gamma^2,$$

so that $a \equiv e^{-1} \circ f$. Then

$$\begin{aligned} p_{(\delta,e,f,V)}(x_1,x_1^+,x_2,x_2^+,w) =& |\Delta|_P^2 - \delta|\Delta|^2 + |\Delta^+|_P^2 - 2(P\Delta^+)'(A\Delta) \\ \geq& |\Delta|_P^2 - |A\Delta|_P^2 - \delta|\Delta|^2 \geq 0, \end{aligned}$$

where $\Delta = x_1 - x_2$, $\Delta^+ = x_1^+ - x_2^+$, and the first inequality follows from explicit minimization w.r.t. Δ^+. Similarly,

$$\begin{aligned} q_{(e,f,V,r)}(x,x^+,\xi,\xi^+,w) &= |\epsilon|_\Gamma^2 + |\Delta|_P^2 - |\Delta|_Q^2 + |\Delta^+|_P^2 - 2(P\Delta_+)'(A\Delta+\epsilon) \\ &\geq |\epsilon|_\Gamma^2 + |\Delta|_P^2 - |A\Delta+\epsilon|_P^2 - |\Delta|_Q^2 \geq 0, \end{aligned}$$

where $\Delta := x - \xi$, $\Delta^+ = x^+ - \xi^+$ and $\epsilon = \xi^+ - A\xi - Bw$.

As Ψ and Φ span all linear functions, there exist choices of θ, and ω, such that $e = e_\theta, f = f_\theta$, and $V_\omega = V$. Additionally, taking $\lambda([\xi_+;\xi;w]) = [\xi_+;\xi;w]$, and

$$R = \begin{bmatrix} I & -A & -B \end{bmatrix}' \Gamma \begin{bmatrix} I & -A & -B \end{bmatrix}$$

one has $R = R' \geq 0$, $\|R\|_F \leq \kappa$ and $r(\cdot) \equiv |\lambda(\cdot)|_R^2$. As every non-negative quadratic polynomial is also a SOS, (θ,ω,R) belongs to F_κ, and it follows that $a \in \bar{\mathbf{A}}_\kappa$. □

■ 3.7.2 Proof of Lemma 3.12

The following additional notation will aid in the discussion of multi-variable polynomials. For $\alpha, \beta \in \mathbb{Z}_+^{n_z}$ with $\beta \leq \alpha$, let

$$\binom{\alpha}{\beta} = \prod_{k=1}^{n} \binom{\alpha_k}{\beta_k}.$$

With this notation, for any $u, v \in \mathbb{R}^n$ and $\alpha \in \mathbb{Z}_+^n$, one has

$$(u+v)^\alpha = \sum_{\beta \leq \alpha} \binom{\alpha}{\beta} u^\beta v^{\alpha-\beta}.$$

For any of functions $\mu : \mathbb{Z}_+^{n_z} \to \mathbb{R}$ and $\nu : \mathbb{Z}_+^{n_z} \to \mathbb{R}$ satisfying

$$\mu(0) = \nu(0) = 1, \tag{3.16}$$

let $\bar{\mu}_{(\mu,\nu)} : \mathbb{Z}_+^{n_z} \times \mathbb{Z}_+^{n_z} \to \mathbb{R}$ be defined by

$$\bar{\mu}(\alpha, \iota) = \bar{\mu}_{(\mu,\nu)}(\alpha, \iota) := \sum_{\beta \leq \alpha} \binom{\alpha}{\beta} \mu(\alpha - \beta + \iota)\nu(\beta). \tag{3.17}$$

Clearly, (3.16) and (3.17) provides a recursive system on nonlinear equations allowing one to calculate $\mu(\alpha)$ and $\nu(\alpha)$ from the values of $\bar{\mu}(\beta, \iota)$ and $\nu(\iota)$ for $(\beta, \iota) \in \mathcal{B}_\alpha$. Specifically, when $\alpha_k > 0$ equation (3.17) provides an explicit equation for $\mu(\alpha)$ as a function of $\bar{\mu}(\alpha - \iota_k, \iota_k)$, and the values of $\mu(\beta)$ and $\nu(\beta)$ for $\beta < \alpha$. Next, one can solve for $\nu(\alpha)$ as a function of $\mu(\alpha)$, $\bar{\mu}(\alpha, 0)$, and the values $\mu(\beta)$ and $\nu(\beta)$ for $\beta < \alpha$. The above argument describes a (non-unique) real-valued polynomial function $\hat{m}_\alpha$ that satisfies

$$\mu(\alpha) = \hat{m}_\alpha(\bar{\mu}_{(\mu,\nu)}|_{\mathcal{B}_\alpha}, [\nu(\iota_1); \ldots; \nu(\iota_{n_z})])$$

for any pair of functions μ, ν satisfying (3.16). We next demonstrate that, for each $\alpha \in \mathbb{Z}_+^{n_z}$, the function m_α defined by

$$m_\alpha(\cdot) = \hat{m}_\alpha(\cdot, [0; 0; \ldots; 0])$$

has the properties required by the lemma.

For each positive integer T, define $\bar{\mu}_T : \mathbb{Z}_+^{n_z} \times \mathbb{Z}_+^{n_z} \to \mathbb{R}$ to be

$$\bar{\mu}_T(\alpha, \iota) := \sum_{\beta \leq \alpha} \binom{\alpha}{\beta} \mathbf{S}_T\Big[\bar{z}_1^{\alpha-\beta+\iota}\Big] \mathbf{S}_T\Big[\zeta_1^\beta\Big].$$

For every $\alpha \in \mathbb{Z}_+^{n_z}$, the definition of m_α implies that

$$\mathbf{S}_T\Big[\bar{z}_1^\alpha\Big] = \hat{m}_\alpha\Big(\bar{\mu}_T|_{\mathcal{B}_\alpha}, \mathbf{S}_T\Big[\zeta_1\Big]\Big).$$

Assumption (A3) implies that $\lim_{T\to\infty} \mathbf{S}_T\Big[\zeta_1\Big] = 0$. We next show that $\tilde{\mu}_T$ converges to $\bar{\mu}_T$ point-wise. This will complete the proof by a uniform continuity argument based on the boundedness of each sequence $\{\tilde{\mu}_T(\alpha, \iota)\}_{T=1}^\infty$ (assumption (A2)) and the continuity of $\hat{m}_\alpha$.

Take $(\alpha, \iota) \in \mathbb{Z}_+^{n_z} \times \{0, \iota_1, \ldots, \iota_{n_z}\}$. Recall that $\zeta_i(t) := \tilde{z}_i(t) - \bar{z}_i(t)$, and

$$\tilde{z}_1(t)^\alpha = \sum_{\beta \leq \alpha} \binom{\alpha}{\beta} \bar{z}_1(t)^{\alpha-\beta} \zeta_1(t)^\beta.$$

Thus, assumption (A3) immediately implies $\tilde{\mu}_T(\alpha, 0) - \bar{\mu}_T(\alpha, 0)$ converges to zero. For $\iota = \iota_k$, one has

$$\begin{aligned}\tilde{\mu}_T(\alpha, \iota) &= \mathbf{S}_T\left[\tilde{z}_1^{\alpha}\tilde{z}_2^{\iota}\right] \\ &= \sum_{\beta \le \alpha} \binom{\alpha}{\beta} \left(\mathbf{S}_T\left[\bar{z}_1^{\alpha-\beta}\zeta_1^{\beta}\bar{z}_2^{\iota}\right] + \mathbf{S}_T[\bar{z}_1^{\alpha-\beta}\zeta_1^{\beta}\zeta_2^{\iota}]\right).\end{aligned}$$

As $\lim_{T\to\infty} \mathbf{S}_T[\zeta_2] = 0$, assumptions (A2) and (A3) guarantee that $\mathbf{S}_T[\bar{z}_1^{\beta}\zeta_1^{\alpha-\beta}\zeta_2^{\iota}]$ converges to zero for each $\beta \le \alpha$. By assumption, $\bar{z}_1$ and ζ_1 are bounded and $\lim_{t\to\infty} \bar{z}_1(t) - \bar{z}_2(t) = 0$, so condition (A3) implies $\mathbf{S}_T[\bar{z}_1^{\alpha-\beta}\zeta_1^{\beta}(\bar{z}_1^{\iota} - \bar{z}_2^{\iota})]$ converges to zero. This completes the proof. □

■ 3.7.3 Proof of Lemma 3.13

For each positive integer T define $\bar{M}_T \in \mathbb{R}^{n_\lambda \times n_\lambda}$ via

$$\bar{M}_T := \frac{1}{T}\sum_{t=1}^{T} \lambda(\bar{z}_1(t))\lambda(\bar{z}_1(t))',$$

so that $J_\kappa(a, \bar{w}_1^{(T)}, \bar{x}_1^{(T)}) = \hat{J}_\kappa(a, \bar{M}_T)$ for each $a \in \mathbf{A}_\kappa$. As a_T is optimal, for any $a \in \mathbf{A}_\kappa$ one has

$$\hat{J}_\kappa(a, \hat{M}_T) \ge \hat{J}_\kappa(a_T, \hat{M}_T).$$

As noted in Proposition 3.7, $\hat{J}_\kappa$ is a κ-Lipschitz function of its second argument, so that

$$\hat{J}_\kappa(a, \bar{M}_T) - \hat{J}_\kappa(a_T, \bar{M}_T) \ge -2\kappa\|\hat{M}_T - \bar{M}_T\|_F.$$

To complete the proof we show that $\lim_{T\to\infty} \|\hat{M}_T - \bar{M}_T\|_F = 0$.

Let $\Pi : \mathbb{R}^{n_\lambda \times n_\lambda} \to \mathbb{R}^{n_\lambda \times n_\lambda}$ denote projection onto the positive semidefinite cone. Lemma 3.12 implies that $\tilde{M}_T - \bar{M}_T$ converges to zero. As $\bar{z}_1$ and $\tilde{z}_1$ are a bounded signals (assumption (A1) and (A2)), $\tilde{M}_T$ and $\bar{M}_T$ lie in a compact set for sufficiently large T. As Π is a continuous function, it is uniformly continuous on this set. Thus the desired result follows from the face that each $\bar{M}_T$ is positive semidefinite so that $\Pi(\bar{M}_T) = \bar{M}_T$.

■ 3.7.4 Proof of Theorem 3.14

For each positive integer T there exists a tuple $(\theta_T, \omega_T, R_T)$ feasible for (3.6) such that $a_T = e_{\theta_T}^{-1} \circ f_{\theta_T}$ and

$$\hat{J}_\kappa(a_T, \bar{M}_T) = \mathrm{tr}(R_T\bar{M}_T). \tag{3.18}$$

For all positive integers T and $(x, w) \in \mathbb{R}^{n_x} \times \mathbb{R}^{n_w}$, one has

$$0 \leq q_{(e_{\theta_T}, f_{\theta_T}, V_{\omega_T}, |\lambda(\cdot)|^2_{R_T})}(x, a_T(x,w), x, a^\star(x,w), w) \tag{3.19}$$
$$+ p_{(\delta, e_{\theta_T}, f_{\theta_T}, V_{\omega_T})}(a_T(x,w), 0, a^\star(x,w), 0, 0)$$
$$= |\lambda([a^\star(x,w); x; w])|^2_{R_T} - \delta |a_T(x,w) - a^\star(x,w)|^2. \tag{3.20}$$

Thus it is sufficient to show that $|\lambda([a^\star(x,w); x; w])|^2_{R_T}$ converges to zero whenever $(x, w) \in \Omega$.

By definition, $a^\star \in \bar{\mathbf{A}}_\kappa$ implies the existence of a $(\theta^\star, \omega^\star, R^\star)$ feasible for (3.6) such that $a^\star = e^{-1}_{\theta^\star} \circ f_{\theta^\star}$ and $|\lambda([a^\star(x,w); x; w])|^2_{R^\star} \equiv 0$. Since

$$\mathrm{tr}(R^\star \bar{M}_T) = \frac{1}{T} \sum_{t=1}^{T} |\lambda([a^\star(\bar{x}_1(t-1); \bar{w}_1(t)); \bar{x}_1(t-1); \bar{w}_1(t)])|^2_{R^\star},$$

one has $\hat{J}_\kappa(a^\star, \bar{M}_T) = 0$. As each $\hat{J}_\kappa(\cdot, \bar{M}_T)$ is a non-negative function, Lemma 3.13 implies $\hat{J}_\kappa(a_T, \bar{M}_T)$ (and thus $\mathrm{tr}(R_T \bar{M}_T)$) converges to zero.

Fix $(\hat{x}, \hat{w}) \in \Omega$. Then there exists a compact neighborhood K of $(\hat{x}, \hat{w})$ and a positive constant c such that

$$\mathrm{tr}(R_T \bar{M}_T) \geq c \int \int_K |\lambda([a^\star(x,w); x; w]))|^2_{R_T} dx\, dw.$$

Note that the set of functions

$$\{|\lambda(\cdot)|^2_R \ : \ R = R' \in \mathbb{R}^{n_\lambda \times n_\lambda}, \|R\|_F \leq \kappa\}$$

is clearly equicontinuous on any compact set as λ is locally Lipschitz. As $a^\star$ is continuously differentiable, this implies that the sequence of functions $(x, w) \mapsto |\lambda([a^\star(x,w); x; w]))|^2_{R_T}$ is equicontinuous on K. Thus, for each $\epsilon > 0$ there exists an open neighborhood U of $(\hat{x}, \hat{w})$ such that $U \subset K$ and

$$|\lambda([a^\star(x,w); x; w])|^2_{R_T} \geq |\lambda([a^\star(\hat{x}, \hat{w}); \hat{x}; \hat{w}])|^2_{R_T} - \epsilon$$

for all $(x, w) \in U$ and positive integers T. As a result,

$$\mathrm{tr}(R_T \bar{M}_T) \geq \left(|\lambda([a^\star(\hat{x}, \hat{w}); \hat{x}; \hat{w}])|^2_{R_T} - \epsilon \right) \cdot c \int \int_U dx dw.$$

As $\mathrm{tr}(R_T \bar{M}_T)$ converges to zero, it follows that

$$\epsilon \geq \limsup_{T \to \infty} |\lambda([a^\star(\hat{x}, \hat{w}); \hat{x}; \hat{w}])|^2_{R_T}.$$

As ϵ was arbitrary, this completes the proof. □

Chapter 4

Robust Simulation Error

This chapter introduces an improved family of convex upper bounds for simulation error applicable to *state-affine* models. Section 4.1 provides the definition of the class of models examined, and defines a weighted notion of simulation error. Section 4.2 then introduces the *robust weighted simulation error* (RWSE), a family of convex upper bounds for the weighted simulation error. These upper bounds depend on a fixed auxiliary parameter and it is shown that:

(i) For an appropriate choice of this additional parameter, the RWSE is a lower bound for the simulation error upper bounds of the previous two chapters.

(ii) For every well-posed state-affine model, there is a choice of this additional parameter such that the RWSE is equal to the weighted simulation error.

This second feature leads to an iterative identification method described in Section 4.4, and applied to two examples. Section 4.3 provides a frequency domain analysis of the RWSE for SISO LTI models.

4.1 Preliminaries

4.1.1 State-Affine Models

This chapter addresses systems determined by a collection of matrix-valued functions $G_k : \mathbb{R}^{n_w} \to \mathbb{R}^{n_y \times n_y}$, for $k \in \{0, \dots, n\}$ and a function $p : \mathbb{R}^{n_w} \to \mathbb{R}^{n_y}$ according to

$$0 = g(y(t), \dots, y(t-n), w(t)) = \sum_{k=0}^{n} G_{n-k}(w(t))y(t-k) + p(w(t)), \qquad (4.1)$$

where $w(t) \in \mathbb{R}^{n_w}$ represents an input signal, and $y(t) \in \mathbb{R}^{n_y}$ represents an output signal. Similarly to earlier chapters, well-posedness of (4.1) will refer to global

invertibility of $G_n(\cdot)$. When (4.1) is well-posed one can equivalently write

$$y(t) = -G_n(w(t))^{-1}\left(\sum_{k=1}^{n} G_{n-k}(w(t))y(t-k) + p(w(t))\right).$$

For every fixed input signal $w(\cdot)$, (4.1) defines a linear time-varying (LTV) system dynamics. Note that the absence of delays in the signal $w(t)$ is superficial, as given an input signal $u(t) \in \mathbb{R}^{n_u}$ and positive integer d_u one could take

$$w(t) = \begin{bmatrix} u(t) \\ u(t-1) \\ \vdots \\ u(t-d_u) \end{bmatrix}.$$

■ 4.1.2 Error Dynamics

Fix a positive integer N, a pair of signals $\tilde{y} \in \ell_{N+n-1}(\mathbb{R}^{n_y})$ and $\tilde{w} \in \ell_N(\mathbb{R}^{n_w})$. For an arbitrary function g such that (4.1) is well-posed, let $y(\cdot)$ be the solution of (4.1) with $y(t) = \tilde{y}(t)$ for $t \in \{0, \ldots, n-1\}$ and $w(t) \equiv \tilde{w}(t-n+1)$ for $t \in \{n, n+1, \ldots, N+n-1\}$. Then the vector

$$\Delta = \begin{bmatrix} y(n) - \tilde{y}(n) \\ y(n+1) - \tilde{y}(n+1) \\ \vdots \\ y(N+n-1) - \tilde{y}(N+n-1) \end{bmatrix} \in \mathbb{R}^{Nn_y}$$

can be seen to satisfy

$$0 = G(\tilde{w})\Delta + \epsilon(\tilde{w}, \tilde{y})$$

where $\epsilon(\tilde{w}, \tilde{y}) \in \mathbb{R}^{Nn_y}$ is defined by

$$\epsilon(\tilde{w}, \tilde{y})_t = \sum_{k=0}^{n} G_{n-k}(\tilde{w}(t))\tilde{y}(t+n-k-1) + p(\tilde{w}(t)), \tag{4.2}$$

and $G(\tilde{w}) \in \mathbb{R}^{Nn_y \times Nn_y}$ is given by

$$G(\tilde{w}) = \begin{bmatrix} G_n(\tilde{w}(1)) & 0 & 0 & \ldots \\ G_{n-1}(\tilde{w}(2)) & G_n(\tilde{w}(2)) & 0 & \ldots \\ G_{n-2}(\tilde{w}(3)) & G_{n-1}(\tilde{w}(3)) & G_n(\tilde{w}(3)) & \ddots \\ \vdots & \ddots & \ddots & \ddots \end{bmatrix}. \tag{4.3}$$

Note that when (4.1) is well-posed, $G(\tilde{w})$ is invertible.

Definition 4.1. *Fix $N \in \mathbb{N}$ and $W \in \mathbb{R}^{Nn_y \times Nn_y}$ such that $W = W'$ is positive-semidefinite. For any function g defining a well-posed model* (4.1) *and pair of signals $\tilde{y} \in \ell_{N+n-1}(\mathbb{R}^{n_y})$ and $\tilde{w} \in \ell_N(\mathbb{R}^{n_w})$ let the* **weighted simulation error** *be defined by*

$$\bar{J}_W(g, \tilde{y}, \tilde{w}) = |G(\tilde{w})^{-1}\epsilon(\tilde{w}, \tilde{y})|_W^2$$

where G and ϵ are defined as in (4.3) *and* (4.2)*.*

4.2 A Family of Upper Bounds on Weighted Simulation Error

The following definition provides family of upper bounds for the weighted simulation error.

Definition 4.2. *Fix a positive integer N, a symmetric positive-semidefinite matrix $W \in \mathbb{R}^{Nn_y \times Nn_y}$, and a function $P : \ell_N(\mathbb{R}^{n_w}) \to \mathbb{R}^{Nn_y \times Nn_y}$. Then for each function g as in* (4.1) *the* **robust weighted simulation error (RWSE)** *is defined by*

$$J_{W,P}^{\mathrm{RSE}}(g, \tilde{w}, \tilde{y}) = \sup_{\Delta \in \mathbb{R}^{Nn_y}} \left\{ |\Delta|_W^2 - 2(P(\tilde{w})\Delta)'(G(\tilde{w})\Delta + \epsilon(\tilde{w}, \tilde{y})) \right\},$$

for all $\tilde{w} \in \ell_N(\mathbb{R}^{n_w})$ and $\tilde{y} \in \ell_{N+n}(\mathbb{R}^{n_y})$. Here G and ϵ are defined as in (4.2) *and* (4.3)*. The* **robust simulation error** *will refer to $J_{I,I}^{\mathrm{RSE}}$.*

It should be note that the $J_{I,I}^{\mathrm{RSE}}$ is closely related to an upper bound for simulation error presented in [88].

4.2.1 Analysis of the RWSE

The next two propositions provide some guarantees as to the values taken on by the RWSE. The first proposition establishes that for any fixed model g there is a specific choice of P such that the RWSE is equal to the weighted simulation error.

Proposition 4.3. *Letting g be a function such that* (4.1) *is well-posed, N be a positive integer, and $W \in \mathbb{R}^{Nn_y \times Nn_y}$ be a fixed positive semidefinite matrix. Define $P : \ell_N(\mathbb{R}^{n_w}) \to \mathbb{R}^{Nn_y}$ by*

$$P(\tilde{w})'G(\tilde{w}) = W,$$

where G is defined as in (4.3)*. Then*

$$J_{W,P}^{\mathrm{RSE}}(g, \tilde{w}, \tilde{y}) = \bar{J}_W(g, \tilde{w}, \tilde{y}).$$

Proof. Note that

$$\begin{aligned}|\Delta|_W^2 - 2(P(\tilde{w})\Delta)'(G(\tilde{w})\Delta + \epsilon(\tilde{w},\tilde{y})) &= -2\Delta' W G(\tilde{w})^{-1}\epsilon(\tilde{w},\tilde{y}) - |\Delta|_W^2 \\ &= -2\Delta' W G(\tilde{w})^{-1}\epsilon(\tilde{w},\tilde{y}) - |W\Delta|_{W^\dagger}^2,\end{aligned}$$

where $W^\dagger$ is the Moore-Penrose pseudo-inverse of W. Taking $\Gamma = W\Delta$, the supremum of this expression with respect to Δ is equivalent to

$$\sup\left\{-2\Gamma' G(\tilde{w})^{-1}\epsilon(\tilde{w},\tilde{y}) - |\Gamma|_{W^\dagger}^2\right\} = |G(\tilde{w})^{-1}\epsilon(\tilde{w},\tilde{y})|_W^2,$$

where the supremum is taken over Γ in the range of W. □

Next, we note that the form of the equations (4.1) can be cast as a model in the form (2.4) with $n_x = n_y n$. We reproduce (2.4) here:

$$\begin{aligned}0 &= h(v(t), x(t-1), w(t)), \\ x(t) &= \begin{bmatrix} v(t) \\ \bar{a}(x(t-1), w(t)) \end{bmatrix}.\end{aligned} \tag{4.4}$$

In particular, take

$$h(y_0, [y_1; \ldots; y_n], w) \equiv g(y_0, y_1, \ldots, y_n, w) \tag{4.5}$$

and

$$\bar{a}(x, w) = \begin{bmatrix} I_{(n-1)n_y} & 0_{(n-1)n_y \times n_y} \end{bmatrix} x, \quad (x \in \mathbb{R}^{n_x}, w \in \mathbb{R}^{n_w}). \tag{4.6}$$

The interpretation here is that

$$x(t-1) = \begin{bmatrix} y(t-1) \\ y(t-2) \\ \vdots \\ y(t-n) \end{bmatrix}.$$

The next definition and proposition relates the RWSE to the RIE for a particular choice of P and W.

Proposition 4.4. *Fix a positive integer N and a function g as in* (4.1)*. Let h and $\bar{a}$ be defined as in* (4.5) *and* (4.6)*. Then for every symmetric positive-semidefinite matrix $Q \in \mathbb{R}^{n_x \times n_x}$ and non-negative function $V : \mathbb{R}^{n_x} \times \mathbb{R}^{n_x} \to \mathbb{R}$,*

$$J_Q^{\mathrm{RIE}}(h, V, \tilde{w}, \tilde{x}) \geq J_{W,I}^{\mathrm{RSE}}(g, \tilde{w}, \tilde{y}) \quad \forall\ \tilde{w} \in \ell_N(\mathbb{R}^{n_w}), \tilde{y} \in \ell_{N+n-1}(\mathbb{R}^{n_y}),$$

where:

(i) $\tilde{x} \in \ell_N(\mathbb{R}^{n_x})$ *is defined by*

$$\tilde{x}(t-1) = \begin{bmatrix} \tilde{y}(t+n-2) \\ \tilde{y}(t+n-3) \\ \vdots \\ \tilde{y}(t-1) \end{bmatrix} \quad \forall\, t \in \{1, \ldots, N+1\},$$

(ii) $W \in \mathbb{R}^{Nn_y \times Nn_y}$ *is the unique symmetric matrix satisfying*

$$\left\| \begin{bmatrix} \Delta_{n+1} \\ \Delta_{n+2} \\ \vdots \\ \Delta_{n+N} \end{bmatrix} \right|_W^2 = \sum_{t=0}^{N-1} \left\| \begin{bmatrix} \Delta_{t+n} \\ \vdots \\ \Delta_{t+1} \end{bmatrix} \right|_Q^2, \forall\, \Delta_1, \ldots, \Delta_{N+n} \in \mathbb{R}^{n_y}, \Delta_1 = \ldots = \Delta_n = 0.$$

The proof is contained in Section 4.6.

■ 4.2.2 A Simple Example

We provide a computational example as evidence of the benefit of identifying models by minimizing the RWSE with $W = P(\tilde{w}) = I$. This experiment examines identification of a model of the form

$$ex(t) = fx(t-1) + kw(t),$$

where $e, f, k \in \mathbb{R}$ and $e > 0$, to match a data set $\tilde{x}, \tilde{w} \in \ell_{5000}(\mathbb{R})$ generated as follows. The signal $\tilde{w}$ was taken to be a realization of an i.i.d. standard normal stochastic process. The signal $\tilde{x}$ was taken to be a solution of

$$\bar{x}(t) = 0.9\bar{x}(t-1) + \tilde{w}(t), \quad \bar{x}(0) = 0, \quad \tilde{x}(t) = x(t) + \eta(t),$$

where $\eta(t)$ is a realization of an i.i.d zero mean Gaussian random process with variance σ_η^2.

A model is then identified by minimizing the RSE over the choice of e and f with $k = e$. This process was repeated for 100 Monte Carlo trials with independent output noise, but a common input sequence. Figure 4.1 compares the average estimated pole, $\hat{a} = e/f$, with the pole obtained by minimizing the RIE and equation error (EE) respectively (see Section 3.2). Also provided is a plot (on log-scale) that compares the average normalized asymptotic simulation error of the models:

$$\frac{\|H - \hat{H}\|_2}{\|H\|_2}, \tag{4.7}$$

where $H(z) = \frac{z}{z-a}$ and $\hat{H}(z) = \frac{z}{z-\hat{a}}$ are the transfer functions of the true system and model system respectively and $\|\cdot\|_2$ denotes the $\mathcal{L}_2$-norm defined for functions on $\mathbb{T}$.

4.3 Frequency Domain Analysis

This section provides a frequency domain interpretation of the RSE for SISO LTI models.

4.3.1 Notation

In this section we introduce the following additional notation. For $p \in [1, \infty)$, let $\mathcal{L}^p$ denote the standard Lebesgue space of measurable functions $f : \mathbb{T} \to \mathbb{C}$ for which

$$\|f\|_p = \left(\int_{\mathbb{T}} |f(z)|^p d\lambda(z) \right)^{1/p} < \infty,$$

where $d\lambda$ denotes the normalized Lebesgue measure on $\mathbb{T}$. Naturally, $\mathcal{L}^\infty$ is the space of essentially bounded measurable complex-valued functions on $\mathbb{T}$. For every $a \in \mathcal{L}^1$, let $\{a_k\}_{k=-\infty}^{\infty}$ be its Fourier coefficients, i.e.

$$a_k = \int_{\mathbb{T}} z^{-k} a(z) d\lambda(z), \quad k \in \mathbb{Z}.$$

For a set J, let $\ell^2(J)$ denote the Hilbert space of functions $x : J \to \mathbb{C}$ which are square summable, i.e.

$$\sum_{t \in J} |x(t)|^2 < \infty,$$

equipped with the standard inner product. We generally take J to be $\mathbb{Z}, \mathbb{N}$, or $\{1, \ldots, N\}$ for some $N \in \mathbb{N}$. For every $a \in \mathcal{L}^\infty$, let $L(a) : \ell^2(\mathbb{Z}) \to \ell^2(\mathbb{Z})$ be the *Laurent operator* defined by

$$(L(a)x)(t) = \sum_{\tau=-\infty}^{\infty} a_{t-\tau} x(\tau) \quad (x \in \ell^2(\mathbb{Z}))$$

and let $T(a) : \ell^2(\mathbb{N}) \to \ell^2(\mathbb{N})$ be the *Toeplitz operator* defined by the infinite matrix

$$T(a) = \begin{bmatrix} a_0 & a_{-1} & a_{-2} & \ldots \\ a_1 & a_0 & a_{-1} & \ddots \\ a_2 & a_1 & a_0 & \ddots \\ \vdots & \ddots & \ddots & \ddots \end{bmatrix}$$

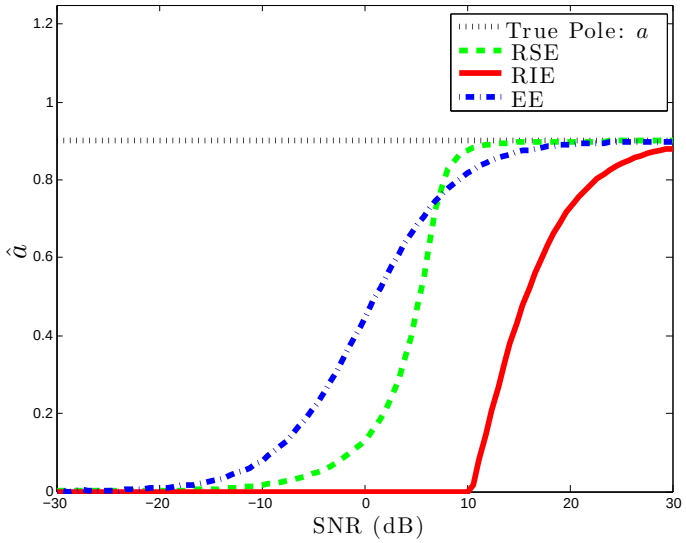

(a) Pole $\hat{a}$ of the identified models for varying SNR.

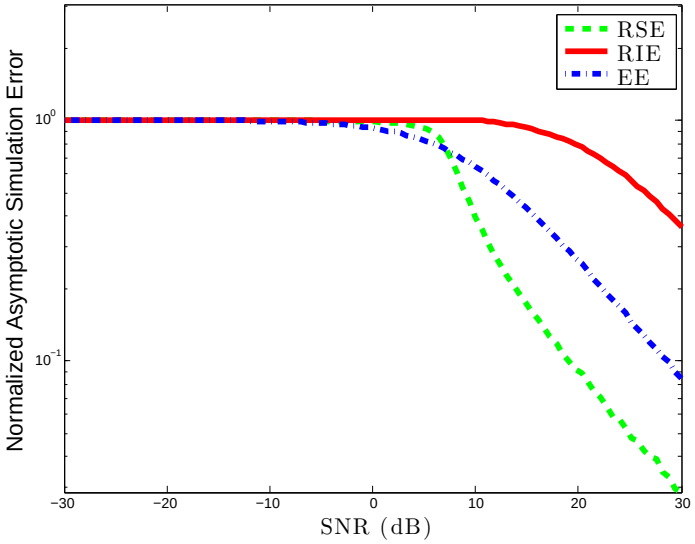

(b) A comparison of the normalized asymptotic simulation error (see (4.7)) for models identified at different SNRs.

Figure 4.1. A comparison of first-order LTI models identified by minimizing the equation error (EE), robust identification error (RIE), and robust simulation error (RSE) for varying SNRs. Figure (a) compares the identified poles whereas (b) compares the simulation performance. For SNRs above 10dB (resp. 20dB) the the asymptotic simulation error of the RSE minimizer is less than one half (resp. one third) of the corresponding EE minimizer.

in the standard basis for $\ell^2(\mathbb{N})$. Similarly, define

$$T_N(a) = \begin{bmatrix} a_0 & a_{-1} & \dots & a_{-N+1} \\ a_1 & a_0 & \ddots & \vdots \\ \vdots & \ddots & \ddots & a_{-1} \\ a_{N-1} & \dots & a_1 & a_0 \end{bmatrix} \in \mathbb{C}^{N\times N}, \quad (N \in \mathbb{Z}_+, a \in \mathcal{L}^\infty).$$

For all positive integers N, let $Q_N : \ell^2(\mathbb{Z}) \to \mathbb{C}^N$ be defined by

$$Q_N x = \begin{bmatrix} x(1) \\ x(2) \\ \vdots \\ x(N) \end{bmatrix}, \quad \forall x \in \ell^2(\mathbb{Z}).$$

Finally, let P denote projection of $\ell(\mathbb{Z})$ onto $\ell(\mathbb{N})$, viewed as a closed subspace, and let S denote the right shift operator on $\ell^2(\mathbb{Z})$.

■ 4.3.2 Analysis

This section studies the asymptotic behavior of the RSE when applied to a LTI SISO difference equation,

$$\sum_{k=0}^{n} q_k y(t+k) = \sum_{k=0}^{n} p_k u(t+k), \tag{4.8}$$

with each $q_k, p_k \in \mathbb{R}$ and $q_n \neq 0$, or equivalently with

$$g(y_0, y_1, \dots, y_n, [u_0; u_1; \dots; u_n]) = \sum_{k=0}^{n} q_k y_{n-k} - p_k u_{n-k}. \tag{4.9}$$

Associated with such an equation are the polynomials

$$q(z) = \sum_{k=0}^{n} q_k z^k, \quad p(z) = \sum_{k=0}^{n} q_k z^k.$$

For the remainder of this section we consider the choice of p and q above to be fixed.

The following notation will be used to simplify discussion of the RSE. For each positive integer N, define $\hat{J}_N : \mathbb{C}^N \to \mathbb{R}$ by

$$\hat{J}_N(\epsilon) := \sup_{\Delta\in\mathbb{C}^N} \left\{ |\Delta|^2 - 2\mathrm{Re}\{\Delta'(T_N(q^*)\Delta + \epsilon)\} \right\}$$

where $q^*(z) = z^n q(z^{-1})$. This quantity is related to the RSE as follows. Fix N, $\tilde{y}, \tilde{u} \in \ell_{N+n-1}(\mathbb{R})$ and define $\tilde{w} \in \ell_N(\mathbb{R}^{n+1})$ by $\tilde{w}(t) = [\tilde{u}(t+n-1); \ldots; \tilde{u}(t-1)]$. Then

$$\hat{J}_N(\epsilon(\tilde{w}, \tilde{y})) = J_{I,I}^{\mathrm{RWSE}}(g, \tilde{w}, \tilde{y})$$

where g is defined by (4.9) and ϵ is defined by (4.2) (this follows from the fact that $G(\tilde{w}) = T_N(q^*)$).

The index N will represent the length of the available data and the case of interest will be as $N \to \infty$. For the remainder of this section we fix a pair of signals $\tilde{u}, \tilde{y} \in \ell^2(\mathbb{Z})$ and let $\tilde{U}$ and $\tilde{Y}$ denote their Fourier transforms. The *equation errors*, $\tilde{\epsilon} \in \ell^2(\mathbb{Z})$, associated with the polynomials p and q and such a pair of signals are defined by

$$\tilde{\epsilon}(t) = \sum_{k=0}^{n} q_k \tilde{y}(t+k) - \sum_{k=0}^{n} p_k \tilde{u}(t+k). \tag{4.10}$$

Upper Bound and Stability

The following fact is a standard result from complex analysis and is stated without proof.

Lemma 4.5. *If q is a polynomial such that the real part $q^*(z) = z^n q(z^{-1})$ is strictly positive on $\mathbb{T}$, then the roots of q lie in the open unit disc.*

This observation has been employed in convex optimization approaches to filter design (e.g. [28],[36]), fixed order LTI controller design (see [52]), and model order reduction (see [123]).

Let $r : \mathbb{T} \to \mathbb{R}$ be defined by

$$r(z) := 2\mathrm{Re}\{q^*(z)\} - 1. \tag{4.11}$$

We will be establishing a relationship between the behavior of $\hat{J}_N$ as $N \to \infty$ and certain integrals in the frequency domain. The connection will be made using the following lemma which is based on the asymptotic analysis of Toeplitz matrices (e.g. [14]).

Lemma 4.6. *If q is a polynomial such that r is positive on $\mathbb{T}$, then each matrix $T_N(r)$ is positive definite, and*

$$\lim_{\tau \to \infty} \lim_{N \to \infty} (S^{-\tau} Q_N' T_N(r)^{-1} Q_N S^{\tau}) x = L(r^{-1}) x, \quad \forall x \in \ell^2(\mathbb{Z}).$$

Proof. As r is continuous and positive, $r \geq \delta$ for some positive constant δ, and

$$v'T_N(r)v = \int_{\mathbb{T}} r(z) \left| \sum_{k=1}^{N} v_k z^k \right|^2 d\lambda(z) \geq \delta |v|^2, \quad \forall\, N \in \mathbb{N}, v \in \mathbb{C}^N.$$

As r has a finite number of non-zero Fourier coefficients and is positive, $T(r)$ is invertible (see [14] Corollary 1.11), and

$$T(r)^{-1} - T(r^{-1}) = K$$

where $K : \ell^2(\mathbb{N}) \to \ell^2(\mathbb{N})$ is a compact operator (see [14], Propositions 1.2 and 1.3). It is clear that

$$\lim_{\tau \to \infty} S^{-\tau} P' T(r^{-1}) P S^{\tau} x = L(r^{-1})x \quad \forall\, x \in \ell^2(\mathbb{Z}).$$

Furthermore, as K is compact,

$$\lim_{\tau \to \infty} S^{-\tau} P' K P S^{\tau} x = 0 \quad \forall\, x \in \ell^2(\mathbb{Z}),$$

as $S^{\tau}x$ converges weakly to zero as $\tau \to \infty$. As $Q_N P = Q_N$, the proof will be completed by showing that

$$\lim_{N \to \infty} P' Q_N' T_N(r)^{-1} Q_N P x = P' T(r)^{-1} P x \quad \forall x \in \ell^2(\mathbb{N}).$$

For $N \in \mathbb{N}$, define $\bar{T}_N : \ell^2(\mathbb{N}) \to \ell^2(\mathbb{N})$ by the infinite matrix

$$\bar{T}_N = \begin{bmatrix} T_N(r) & 0 \\ 0 & T(r) \end{bmatrix},$$

in the standard basis for $\ell^2(\mathbb{N})$. Let P_N denote the orthogonal projection of $\ell^2(\mathbb{N})$ onto $\ell^2(\{1, \ldots, N\})$. Then

$$P' Q_N' T_N(r)^{-1} Q_N P x = P' \bar{T}_N^{-1} P_N P x.$$

Thus it is sufficient to show that $\bar{T}_N^{-1} P_N$ converges pointwise to $T(r)^{-1}$. Clearly $(x, \bar{T}_N x) \geq \delta |x|^2$ for all $x \in \ell^2(\mathbb{N})$, where δ again is defined so that $r \geq \delta > 0$. Thus,

$$\begin{aligned} |\bar{T}_N^{-1} P_N x - T(r)^{-1} x| &= |\bar{T}_N^{-1}(I - P_N)x - (\bar{T}_N^{-1} - T(r)^{-1})x| \\ &\leq |\bar{T}_N^{-1}(I - P_N)x| + |(\bar{T}_N^{-1} - T(r)^{-1})x| \\ &= |\bar{T}_N^{-1}(I - P_N)x| + |\bar{T}_N^{-1}(T(r) - \bar{T}_N)T(r)^{-1}x| \\ &\leq \frac{1}{\delta} \left(|(I - P_N)x| + |(T(r) - \bar{T}_N)T(r)^{-1}x| \right). \end{aligned}$$

As $I - P_N$ and $T(r) - \bar{T}_N$ both converge pointwise to zero, this completes the proof. □

The next statement is the main result of this section.

Theorem 4.7. *If q is a polynomial such that r, defined in* (4.11)*, is positive then*

$$\lim_{\tau\to\infty}\lim_{N\to\infty}\hat{J}_N(Q_N S^\tau\tilde{\epsilon}) = \int_{\mathbb{T}}\left|\tilde{Y}(z)-\frac{p(z)}{q(z)}\tilde{U}(z)\right|^2\left(\frac{|q(z)|^2}{2\mathrm{Re}\{q^*(z)\}-1}\right)d\lambda(z).$$

Proof. It can be readily verified that

$$\sum_{t=1}^{N}2\Delta'_{t+n}\left(\epsilon_t-\sum_{k=0}^{n}q_k\Delta_{t+k}\right)+|\Delta_{t+n}|^2 = 2\bar{\Delta}'\epsilon-\bar{\Delta}'T_N(r)\bar{\Delta},$$

for all $N\in\mathbb{N}$, $\epsilon\in\mathbb{C}^m$, and $\Delta=[0_n;\bar{\Delta}]\in L_N$. As r is strictly positive, $T_N(r)$ is positive definite and the supremum in the definition of $\hat{J}_N(Q_NS^\tau\tilde{\epsilon})$ can be evaluated explicitly:

$$\hat{J}_N(Q_NS^\tau\tilde{\epsilon}) = |Q_NS^\tau\tilde{\epsilon}|^2_{T_N(r)^{-1}}.$$

It follows from Lemma 4.6, continuity of the inner product and Parseval's theorem that

$$\lim_{\tau\to\infty}\lim_{N\to\infty}\hat{J}_N(Q_NS^\tau\tilde{\epsilon}) = \tilde{\epsilon}'L(r^{-1})\tilde{\epsilon} = \int_{\mathbb{T}}|\tilde{\mathcal{E}}(z)|^2\frac{1}{r(z)}d\lambda(z),$$

where $\tilde{\mathcal{E}}$ is the Fourier transform of $\tilde{\epsilon}$ and satisfies

$$\tilde{\mathcal{E}}(z) = q(z)\tilde{Y}(z)-p(z)\tilde{U}(z),\quad\forall\, z\in\mathbb{T}.$$

The desired result follows from simple algebraic manipulations and the definition of r.

□

■ 4.4 An Iterative Identification Scheme

Propositions 4.3 and 4.4 naturally suggest the following iterative identification scheme. We fix an affine parameterization of models of the form (4.1), i.e. for some fixed functions $\phi_{i,j}:\mathbb{R}^{n_w}\to\mathbb{R}^{n_y\times n_y}$ and $\psi_i:\mathbb{R}^{n_w}\to\mathbb{R}^{n_y}$ we take

$$g_\theta(y(t),\dots,y(t-n),u(t),w(t)) = \sum_{k=0}^{n}G_{\theta,n-k}(w(t))y(t-k)+p_\theta(w(t)),\quad(\theta\in\mathbb{R}^{n_\theta})$$

where

$$G_{\theta,j}(w(t)) = \phi_{i,0}(w(t))+\sum_{i=1}^{n_\theta}\theta_i\phi_{i,j}(w(t)),$$

$$p_\theta(w(t)) = \psi_0(w(t))+\sum_{i=1}^{n_\theta}\theta_i\psi_i(w(t)).$$

.

Fix a positive integer N and weight matrix $W \in \mathbb{R}^{Nn_y \times Nn_y}$. For a given data set $\tilde{y} \in \ell_{N+n-1}(\mathbb{R}^{n_y})$ and $\tilde{w} \in \ell_N(\mathbb{R}^{n_w})$, we identify a model by performing the following steps:

(i) Let $\theta^{(0)} = \operatorname{argmin}_\theta \left\{ J^{\mathrm{RSE}}_{I,W}(g_\theta, \tilde{y}, \tilde{w}) \right\}$ and $m = 0$.

(ii) Take $P_m(\tilde{w}) = (G(\tilde{w})^{-1})'W$ where G is defined by (4.3) with $g = g_{\theta^{(m)}}$.

(iii) Let $\theta^{(m+1)} = \operatorname{argmin}_\theta \{ J^{\mathrm{RSE}}_{P_m,W}(g_\theta, \tilde{y}, \tilde{w}) \}$.

(iv) If

$$\frac{\bar{J}_W(g_{\theta^{(m)}}, \tilde{y}, \tilde{w}) - \bar{J}_W(g_{\theta^{(m+1)}}, \tilde{y}, \tilde{w})}{|\bar{J}_W(g_{\theta^{(m)}}, \tilde{y}, \tilde{w})|} < \texttt{tol}$$

terminate, otherwise increment m and repeat steps (ii)-(iv).

From Proposition 4.3 we know the sequence $\bar{J}_W(g_{\theta^{(m)}}, \tilde{y}, \tilde{w})$ decreases monotonically and (as it is bounded below) will converge. The termination condition given in (iv), however, is simply heuristic.

4.5 Examples

4.5.1 Heat Exchanger Example

This section makes use of a benchmark system identification example from the DaISy system identification database [31]. The data set is from an experiment involving a liquid-saturated steam heat exchanger which heats water using pressurized steam in a copper tube. The data set consists of 4000 input-output data samples taken with a sampling rate of 1 Hz. The input time series is the liquid flow rate and the output time series is outlet liquid temperature. The system is described in more detail in [12].

The first 1,500 samples are used for model identification whereas the complete data set is used for model validation. We identify models of the form

$$q_n(w(t))y(t) = \sum_{k=1}^{n} q_{n-k} y(t-k) + p(w(t)), \quad w(t) = \begin{bmatrix} u(t) \\ u(t-1) \\ \vdots \\ u(t-n) \end{bmatrix},$$

where q_n is parameterized as an arbitrary quadratic polynomial and p is parameterized as an arbitrary cubic polynomial. For simplicity, the proposed method is halted after five iterations.

Table 4.1. Test Error (%) Comparison for the Heat Exchanger Example

	Model Order (n)		
Method	2	3	4
`nlhw`	29.1	76.4	43.9
`nlarx` (Eqn. Err. Min.)	22.1	21.9	22.0
`nlarx` (Sim. Err. Min.)	26.7	26.4	26.4
RIE	27.9	24.4	20.5
Proposed (1^{st} Iter.)	20.7	17.7	13.7
Proposed (5^{th} Iter.)	13.7	11.4	9.7

For comparison, several models are computed using MATLAB® System Identification Toolbox™, specifically the `nlarx` and `nlhw` functions which compute nonlinear ARX and nonlinear Hammerstein-Wiener models respectively (see [78]). The function `nlarx` has options both for performing simulation error and equation error minimization. Table 4.1 compares these models based on a normalized simulation error calculated as

$$\sqrt{\sum_{t=1}^{4000} |y(t) - \tilde{y}(t)|^2} \Bigg/ \sqrt{\sum_{t=1}^{4000} \left| \tilde{y}(t) - \frac{1}{4000} \sum_{t=1}^{4000} \tilde{y}(t) \right|^2},$$

where $\tilde{y}(t)$ are output the samples of the data-set and $y(t)$ are the corresponding model simulations with zero initial conditions For each examined model order, the best identified models are provided by the final iterate of proposed method and the second best models are provided by the first iterate. There is also a significant gap between the performance of the RIE minimizer and the first iterate of the proposed method (between 25 to 35 percent improvement).

■ 4.5.2 Wiener-Hammerstein Benchmark Example

Next, we examine the performance of the proposed iterative scheme on a benchmark data set described in [117]. The data set consists of a input and output time series consisting of 188,000 samples. A random excitation was applied to a circuit consisting linear filter, cascaded with a passive nonlinear circuit element followed by another linear filter (see [117] for details). The data is divided into an *estimation* portion, consisting of the first 100,000 data samples, and a *test* portion which consists of the remaining samples. Model parameters and order

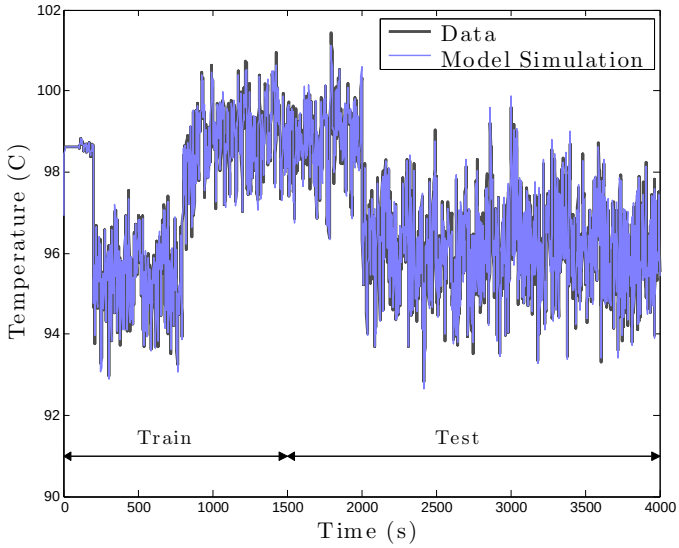

(a) Simulation of the best fitting model versus the true data set.

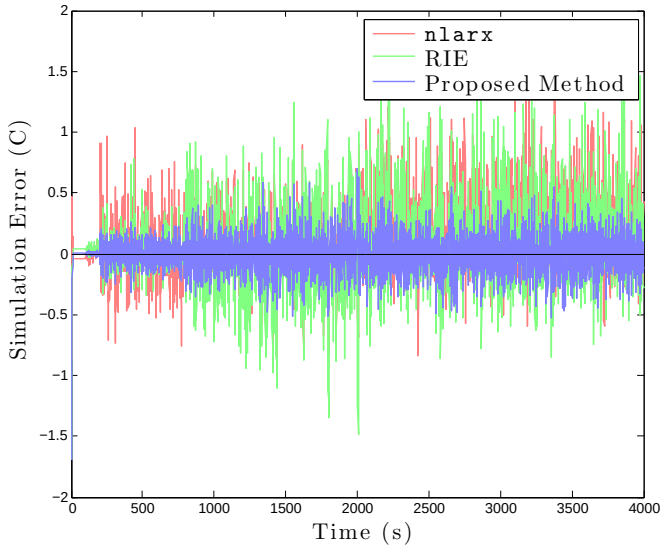

(b) Comparison of simulation errors.

Figure 4.2. Two plots presenting the fitting results for the heat exchanger example. The best fitting model (5^{th} iteration of the proposed method with $n = 4$) is compared to the true data and models fit via `nlarx` and minimization of the RIE with the same model order.

are selected based purely on the estimation data then compared on the test data in terms of the square root of the MSSE.

Proposed Method

For identifying a model using the proposed method, the estimation data set was further divided into a training data set consisting of the samples in the range $\{10001, 10002, \ldots, 14000\}$ and a *validation* data set consisting of the samples in the range $\{80001, 80002, \ldots, 100000\}$. Iterations are performed minimizing the RWSE for the training data until less than a 1% improvement on MSSE is observed. The iterate with the lowest MSSE on the validation data is taken to be the final model. The proposed method is used to identify models of the form

$$\sum_{k=0}^{n} q_{n-k} y(t-k) = p(u(t), \ldots, u(t-n)),$$

where p is parameterized to be an arbitrary cubic nonlinear function and the model order, n, is variable.

Alternative Methods

The proposed method is compared with four standard functions from the System Identification Toolbox™ (using MATLAB® version R2012b):

(i) `oe` produces a SISO LTI model by minimizing simulation error.

(iii) `nlarx` identifies a nonlinear ARX model.

(iv) `nlhw` identifies a Hammerstein-Wiener model.

(ii) `n4sid` is an implementation of [98] and produces a linear state-space model.

Details can be found in [78]. The methods were provided with the entirety of the estimation data set. The first three methods were configured to use $y(t-1), \ldots, y(t-n), u(t), u(t-1), \ldots, u(t-n)$ as regressors, whereas the final method was constrained to produce a state-spaced model of order n.

Results

Table 4.2 provides a comparison of the resulting models in terms of normalized simulation error:

$$\sqrt{\sum_{t=100001}^{180000} |y(t) - \tilde{y}(t)|^2} \Bigg/ \sqrt{\sum_{t=100001}^{180000} |\tilde{y}(t)|^2},$$

where $\tilde{y}(t)$ are the samples of the data-set and $y(t)$ are the corresponding model simulations with zero initial conditions. For the proposed method, the simulation error is reported both for the first iteration (minimization of the RSE) and final iteration. Two aspects of this table should be highlighted. First, the final iteration of the proposed method outperforms the alternative methods irrespective of their model order. Second, minimization of the RSE (i.e. the first iteration) actually performs worse on this data set than any of the alternative methods (particularly for low model orders).

A further comparison is made between the best performing model (on the validation data) for the proposed method and eight other studies which have identified models to fit the benchmark data-set. The relevant comparison is provided in Table 4.3. The root MSSE on the test data is reported in terms of volts (as opposed to being normalized). Model orders presented in parenthesis (d_y, d_u) refer to the number of delays of the input and output respectively used in a difference equation model. Numbers presented without parenthesis indicate the number of states in a state-space models. The proposed method outperforms [102] which performed direct simulation error minimization. It should be noted that three recently published results ([99], [87], and [118]) achieve much higher accuracy than the proposed method or other methods in the comparison. The models in both [99] and [87] result from carefully initialized simulation error minimization. The model found by [118] is more specific to the structure of the identified system. The method introduced in this chapter optimizes an upper bound for simulation error which is accurate only at the initial guess and subsequent iterates. It is unavoidable that careful initialization of other general descent methods can out potentially out perform the proposed method. The proposed method can also benefit from insight into model initialization, a possibility which was not explored in this work.

4.6 Proofs

Proof of Proposition 4.4. Fix $N \in \mathbb{Z}_+$, $\tilde{y} \in \ell_{N+n-1}(\mathbb{R}^{n_x})$, and $\tilde{w} \in \ell_N(\mathbb{R}^{n_w})$. Recall that

$$J_Q^{\mathrm{RIE}}(h, V, \tilde{w}, \tilde{x}) = V(\tilde{x}(0), \tilde{x}(0)) + \sum_{t=1}^{N} \sup_{x \in \mathbb{R}^{n_x}, v \in \mathbb{R}^{n_y}} \left\{ q_{(h,V)}(x, v, \tilde{x}(t-1), \tilde{x}(t), \tilde{w}(t)) \right\},$$

where $q_{(h,V)}$ is defined by (2.28) on page 39. This expression can be rewritten as

$$\sup \left\{ V(\tilde{x}(0), \tilde{x}(0)) + \sum_{t=1}^{N} q_{(h,V)}(x(t-1), v(t-1), \tilde{x}(t-1), \tilde{x}(t), \tilde{w}(t)) \right\},$$

Table 4.2. Test Error (%) Comparison with the System Identification Toolbox™.

	Model Order (n)		
Method	3	5	7
`n4sid`	38.4	23.7	23.2
`oe`	23.9	23.2	23.2
`nlarx`	49.7	16.4	16.2
`nlhw`	10.8	8.9	9.0
Proposed (First Iter.)	99.9	66.0	31.0
Proposed (Final Iter.)	6.5	4.9	5

Table 4.3. Test Error for Wiener-Hammerstein Benchmark

Citation	Order	RMSE (V)
Ase et al. 2009 ([5])	(3,3)	0.0335
Han et al. 2012 ([49])	(3,3)	0.0345
Truong et al. 2009 ([134])	(6,6)	0.0145
Piroddi et al. 2012 ([102])	(4,9)	0.0131
Proposed Method	(5,5)	0.0119
dos Santos et al. 2012 ([34])	5	0.0109
Paduart et al. 2012 ([99])	10	0.0027
Marconato et al. 2012 ([87])	6	0.0026
Paduart et al. 2012 ([99])	6	0.0004
Sjöberg et al. 2012 ([118])	6	0.0003

where the supremum is now taken over all pairs of signals $x \in \ell_{N-1}(\mathbb{R}^{n_x}), v \in \ell_{N-1}(\mathbb{R}^{n_y})$. Substituting in the definition of $q_{(h,V)}$ yields

$$J_Q^{\mathrm{RIE}}(h, V, \tilde{w}, \tilde{x}) = \sup \Bigg\{ V(\tilde{x}(0), \tilde{x}(0)) + \sum_{t=1}^{N} |x(t-1) - \tilde{x}(t-1)|_Q^2 \\ - 2(v(t-1) - \tilde{y}(t+n))' h(v(t-1), x(t-1), \tilde{w}(t)) \\ - V(\tilde{x}(t-1), x(t-1)) + V(\tilde{x}(t),) \Bigg\}.$$

where the supremum is again taken over all pairs of signals $x \in \ell_{N-1}(\mathbb{R}^{n_x}), v \in \ell_{N-1}(\mathbb{R}^{n_y})$. We now restrict the supremum to be taken over only those $x \in \ell_{N-1}(\mathbb{R}^{n_x})$ for which $x(0) = \tilde{x}(0)$ and

$$x(t) = \begin{bmatrix} v(t-1) \\ \bar{a}(x(t-1), \tilde{w}(t)) \end{bmatrix} \quad \forall t \in \{0, \ldots, N-1\}.$$

For $\bar{a}$ defined by (4.6), this is equivalent to taking the supremum over signals $y \in \ell_{N+n}(\mathbb{R}^{n_y})$ with

$$v(t-1) \equiv y(t+n), \quad x(t-1) \equiv \begin{bmatrix} y(t+n-2) \\ \vdots \\ y(t-1) \end{bmatrix}.$$

and $y(t) = \tilde{y}(t)$ for $t \in \{0, \ldots, n-1\}$. It is then immediate that

$$J_Q^{\mathrm{RIE}}(h, V, \tilde{w}, \tilde{x})$$

$$\geq$$

$$\sup \Bigg\{ V\left(\tilde{x}(N), \begin{bmatrix} y(N+n) \\ \vdots \\ y(N+1) \end{bmatrix}\right) + \sum_{t=1}^{N} |x(t-1) - \tilde{x}(t-1)|_Q^2 \\ - 2(y(t+n) - \tilde{y}(t+n))' h(y(t), x(t-1), \tilde{w}(t)) \Bigg\},$$

$$\geq$$

$$\sup\left\{\sum_{t=1}^{N}\left\|\begin{bmatrix} y(t+n-2)-\tilde{y}(t+n-2) \\ \vdots \\ y(t-1)-\tilde{y}(t-1)\end{bmatrix}\right\|_Q^2 \right.$$
$$\left. -2(y(t+n)-\tilde{y}(t+n))'h\left(v(t),\begin{bmatrix} y(t+n-1) \\ \dots \\ y(t)\end{bmatrix},\tilde{w}(t)\right)\right\},$$

where the first inequality holds due to algebraic cancellations and the second inequality holds due to the non-negativity of V. Letting

$$\Delta = \begin{bmatrix} y(n)-\tilde{y}(n) \\ \vdots \\ y(n+N)-\tilde{y}(n+N)\end{bmatrix}$$

and examining the definitions of G, ϵ, P, and W establishes the result. □

Part II:
Robustness Analysis of Dynamic Trajectories

Chapter 5

Introduction

Trajectory libraries have recently emerged as a powerful and flexible methodology for tackling highly dynamic motion planning and control tasks such as robotic juggling [17], acrobatic autonomous helicopter maneuvers [41], quadrapedal and bipedal robot locomotion [125, 138], and aggressive post-stall flight maneuvers for unmanned aerial vehicles [93]. These techniques sequentially compose a small set of basic control actions to achieve higher level goals. In practice, the open-loop plans contained in such a library must be combined with feedback controllers to overcome state and model uncertainty and provide disturbance rejection. A practical question arises when applying these techniques: how close to a nominal trajectory must the state of a system be for a feedback controller to successfully "capture" it?

This chapter addresses this question by providing algorithms for computing "funnels" around trajectories of a dynamical system: that is a set of initial conditions whose solutions are guaranteed to enter a certain goal region at a particular time. More formally, consider the time-varying ordinary differential equation

$$\dot{\xi}(t) = f(t, \xi(t)), \tag{5.1}$$

where $t \in [t_0, t_f]$ denotes time, $\xi(t) \in \mathbb{R}^{n_x}$ denotes the system state, and the function f is assumed to be piecewise continuous in its first argument and locally Lipschitzian in its second argument (see, for example, [48] Section 1.3). A funnel is defined as follows.

Definition 5.1. *Given a dynamical system* (5.1) *we say a function* $\mathcal{F}$ *mapping times* $t \in [t_a, t_b] \subset [t_0, t_f]$ *to sets* $\mathcal{F}(t) \subset \mathbb{R}^{n_x}$ *is a funnel if the following condition is satisfied. For each* $t \in [t_a, t_b]$ *and* $x \in \mathcal{F}(t)$ *the solution of* (5.1) *with* $\xi(t) = x$ *can be extended to the whole interval* $[t, t_b]$*, and*

$$\xi(\tau) \in \mathcal{F}(\tau), \quad \forall\, \tau \in [t, t_b].$$

The intuition behind this definition is sketched in Figure 5.1. Solutions are allowed to "enter" a funnel at any time, but can never exit. There is also no

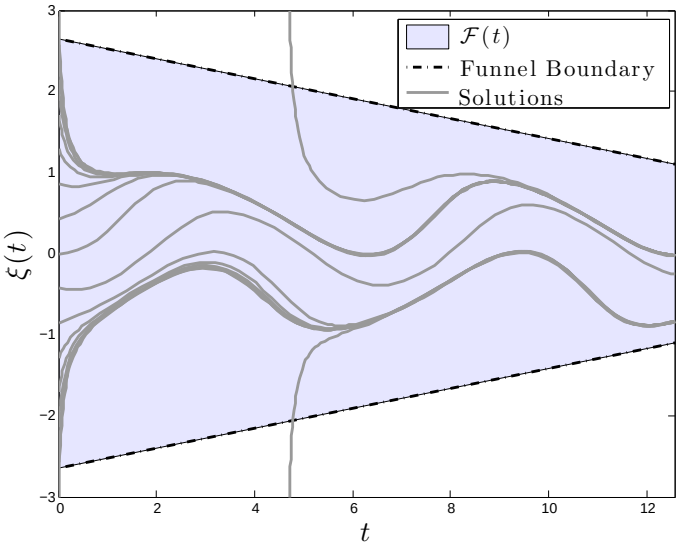

Figure 5.1. Schematic representation of a funnel. Solutions can enter the funnel at any time, but are guaranteed never to exit.

guarantee that solutions starting outside of a funnel should ever enter. This chapter presents algorithms for constructing such funnels and maximizing their size subject to the constraint that

$$\mathcal{F}(t_f) \subset \mathcal{E}$$

for some "target set" $\mathcal{E} \subset \mathbb{R}^{n_x}$ (generally an ellipse). The proposed algorithm exploits access to approximate solutions of (5.1) and uses sum-of-squares (SOS) optimization to optimize time-varying quadratic Lyapunov functions.

5.1 Constructing Funnels with Lyapunov Functions

For any continuously differentiable function $V : [t_a, t_b] \times \mathbb{R}^{n_x} \to \mathbb{R}$ define

$$\mathcal{F}_V(t) = \{x \in \mathbb{R}^{n_x} \ : \ V(t,x) \leq 1\}, \quad t \in [t_a, t_b].$$

This section describes constraints that can be placed on V to ensure that $\mathcal{F}_V$ is a funnel. The basic approach is to require that for each trajectory of (5.1) the function $t \mapsto V(t, \xi(t))$ must decrease near the boundary of $\mathcal{F}_V(t)$ (i.e. when $V(t, \xi(t)) = 1$). The lemmas in this section are stated without proof. Variants of these results can be found in texts on nonlinear systems such as [63].

Lemma 5.2. *Let $V : [t_a, t_b] \times \mathbb{R}^{n_x} \to \mathbb{R}$ be a continuously differentiable function. If the set*

$$\{(t, x) \in [t_a, t_b] \times \mathbb{R}^{n_x} \ : \ V(t, x) \leq 1\}$$

is bounded and

$$\frac{\partial V}{\partial t}(t, x) + \frac{\partial V}{\partial x}(t, x) f(t, x) < 0 \quad \forall\, (t, x) \ : \ V(t, x) = 1, \tag{5.2}$$

then $\mathcal{F}_V$ defines a funnel.

The boundedness requirement above is primarily to preclude finite escape. Note that the above result establishes very little about the behavior of solutions *inside* of $\mathcal{F}_V(t)$, other than the fact that they remain there. It is tempting to to replace the strict equality of (5.2) with a non-strict inequality. However, this revised claim would not hold, as demonstrated by the following example.

Example 5.1.1. Consider the first-order dynamical system and Lyapunov function given by

$$f(t, x) = 1, \quad V(t, x) = 1 + (|x|^2 - 1)^3, \quad (x \in \mathbb{R}, t \in [0, 3]).$$

Here $V(t, x) = 1$ holds only for $x \in \{1, -1\}$. Furthermore, $\frac{\partial V}{\partial t}(t, x) \equiv \frac{\partial V}{\partial x}(t, 1) \equiv \frac{\partial V}{\partial x}(t, -1) \equiv 0$. Thus (5.2) holds with a non-strict inequality. However, any solution of (5.1) with $\xi(0) \in \mathcal{F}_V(0)$ has $\xi(t) \notin \mathcal{F}_V(t)$ for $t > 1 - \xi(0)$.

The following alternative theorem provides stronger guarantees about the behavior of solutions.

Lemma 5.3. *Let $V : [t_a, t_b] \times \mathbb{R}^{n_x} \to \mathbb{R}$ be a continuously differentiable function. If the set*

$$\{(t, x) \in [t_a, t_b] \times \mathbb{R}^{n_x} \ : \ V(t, x) \leq 1\}$$

is bounded and there exist constants $\lambda > 0$ and $\sigma \in [0, 1)$ such that

$$\frac{\partial V}{\partial t}(t, x) + \frac{\partial V}{\partial x}(t, x) f(t, x) \leq \lambda(\sigma - V(t, x)) \quad \forall\, (t, x) \ : \ V(t, x) \leq 1, \tag{5.3}$$

then the following holds:

(i) The function $\mathcal{F}_{(V/r)}$ is a funnel for every $r \in (\sigma, 1]$.

(ii) For each solution $\xi(\cdot)$ of (5.1), if $V(\tau, \xi(\tau)) \in (\sigma, 1]$ for some $\tau \in [t_a, t_b]$, then

$$V(t, \xi(t)) \leq \sigma + e^{-\lambda(t-\tau)}(V(\tau, \xi(\tau)) - \sigma), \quad \forall\, t \in [\tau, t_b]. \tag{5.4}$$

5.1.1 Rational Parameterizations

In later chapters, we consider Lyapunov functions of the form

$$V(t,x) = \frac{W(t,x)}{\rho(t)},$$

where $W : [t_a, t_b] \times \mathbb{R}^{n_x} \to \mathbb{R}$ and $\rho : [t_a, t_b] \to \mathbb{R}$ are continuously differentiable functions and ρ is strictly positive. The following proposition, which follows immediately from the chain rule, provides simple conditions on W and ρ to ensure V satisfies the hypotheses of Lemmas 5.2 and 5.3.

Proposition 5.4. *For the functions V, W and ρ as above,* (5.2) *is equivalent to*

$$\frac{\partial W}{\partial t}(t,x) + \frac{\partial W}{\partial x}(t,x) f(t,x) < \dot{\rho}(t) \quad \forall\ (t,x)\ :\ W(t,x) = \rho(t). \tag{5.5}$$

For arbitrary constants $\lambda_0 > 0$ and $\sigma \in [0,1)$, if

$$\rho(t)\left(\frac{\partial W}{\partial t}(t,x) + \frac{\partial W}{\partial x}(t,x) f(t,x)\right) - \dot{\rho}(t) W(t,x) \leq \lambda_0(\sigma\rho(t) - W(t,x)) \tag{5.6}$$

holds for all (t,x) s.t. $W(t,x) \in (\rho(t)\sigma, \rho(t)]$, then (5.3) *holds with*

$$\lambda = \min_t \left\{ \frac{\lambda_0}{\rho(t)} \right\}.$$

5.1.2 A Simple Example

The following example illustrates the difference between these two lemmas.

Example 5.1.2. Consider the first-order dynamical system defined by (5.1) with

$$f(t,x) = -\frac{1}{2}x + \frac{1}{2}\sin(t) - x^3, \quad (t \in [0, 4\pi],\ x \in \mathbb{R}).$$

Let $V(t,x) = W(t,x)/\rho(t)$ with $W(t,x) = x^2$ and $\rho(t) = a_0 + t\frac{a_1 - a_0}{4\pi}$ for $a_0, a_1 > 0$. Note that $\{x\ :\ V(t,x) = 1\} = \{\pm\sqrt{\rho(t)}\}$ and

$$\frac{\partial W}{\partial t}(t,x) + \frac{\partial W}{\partial x}(t,x) f(t,x) = x^2 + x\sin(t) - 2x^4.$$

It can be verified explicitly that the conditions of Lemma 5.2 are satisfied with $a_0 = 2.65$ and $a_1 = 1.1$. The conditions of Lemma 5.3 are satisfied, for example, with $\rho(t) = 4$, $\sigma = 0.36$, and $\lambda = 3$. Figures 5.2(a) and 5.2(b) compare the guarantees provided by these two results.

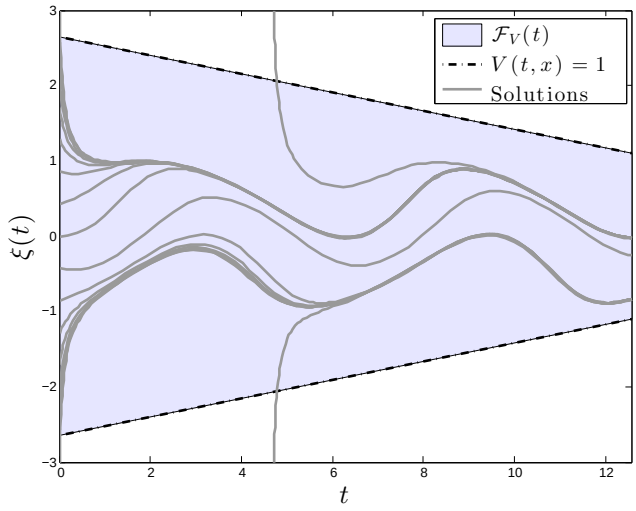

(a) Sample solutions and funnel boundary when applying Lemma 5.2 to Example 5.1.2.

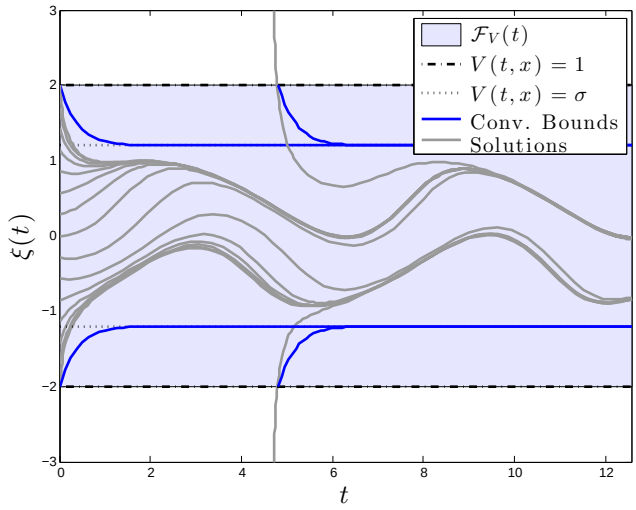

(b) Sample solutions, convergence bounds, and funnel boundary when applying Lemma 5.3 to Example 5.1.2 with $\sigma = 0.36$ and $\lambda = 3$.

Figure 5.2. A comparison of the guarantees provided by applying Lemmas 5.2 and 5.3 to Example 5.1.2. In (a), solutions are guaranteed never to exit $W(t,x) = x^2 \leq 2.65 - (1.55/4\pi)t$, but little is said about their behavior otherwise. In (b), solutions, are guaranteed never to exit $V(t,x) = \frac{1}{4}x^2 \leq r$ for any $r \in (0.36, 1)$. Furthermore, $V(t,\xi(t))$ will approach $\sigma = 0.36$ at an exponential rate so long as $V(t,\xi(t)) \in (\sigma, 1)$. This convergence rate, given by (5.4), is illustrated by dark blue lines for two starting times τ.

5.1.3 Composition and Piecewise Functions

The results of the above lemmas can naturally be extended to the case where both V and f are defined *piecewise* with respect to time. To handle these cases, we make use of the following intuitive "composition" property of funnels. Given a pair of funnels $\mathcal{F}_a$ and $\mathcal{F}_b$ defined on $[t_a, t_b]$ and $[t_b, t_c]$ respectively, with $t_a < t_b < t_c$, if

$$\mathcal{F}_a(t_b) \subset \mathcal{F}_b(t_b),$$

then the function

$$\mathcal{F}(t) = \begin{cases} \mathcal{F}_a(t) & t \in [t_a, t_b) \\ \mathcal{F}_b(t) & t \in [t_b, t_c] \end{cases}$$

is also a funnel.

To see how this fact can be applied, say the time interval $[t_0, t_f]$ has been divided into a sequence of intervals defined by $t_0 < t_1 < t_2 < \ldots < t_k = t_f$. Let f be defined by

$$f(t, x) = \begin{cases} f_i(t, x) & t \in [t_{i-1}, t_i),\ i \in \{1, \ldots, k-1\} \\ f_k(t, x) & t \in [t_{k-1}, t_k] \end{cases},$$

where each $f_i : [t_{i-1}, t_i] \times \mathbb{R}^{n_x} \to \mathbb{R}^{n_x}$ is continuous in its first argument and locally Lipschitzian in its second[1]. Similarly, assume there exists a function $V : [t_0, t_f] \times \mathbb{R}^{n_x} \to \mathbb{R}$ defined by

$$V(t, x) = \begin{cases} V_i(t, x) & t \in [t_{i-1}, t_i),\ i \in \{1, \ldots, k-1\} \\ V_k(t, x) & t \in [t_{k-1}, t_k] \end{cases},$$

where the functions $V_i : [t_{i-1}, t_i] \times \mathbb{R}^{n_x} \to \mathbb{R}$ are continuously differentiable. If the conditions of Lemma 5.2 hold for each f_i and V_i individually, then each $\mathcal{F}_{V_i}$ defines a funnel. If in addition,

$$\{x \in \mathbb{R}^{n_x} \ :\ V_i(t_i, x) \leq 1\} = \mathcal{F}_{V_i}(t_i) \subset \mathcal{F}_{V_{i+1}}(t_i) = \{x \in \mathbb{R}^{n_x} \ :\ V_{i+1}(t_i, x) \leq 1\}$$

for $i \in \{1, \ldots, k-1\}$, then the composition property implies that $\mathcal{F}_V(t)$ defines a funnel.

[1] A "solution" of (5.1) in this setting will mean that (5.1) is satisfied by $\xi(t)$ for $t \in [t_0, t_f] \setminus \{t_0, t_1, t_2, \ldots, t_k\}$.

Chapter 6

Optimization of Funnels

This chapter takes up the question of automatically searching for Lyapunov functions which certify the existence of a funnel. Our interest will be in funnels which are constrained to satisfy a *terminal condition*:

$$\mathcal{F}(t_f) \subset \mathcal{E}_f,$$

where $\mathcal{E}_f$ is a *target set* or *goal region*. In applications, this target region will be taken to be an ellipsoid. In terms of the definitions given in the previous chapter, the optimization problem addressed in this section is

$$\begin{aligned} \underset{V}{\text{maximize}} \quad & \nu(V) \\ \text{subj. to} \quad & \mathcal{F}_V(t_f) \subset \mathcal{E}_f, \\ & \frac{\partial V}{\partial t}(t,x) + \frac{\partial V}{\partial x}(t,x) f(t,x) < 0, \quad \forall\ (t,x)\ :\ V(t,x) = 1. \end{aligned}$$

Here ν denotes a cost function representing the "size" of the funnel $\mathcal{F}_V$ and will be defined later. The function V will be drawn from a fixed class of functions whose one-sublevel sets are bounded.

The remainder of this chapter first provides a parameterization of time-varying quadratic candidate Lyapunov functions. Several natural measures of size for funnels defined by time-varying quadratic functions are defined. Finally, we propose an iterative optimization procedure based on sums-of-squares programming for finding as large a funnel as possible. This procedure is initialized based on a linearized analysis of a sample trajectory.

6.1 Time-Varying Quadratic Candidate Lyapunov Functions

This section makes simple observations about time-varying quadratic Lyapunov candidates. This class of functions has a number of distinct advantages over more general classes, including connections to basic analytical tools available from linear

systems theory and the availability of explicit expressions for the volume of sub-level sets.

In particular, we will examine the following parameterization of time-varying quadratic Lyapunov functions. Let $\xi_0 : [t_a, t_b] \to \mathbb{R}^{n_x}$ be a differentiable function (in applications it will generally be an approximate solution of (5.1)). For any pair of functions $P : [t_a, t_b] \to \mathbb{R}^{n_x \times n_x}$, and $\rho : [t_a, t_b] \to \mathbb{R}$ such that

$$P(t) = P(t)' > 0 \quad \text{and} \quad \rho(t) > 0 \quad \forall\, t \in [t_a, t_b],$$

define

$$W(t, x) = W_{(\xi_0, P)}(t, x) = |x - \xi_0(t)|^2_{P(t)},$$

and

$$V(t, x) = V_{(\xi_0, P, \rho)}(t, x) := \frac{W(t, x)}{\rho(t)}.$$

6.1.1 Quantifying Size

The following two statements are used in the later sections of this chapter to quantify the size of funnels defined by a function V given as above:

(i)
$$\mathrm{vol}(\mathcal{F}_V(t)) \propto \sqrt{\frac{\rho(t)^{n_x}}{\det(P(t))}}, \tag{6.1}$$

where the constant of proportionality is the volume of the unit n_x-sphere.

(ii) For any function $P_0 : [t_a, t_b] \to \mathbb{R}^{n_x \times n_x}$ s.t. $P_0(t) = P_0(t)' > 0$ and $r > 0$,

$$\{x \in \mathbb{R}^{n_x} \ : \ |x - \xi_0(t)|^2_{P_0(t)} \le r\} \subset F_V(t), \quad \forall\, t \in [t_a, t_b]$$

if and only if

$$\rho(t) P_0(t) \ge r P(t) \quad \forall\, t \in [t_a, t_b].$$

6.1.2 Linearized Analysis

Part of our interest in time-varying quadratic Lyapunov functions is their connection to analysis tools available from linear systems theory. We briefly recall a result describing how (potentially very conservative) funnels can be related to the solution of a time-varying Lyapunov differential equation.

Let $\xi_0 : [t_a, t_b] \to \mathbb{R}^{n_x}$ be a solution of (5.1) and define

$$A(t) = \frac{\partial f}{\partial x}(t, \xi_0(t)).$$

For any symmetric positive-definite matrices $Q \in \mathbb{R}^{n_x \times n_x}$ and $P_f \in \mathbb{R}^{n_x \times n_x}$ let $P_0 : [t_a, t_b] \to \mathbb{R}^{n_x \times n_x}$ be the solution of the Lyapunov differential equation

$$\dot{P}(t) = -A(t)'P(t) - P(t)A(t) - Q, \tag{6.2}$$

that satisfies $P(t_f) = P_f$ (a unique solution exists as this is a linear differential equation). The following proposition shows that such a solution provides a natural, albeit conservative, method for generating funnels. The proof is relatively standard and omitted.

Proposition 6.1. *For ξ_0 and P_0 as above, there exists a positive constant function ρ sufficiently small such that $\mathcal{F}_{V_{(\xi_0, P_0, \rho)}}$ defines a funnel.*

It is important to note that no immediate formula is available for calculating the positive constant value of ρ. The above proposition only establishes that such a value should exist.

The following similar statement will be used below:

Proposition 6.2. *Let ξ_0 and P_0 be given as above. There exists a $c > 0$ such that $\mathcal{F}_{V_{(\xi_0, P_0, \rho)}}$ defines a funnel where*

$$\rho(t) = \exp\left(-c\frac{t_f - t}{t_f - t_0}\right). \tag{6.3}$$

■ 6.1.3 Parameterizations of Quadratic Lyapunov Functions

This section describes a well-known parameterization of matrix-valued functions $P : [t_0, t_f] \to \mathbb{R}^{n_x}$ which guarantee that

$$P(t) = P(t)' > 0 \quad \forall\, t \in [t_0, t_f].$$

The provided parameterization is convex, and in particular can be represented via LMIs involving the coefficients that determine the function P.

If P is parameterized as a general polynomial function, a sufficient condition is to ensure the above positivity is to require that

$$\Delta' P(t)\Delta = s_0(t, \Delta) + s_1(t, \Delta)(t - t_a)(t_b - t), \quad \forall\, t \in \mathbb{R}, \Delta \in \mathbb{R}^{n_x}$$

where s_0 and s_1 are SOS polynomials that are quadratic in Δ. The set of matrix polynomials in a single indeterminate that are positive definite on all of $\mathbb{R}$ are contained in this representation (see [20]). When P is a constant function, this requirement can obviously be simplified to testing that $P(0)$ is positive semidefinite. Additionally, if P is a linear function it is sufficient to require $P(0)$ and $P(1)$ both be symmetric positive semidefinite (due to the convexity of the cone of positive semidefinite matrices). These parameterizations also have clear generalizations for defining functions which are piecewise polynomial in t.

6.2 Optimization Approach

The optimization approach taken up in this chapter hinges on three assumptions:

(P1) The function f defining (5.1) is piecewise polynomial in time and polynomial in the remaining variables.

(P2) The function ξ_0 is piecewise polynomial.

(P3) The functions ρ and P, as in Section 6.1, are to be chosen from an affinely parameterized family of functions which are piecewise polynomial in time.

Without loss of generality, we assume there is a common set of "knot points", $t_0 < t_1 < \ldots < t_N = t_f$, on which the pieces of these piecewise functions are defined. The most burdensome of these assumptions is (P1). In applications one approach to satisfying (P1) is to approximate the true dynamics, for example by Taylor expansion. Methods exist for ensuring such an approximation does not yield incorrect certificates (e.g. [27]).

Specifically, we examine searching for a continuous piecewise polynomial ρ for a fixed time-varying quadratic function W, where it is assumed that the one sublevel set of $W(t_f, \cdot)$ belongs to the goal region $\mathcal{E}_f$. Once we restrict ourselves to piecewise polynomial vector fields and Lyapunov functions, we can approach our optimization task as a bilinear sum-of-squares program:

$$
\begin{aligned}
\underset{\rho, s_0, s_1, \ell_0, \ell_1, \mu}{\text{maximize}} \quad & \int_{t_0}^{t_f} \rho(t) dt \qquad (6.4)\\
\text{subj. to} \quad & \rho_{N-1}(t_f) \leq 1, \\
& \forall\, i \in \{0, \ldots, N-1\} : \\
& \quad \rho_i(t_{i+1}) = \rho_{i+1}(t_{i+1}), \\
& \quad \rho_i(t) \equiv s_{0i}(t) + s_{1i}(t)(t - t_i)(t_{i+1} - t), \\
& \quad \left[\dot{\rho}_i(t) - \frac{\partial W_i}{\partial x}(t,x) f_i(t,x) - \frac{\partial W_i}{\partial t}(t,x) - \epsilon\right] \\
& \quad \equiv \left[\ell_{0i}(t,x) + \ell_{1i}(t,x)(t - t_i)(t_{i+1} - t) + \mu_i(t,x)(\rho_i(t) - W_i(t,x))\right] \\
& \quad s_{0i}, s_{1i}, \ell_{0i}, \ell_{1i} \text{ SOS}.
\end{aligned}
$$

Here ϵ is a small positive constant and the decision parameters are the coefficients determining the pieces of ρ and the polynomials $s_{0i}, s_{1i}, \ell_{0i}, \ell_{1i}$, and μ_i (whose degrees are fixed). The cost function is a surrogate for the true volume (see (6.1)). One can verify that the above SOS conditions imply both that each ρ_i is non-negative on $[t_i, t_{i+1}]$ and that

$$\dot{\rho}_i(t) - \frac{\partial W_i}{\partial x}(t,x) f_i(t,x) - \frac{\partial W_i}{\partial t}(t,x) \geq \epsilon.$$

whenever $t \in [t_i, t_{i+1}]$ and $W_i(t,x) = \rho_i(t)$.

This optimization problem is *bilinear* in the decision variables (note the product of the multipliers μ_i with ρ_i). To address this issue, we take an approach similar to [59] by solving an alternating sequence of optimization problems holding some decision variables fixed.

6.2.1 The L-Step: Finding Multipliers

For a fixed $\rho(t)$ we can compute the multiplier polynomials via the following set of optimizations. For each interval $[t_i, t_{i+1}]$ we optimize over fixed degree polynomials ℓ_{0i}, ℓ_{1i}, and μ_i and a slack variable γ_i:

$$\begin{aligned} \underset{\gamma_i, \ell_{0i}, \ell_{1i}, \mu_i}{\text{minimize}} \quad & \gamma_i \\ \text{subj. to} \quad & \left[\gamma_i + \dot{\rho}_i(t) - \frac{\partial W_i}{\partial x}(t,x) f_i(t,x) - \frac{\partial W_i}{\partial t}(t,x) - \epsilon\right] \\ & \quad \equiv \left[\ell_{0i}(t,x) + \ell_{1i}(t,x)(t-t_i)(t_{i+1}-t) + \mu_i(t,x)(\rho_i(t) - W_i(t,x))\right] \\ & \quad \ell_{0i}, \ell_{1i} \text{ SOS} \end{aligned} \tag{6.5}$$

These programs can be computed in parallel. If all of the γ_i are negative then the combination of ρ and the optimized multipliers are feasible for the original bilinear SOS problem.

An obvious question is how to first obtain a feasible $\rho(t)$. Motivated by Proposition 6.2, we suggest the following search. We search over a positive constant $c \geq 0$, and take $\rho(t)$ to be a continuous piecewise polynomial approximation of:

$$\rho(t) \approx \exp\left(-c\frac{t_f - t}{t_f - t_0}\right).$$

If a given choice of c does not verify a funnel (i.e. if the optimal values of (6.5) are not all negative), we iteratively increase the value of c, and potentially the number of knot points of $\rho(t)$.

6.2.2 The V-Step: Improving $\rho(t)$.

Having solved (6.5) for each time interval, we now attempt to increase the size of the region verified by V by optimizing to increase $\rho(t)$. To do so, we pose the

following optimization with $\{\ell_{0i}, \ell_{1i}, \mu_i\}_{i=0}^{N-1}$ fixed from a solution to (6.5):

$$\begin{aligned}
\underset{\rho, s_0, s_1}{\text{maximize}} \quad & \int_{t_0}^{t_f} \rho(t) dt \qquad (6.6)\\
\text{subj. to} \quad & \rho_{N-1}(t_f) \leq 1, \\
& \forall\, i \in \{0, \ldots, N-1\} : \\
& \quad \rho_i(t_{i+1}) = \rho_{i+1}(t_{i+1}), \\
& \quad \rho_i(t) \equiv s_{0i}(t) + s_{1i}(t)(t - t_i)(t_{i+1} - t), \\
& \quad \left[\dot{\rho}_i(t) - \frac{\partial W_i}{\partial x}(t,x) f_i(t,x) - \frac{\partial W_i}{\partial t}(t,x) - \epsilon_i\right] \\
& \quad \equiv \left[\ell_{0i}(t,x) + \ell_{1i}(t,x)(t - t_i)(t_{i+1} - t) + \mu_i(t,x)(\rho_i(t) - W_i(t,x))\right] \\
& \quad s_{0i}, s_{1i} \text{ SOS}
\end{aligned}$$

Here $\epsilon_i > 0$ can be taken, for example, to be a constant satisfying $\epsilon_i < -\gamma_i$. So long as the class of $\rho_i(t)$ includes the $\rho_i(t)$ used in the optimizations (6.5), this optimization will be feasible, and can only improve the achieved value of the objective.

6.2.3 Variations

6.2.4 Time Sampled Relaxation

In terms of computational complexity, the high degree dependence on t in the above SOS optimization problems is the most immediate limiting factor. We now discuss an approximation to verifying the funnels based on sampling in time.

The proposed approximation verifies the conditions of Lemma 5.2 only at finely sampled times. For each interval $[t_i, t_{i+1}]$ from the above formulation, we choose a finer sampling $t_i = \tau_{i1} < \tau_{i2} < \ldots < \tau_{iM_i} = t_{i+1}$. We adapt the bilinear program of the previous section by testing the resulting conditions only at the time-points τ_{ij}. As a result, the terms involving the multipliers ℓ_{1i} are no longer necessary. Furthermore, the functions $\mu_i : \mathbb{R} \times \mathbb{R}^{n_x} \to \mathbb{R}$ can be replaced by polynomials $\mu_{ij} : \mathbb{R}^{n_x} \to \mathbb{R}$ (one for each τ_{ij}).

We pose the bilinear SOS optimization:

$$
\begin{aligned}
\underset{\rho,s_0,s_1,\ell,\mu}{\text{maximize}} \quad & \int_{t_0}^{t_f} \rho(t)dt \qquad (6.7)\\
\text{subj. to} \quad & \rho_{N-1}(t_f) \leq 1,\\
& \forall\, i \in \{0,\dots,N-1\}:\\
& \quad \rho_i(t_{i+1}) = \rho_{i+1}(t_{i+1}),\\
& \quad \rho_i(t) \equiv s_{0i}(t) + s_{1i}(t)(t-t_i)(t_{i+1}-t),\\
& \quad s_{0i}, s_{1i} \text{ SOS}\\
& \quad \forall j \in \{1,\dots,M_i\}:\\
& \quad\quad \left[\dot{\rho}_i(\tau_{ij}) - \frac{\partial W_i}{\partial x}(\tau_{ij},x) f_i(\tau_{ij},x) - \frac{\partial W_i}{\partial t}(\tau_{ij},x) - \epsilon_i\right]\\
& \quad\quad\quad \equiv \left[\ell_{ij}(x) + \mu_{ij}(x)(\rho_i(\tau_{ij}) - W_i(\tau_{ij},x))\right]\\
& \quad\quad \ell_{ij} \text{ SOS}.
\end{aligned}
$$

We use an analogous strategy of bilinear alternation to approach the problem and the same strategy is used to find an initial feasible $\rho(t)$. This optimization removes the complicated dependence on t, however it only tests a necessary but not sufficient condition for Lemma 5.2 to apply. It can be shown that if $V(t,x)$ does not satisfy the conditions of Lemma 5.2 there exists a sufficiently fine sampling such that the analogous optimization to (6.5) will not be feasible. However, this statement does not provide constraints based on computable quantities to ensure the above certificate is exact.

General Quadratic Lyapunov Functions

Our method thus far has been constrained to rescalings of a fixed computed quadratic function. In this section we present a modification of the method to search over more general quadratic Lyapunov functions. This will, for $n > 1$, increase the number of parameters describing the funnel, but may result in significantly larger volumes being verified.

We adapt the previous optimization problem in the following manner. The function $\rho(t)$ is taken to be a constant, whereas $P(t)$ is now defined to be piecewise linear:

$$P(t) = [(t-t_i)P_{i+1} + (t_{i+1}-t)P_i](t_{i+1}-t_i)^{-1}, \quad t \in [t_i, t_{i+1}],$$

where the matrices P_i are required to be positive-definite. Another important question is the choice of cost function. Similar to the work in [133], at a set of

sample times we measure the size of the sub-level set $\mathcal{F}_V(t)$ by the largest rescaling of another fixed ellipse (defined by a function $P_0(t)$) that is contained in $\mathcal{F}_V(t)$.

$$
\begin{aligned}
\underset{P,\ell_0,\ell_1,\mu}{\text{maximize}} \quad & -\sum_{i=1}^{N} \sigma_i \\
\text{subj. to} \quad & P_N = P_f, \\
& \forall\, i \in \{0,\dots,N-1\}: \\
& \quad \sigma_i P_0(t_i) \geq P_i \geq 0, \\
& \quad \Big[-\frac{\partial W_i}{\partial x}(t,x) f_i(t,x) - \frac{\partial W_i}{\partial t}(t,x) - \epsilon \Big] \\
& \quad \equiv \Big[\ell_{0i}(t,x) + \ell_{1i}(t,x)(t-t_i)(t_{i+1}-t) + \mu_i(t,x)(1-W_i(t,x)) \Big] \\
& \quad \ell_{0i}, \ell_{1i} \text{ SOS}.
\end{aligned}
\tag{6.8}
$$

This optimization problem is then split into a sequence of bilinear alternations as above.

Chapter 7

Examples and Applications

We first illustrate the general procedure with a one-dimensional polynomial system. Our second example is an idealized three degree of freedom satellite model. For this second example we compare numerically the proposed techniques. For both examples, the resulting SDPs are solved using SeDuMi version 1.3 ([126]).

7.1 A One-Dimensional Example

We examine a one dimensional time-varying polynomial differential equation defined by (5.1) with

$$f(t,x) = x - \frac{1}{2}x^2 + 2t - 2.4t^3, \quad (t \in [-1,1],\ x \in \mathbb{R}). \tag{7.1}$$

Our goal region is $\mathcal{E} = [0,1]$. We can solve nearly exact bounds for the backwards reachable set which flows into the goal by computing the solutions to (7.1) with final value conditions $x(1) = 1$ and $x(1) = 0$. To find our inner approximation of this set, we compute an approximate numerical trajectory, $\xi_0(t)$ with final value $\xi_0(1) = x_f = 0.5$. We take $P_f = 4$ so that $\mathcal{E}_f = \{x \mid |x - x_f|^2_{P_f} \leq 1\} = \mathcal{E}$. We numerically solve the Lyapunov equation (6.2).

We use $N = 40$ knot points, $\{t_i\}_{i=1}^N$, chosen to be the steps of a the variable time-step integration of the Lyapunov differential equation. We interpolate $\xi_0(t)$ with a piecewise cubic polynomial and $P(t)$ with a piecewise linear function. To find our initial candidate Lyapunov function, we begin by taking $\rho(t)$ to be a piecewise linear interpolation of $\exp\left(\frac{c(t-1)}{2}\right)$, for $c \geq 0$. Taking $c = 4$ provides a feasible candidate Lyapunov function. This feasible solution is then improved by bilinear alternation. Both the initial and optimized sets are plotted against the known bounds in Figure 7.1.

After a single bilinear alternation, a tight region is found. Note that the symmetry of the Lyapunov function around the trajectory restricts the region being verified. Additional trajectories could be used to continue to grow the verified region.

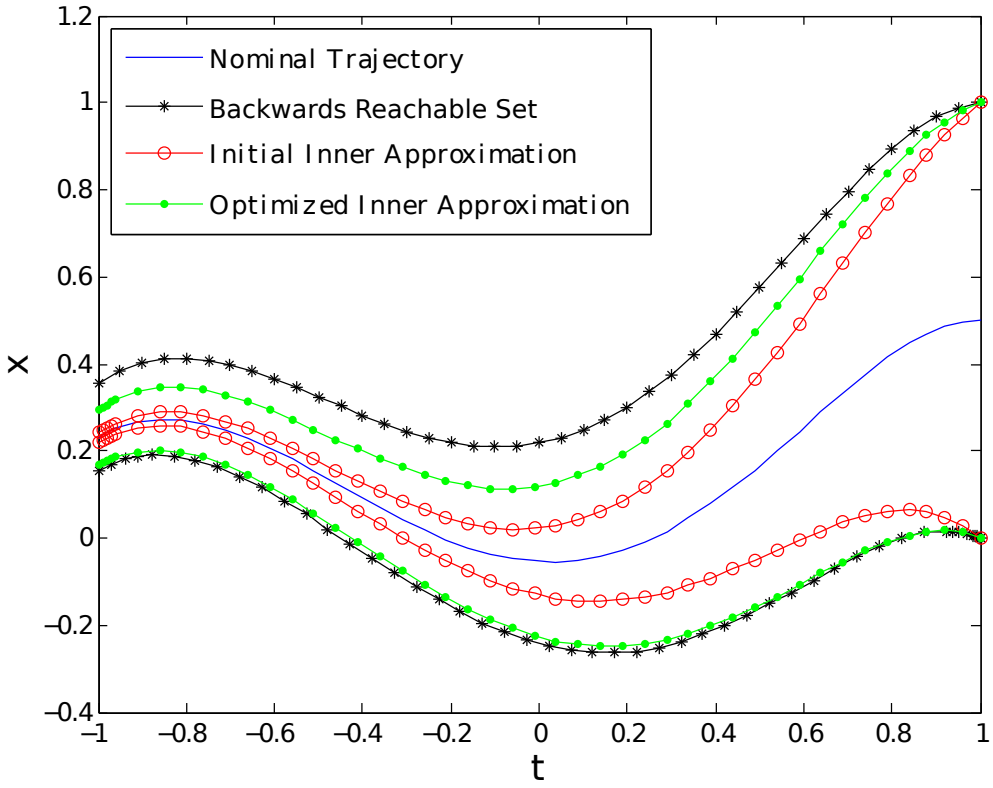

Figure 7.1. The backwards reachable set and inner approximations calculated by the method. Surrounding the nominal trajectory (solid blue) are time-varying intervals. An initial candidate Lyapunov function (red open circle) is improved via the bilinear optimization (solid green circle). In this case, a single step of alternation provided a certificate tight to the known bounds (black stars). Note that the certificate is symmetric about the trajectory, and as a result is generally sub-optimal.

■ 7.2 Trajectory Stabilization of Satellite Dynamics

We next evaluate a time-varying positively invariant region around a feedback stabilized nominal trajectory. In past work, [130], it was demonstrated how trajectory optimization and randomized search can be combined with such certificates to approximate the controllable region for a smooth nonlinear system.

We examine the stabilization of a nominal trajectory for a rigid body floating in space subject to commanded torques. The state of the system is $x = [\sigma', \omega']'$ where $\sigma \in \mathbb{R}^3$ are the Modified Rodriguez parameters and $\omega \in \mathbb{R}^3$ are the angular velocities of the body about its principal axes.

The open-loop dynamics,

$$\dot{\xi}(t) = f_0(\xi(t), u(t)), \tag{7.2}$$

are defined by

$$f_0\left(\begin{bmatrix}\sigma\\ \omega\end{bmatrix}, u\right) = \begin{bmatrix} J(\sigma)\omega \\ -H^{-1}(\omega \times H\omega - u)\end{bmatrix} \quad (\sigma, \omega, u \in \mathbb{R}^3) \tag{7.3}$$

where

$$J(\sigma) = (1 - \|\sigma\|^2)I + 2\sigma\sigma' - 2\begin{bmatrix} 0 & \sigma_3 & \sigma_2 \\ \sigma_3 & 0 & \sigma_1 \\ \sigma_2 & \sigma_1 & 0\end{bmatrix},$$

$H = H' > 0$ is the diagonal, positive-definite inertia matrix of the system and u is a vector of torques. In our example $H = \mathrm{diag}([5, 3, 2])$. We now design a control policy $u(t) = \pi(t, x(t))$ such that the closed loop system defined by (5.1) with

$$f(t, x) = f_0(x, \pi(t, x)) \tag{7.4}$$

satisfies the assumptions of our method.

Our goal region is defined by an ellipse centered on the origin, described by a positive-definite matrix P_G,

$$P_G = \begin{bmatrix} 36.1704 & 0 & 0 & 12.1205 & 0 & 0 \\ 0 & 17.4283 & 0 & 0 & 7.2723 & 0 \\ 0 & 0 & 9.8911 & 0 & 0 & 4.8482 \\ 12.1205 & 0 & 0 & 9.1505 & 0 & 0 \\ 0 & 7.2723 & 0 & 0 & 7.3484 & 0 \\ 0 & 0 & 4.8482 & 0 & 0 & 6.2557 \end{bmatrix}.$$

We begin with a nominal command:

$$u_0(t) = \frac{1}{100} t(t-5)(t+5) \begin{bmatrix} -1 \\ -1 \\ 1 \end{bmatrix}, \quad (t \in [0,5]).$$

We compute the solution, $\xi_0(t)$ to (7.3) with $u(t) \equiv u_0(t)$ and $\xi(5) = 0$. Next, we design a time-varying LQR controller around the trajectory based on the dynamics linearized about the trajectory (see, for example, [47] Chapter 5). Taking $R = 10I_3$ and $Q = I_6$, we solve the Riccati differential equation:

$$-\dot{S}^\star(t) = A(t)'S^\star(t) + S^\star(t)A(t) + Q - S^\star(t)B(t)R^{-1}B(t)'S^\star(t), \quad S^\star(5) = P_f$$

where $P_f = 1.01P_G$, $A(t) = \frac{\partial}{\partial x} f_0(\xi_0(t), u_0(t))$, and $B(t) = \frac{\partial}{\partial u} f_0(\xi_0(t), u_0(t))$.

This procedure gives us a time-varying gain matrix:

$$K(t) = R^{-1}B(t)'S^\star(t)$$

To force $\pi(t,x)$ to be piecewise polynomial in t and polynomial in x we take a piecewise constant approximation of $\hat{K}$ of K and a piecewise cubic interpolation $\hat{\xi}_0(t)$ of $\xi_0(t)$. Our control policy is then:

$$\pi(t,x) = u_0(t) - \hat{K}(t)(x - \hat{\xi}_0(t)).$$

We now examine the closed loop dynamics. We compare three computed certificates in terms of their computation time and performance (funnel volume). In particular, we compute an exact certificate using the $\rho(t)$ parameterization. We then compute time-sampled certificates using both the $\rho(t)$ parameterization and the more general quadratic parameterization. For the $\rho(t)$ parameterization, we take $P_0(t)$ to be a piecewise linear approximation of $S^\star(t)$. All of the above approximations were piecewise with $N = 49$ knot points chosen by a variable time-step integration of the Riccati differential equation. For the time-sampled versions we verify necessary conditions at $M_i = 4$ points equally spaced in each interval $[t_i, t_{i+1}]$.

For an initial $\rho(t)$ we use a linear interpolation of an exponential weighting as suggested by Proposition 6.2. In particular $c = 3$ proved feasible for both methods. We choose the initial $P(t)$ to agree at the knot points with the Lyapunov candidates defined by this initial choice of $\rho(t)$.

We use the following stopping criterion. Let $\mathcal{F}^{(k)}$ be the funnel on the k-th iteration. We halt the iteration if:

$$\frac{\text{vol}(\mathcal{F}^{(k)}) - \text{vol}(\mathcal{F}^{(k-1)})}{\text{vol}(\mathcal{F}^{(k-1)})} < 0.025 \tag{7.5}$$

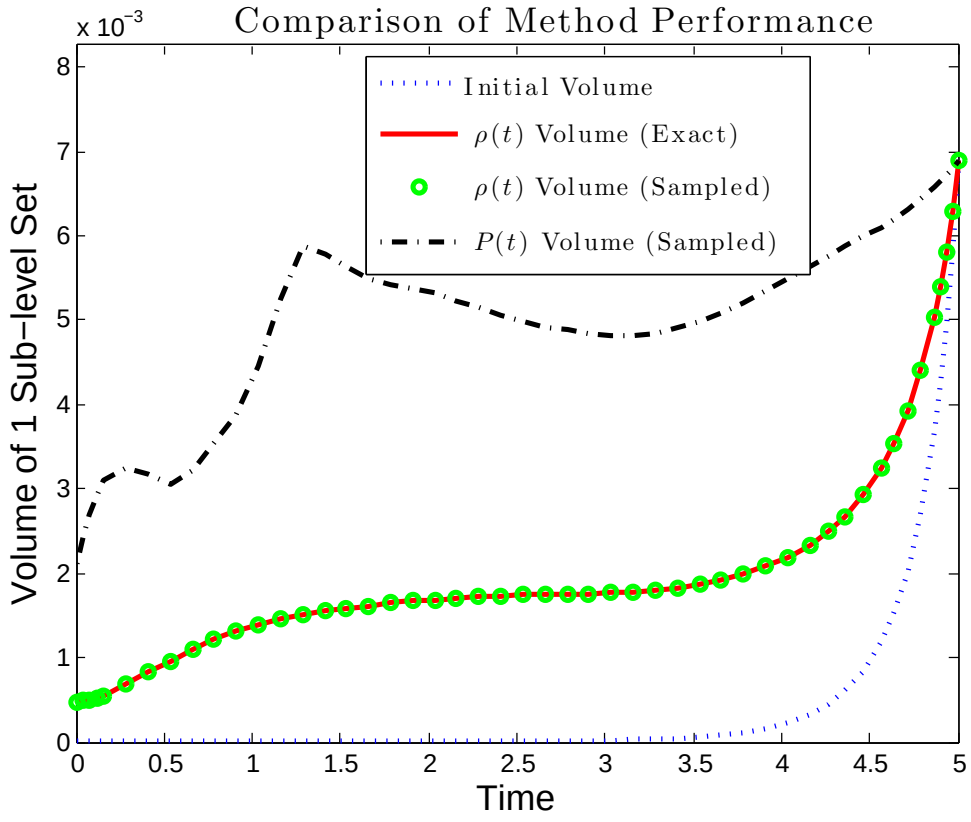

Figure 7.2. Comparison of optimized volumes using the exact and time-sampled methods for the $\rho(t)$ parameterization and the time-sampled method with the general quadratic form ($P(t)$) parameterization of Section 6.1.

Figure 7.2 compares the result of the final iteration for all three methods. The figure plots the volume of Ω_t for each $t \in [0, 5]$. We have found that for the $\rho(t)$ parameterization typically very few iterations are required for the procedure to converge; both time-sampled and exact methods stopped after two iterations. The more complicated $P(t)$ parameterization stopped after 9 iterations. For the $\rho(t)$ formulation, the time-sampled and exact methods produce nearly identical results. The more general Lyapunov function shows a substantial increase in funnel volume. However, this comes at higher computational cost.

Table 7.1 compares the run times. The L-Step consisted of 48 independent SDPs for the exact method and 192 independent SDPs for both time-sampled computations. These computations were performed on a 12-core 3.33 GHz Intel

Table 7.1. Runtime comparison of SDPs for exact and time-sampled approaches.

Method	Iters	L-Step (sec/iter)	V-Step (sec/iter)	Total (min:sec)
$\rho(t)$ Exact	2	5336.5	1378.0	223:49
$\rho(t)$ Sampled	2	45.0	220.0	5:50
$P(t)$ Sampled	9	45.5	887.5	139:57

Xeon computer with 24 Gb of RAM. These L-Step programs can be trivially parallelized for speedup.

Chapter 8

Conclusion

This thesis has provided methods for addressing the identification and analysis of nonlinear dynamical systems. With regards to system identification, a family of algorithms for estimating stable nonlinear discrete time state-space models was introduced based on convex sufficient conditions for stability and easily minimized convex upper bounds for simulation error. Additionally, a computational approach to analyzing the backwards reachable sets for nonlinear, nonautonomous ordinary differential equations was provided. Below I discuss the problems which these techniques are most relevant to, some caveats regarding the scalability of the proposed approaches, and topics of ongoing research.

8.1 Robust Convex Optimization for Nonlinear System Identification

The techniques introduced in Part I of this thesis are of greatest relevance to "black-box" identification of dynamical models, i.e. matching highly flexible models to data without exploiting much in the way of *a-priori* structural information. Black-box identification is important for situations where parameterizations of the "true" dynamics governing a system are prohibitively complex, poorly identifiable, or simply unknown.

One major obstacle to scaling the approaches provided in this work to larger systems lies in the use of polynomial equations. This arises due to our dependence on sums-of-squares programming for ensuring model well-posedness and stability. Using *dense* polynomials limits scalability as the number of coefficients required to describe the space of polynomials of degree d in n variables grows exponentially as both n and d tend to infinity. Using the currently available technologies for solving semidefinite programs, the problems which are tractable for the methods introduced in this work either have a limited dimensionality (a state dimension of at most 6) but potentially a relatively high degree of nonlinearity, or have a very structured nonlinearity (as in the example of Section 3.6) with potentially higher dimension.

8.1.1 Extensions and Future Work

A number of extensions of the techniques presented in this thesis are the subject of ongoing work with collaborators.

Alternative Identification Objectives

While this work focused exclusively on minimizing simulation error, there are many situations where models are more appropriately chosen by optimizing other loss functions. Some obvious situations where simulation error minimization may not be appropriate are:

1. The system being modeled is not ℓ_2-incrementally stable (i.e. has large sensitivities to initial conditions).

2. The experimental condition involves substantial process noise, or generally a noise models is desirable.

3. The final application requires only short term predictions.

The simplest modifications of the techniques described in this work to these situations might look at fixed simulation horizons or "discounted" versions of simulation error involving geometrically decaying weights. A more palatable alternative would be to adapt the methods described in Chapters 2 and 4 to other identification paradigms such as the maximum-likelihood and prediction-error methods. Some initial work indicates that joint estimation of output noise spectrum and open-loop simulation models should be possible in the framework suggested by Chapter 4.

Continuous Time Identification

Preliminary extensions of the methods described in this thesis to the identification of stable continuous time models (i.e. defined by ordinary differential equations) are provided in [132]. In [13] a similar alternative approach was suggested. There are several open challenges in applying these approaches to practical data sets arising from experiments. First, the methods assume access to the derivative of the state signal. Second, the methods require knowledge of the excitation and response signals on the entire time interval (i.e. simulation error bounds contained in these works are not applicable given only data recorded at finite sample points without some additional approximations). One approach to overcoming these difficulties is to approximate data signals by functions for which analytical derivatives and integrals are available such as splines and trigonometric functions.

The latter set of functions may be particularly relevant for approximating nonlinear systems from responses to periodic excitations. Another topic for future research is the identifying an analog to the contribution of Chapter 4 for continuous time systems.

Incremental Passivity and ℓ_2-Gain Bounds

There are straightforward ways to modify the dissipation inequalities used to ensure stability in Chapter 2 to instead guarantee identified models are incrementally passive or possess incremental ℓ_2 input-output gain bounds (see [32] for definitions of these properties). Coverage of the corresponding classes of LTI systems with these properties can be readily established via application of the Positive Real Lemma and the Bounded Real Lemma (see, for example, [143] Chapter 21). Relating the passivity of discrete time models back to passivity that arises in physical systems defined by ODEs presents difficulties which have been touched on for LTI models in [55]. This topic deserves further study in the nonlinear case. Such incremental input-output properties also allow for establishing simulation error bounds for feedback interconnections of subsystems identified individually from closed-loop data. This observation may open the way towards parallelized applications of the methods described in this thesis to structured systems.

Limit Cycle Stability

Another area of ongoing research is the identification of differential equation models which admit stable limit cycles (unforced oscillations). Systems with stable limit cycles naturally cannot be incrementally stable as solutions beginning at different points of the limit cycle never converge toward one another. In a preliminary paper, [86], collaborators and the author explored adaptations of techniques discussed in this thesis to relaxed notions of stability more suitable for the identification of models with such stable oscillations. Figure 8.1, reproduced from [86], compares open-loop simulations of three ODE models (blue) matched to data collected from electrical excitation of a live neuron (grey). The model in (a) is identified by minimizing a cost function similar to equation error. The simulation of this model eventually becomes unstable and diverges. The model in (b) is fit using a technique similar to minimization of the RIE. This yields a model which is excessively damped compared to the experimental system. The final model is identified using the technique suggested in [86]. This last model very accurately reproduces the qualitative behavior of the experimental system. Note that the simulation error for such a model is actually quite large due to the slight differences in phase between the simulated "spikes" and actual "spikes" generated by the neuron. These errors are in agreement with the discussion above regarding

persistence of errors in phase for systems with stable limit cycles. Despite these facts, the qualitative behavior of the model clearly matches the experimental system response.

8.2 Robustness Analysis of Dynamic Trajectories

Part II of this thesis provided methods for analyzing the behavior of solutions of polynomial dynamical systems. In practice, the set of systems with polynomial dynamics is somewhat limited, though there is some progress in applying SOS techniques to systems determined by *semialgebraic* or other nonlinear functional forms (see, for example, [51] Chapter 2 and [4] Chapter 14). In other circumstances, polynomial approximations of dynamics (e.g. Taylor approximations) can be employed. At the expense of additional computational complexity one can ensure that such approximations are conservative (see [27]). Perhaps the greatest limitations of the proposed approach are the difficulty of identifying an initial feasible candidate Lyapunov function, and the lack of systematic methods for choosing the degrees of multiplier polynomials.

8.2.1 Extensions and Future Work

In a straightforward manner the techniques described in this work can be extended to dynamics which are piecewise polynomials including, for example, the effects of actuator saturation (see [130]). It is also straightforward to accommodate parametric uncertainties and worst case analysis with respect to disturbances. Incorporating these extensions, however, rapidly increases the computational complexity of the verification task.

A number of recent papers have extended or modified the approach suggested in Part II (portions of this work were published in [131]). In [85], the author and collaborators demonstrated how ideas similar to Part II of this thesis can be applied to the analysis of limit cycles arising in hybrid dynamics. A related method presented in [93] (though with a different optimization objective) was applied to models of a perching unmanned aerial vehicle. The paper [84] provides an iterative control *design* strategy based on choosing control laws to maximize the size of the funnel which can be verified. Most importantly, this last paper examines experimental applications of the identified control laws and partial experimental validation of the computed funnels.

Perhaps the most pressing topic for future research is the interaction between the theoretical guarantees provided by "funnels" and experimental practice. If an experimental system violates a given funnel at some level one has proven the model used to compute the funnel invalid. Finding a meaningful way to incorporate such

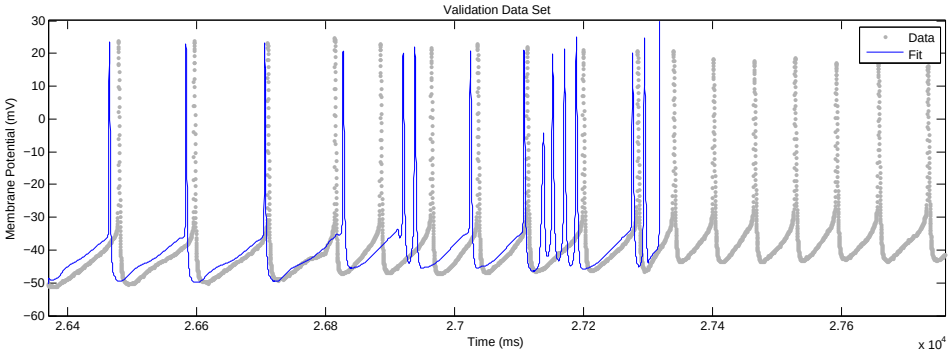

(a) Performance of a model identified using least squares.

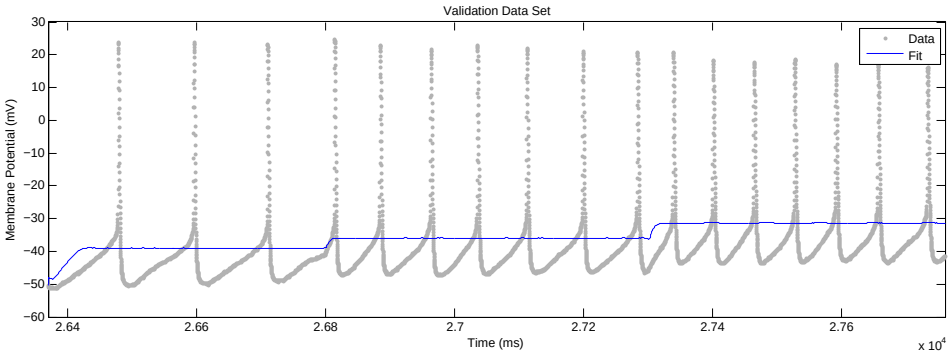

(b) Performance of a model identified using a method related to RIE minimization.

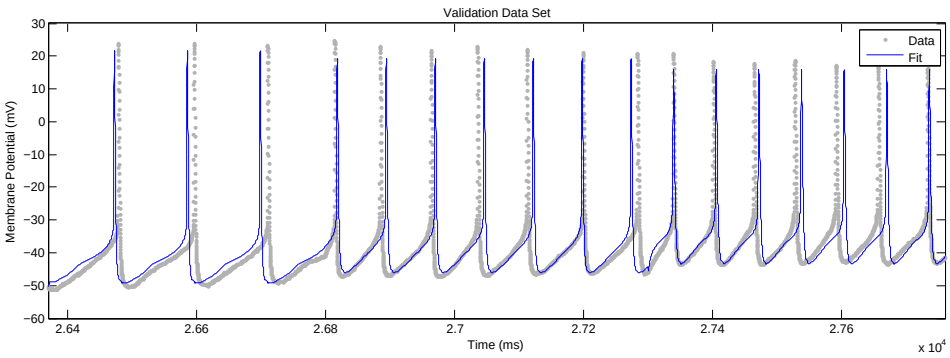

(c) Performance of a model identified using the technique described in [86].

Figure 8.1. A comparison of identification approaches to black-box modeling of the cellular membrane potential (gray) of a live neuron in response to injected current. Open-loop simulations of three ODE models (blue) identified using competing techniques are compared (see [86] for details and the text for discussion).

negative results into improved certificates or models represents a serious challenge (and potential opportunity) for practical application of these techniques.

References

[1] A. Abate, A. D'Innocenzo, and M. Di Benedetto. Approximate abstractions of stochastic hybrid systems. *Automatic Control, IEEE Transactions on*, 56(11):2688–2694, 2011.

[2] R. Alur, T. Henzinger, G. Lafferriere, and G. Pappas. Discrete abstractions of hybrid systems. *Proceedings of the IEEE*, 88(7):971–984, 2000.

[3] D. Angeli. A Lyapunov approach to incremental stability properties. *Automatic Control, IEEE Transactions on*, 47(3):410 –421, Mar. 2002.

[4] M. F. Anjos and J. B. Lasserre, editors. *Handbook on Semidefinite, Conic and Polynomial Optimization*. Springer, New York, 1st edition, 2012.

[5] H. Ase, T. Katayama, and H. Tanaka. A state-space approach to identification of Wiener-Hammerstein benchmark model. In *System Identification, 15th IFAC Symposium on*, volume 15, pages 1092–1097, Jul. 2009.

[6] E.-W. Bai and Y. Liu. Recursive direct weight optimization in nonlinear system identification: A minimal probability approach. *Automatic Control, IEEE Transactions on*, 52(7):1218–1231, 2007.

[7] E.-W. Bai, R. Tempo, and Y. Liu. Identification of IIR nonlinear systems without prior structural information. *Automatic Control, IEEE Transactions on*, 52(3):442–453, 2007.

[8] E.-W. Bai, Y. Ye, and R. Tempo. Bounded error parameter estimation: A sequential analytic center approach. *Automatic Control, IEEE Transactions on*, 44(6):1107 –1117, Jun. 1999.

[9] J. Bernussou, P. Peres, and J. Geromel. A linear programming oriented procedure for quadratic stabilization of uncertain systems. *Systems and Control Letters*, 13(1):65 – 72, 1989.

[10] B. Besselink, N. van de Wouw, and H. Nijmeijer. Model reduction for a class of convergent nonlinear systems. *Automatic Control, IEEE Transactions on*, 57(4):1071 –1076, Apr. 2012.

[11] J. T. Betts. *Practical Methods for Optimal Control and Estimation Using Nonlinear Programming*. SIAM, Philadelphia, 2nd edition, 2010.

[12] S. Bittanti and L. Piroddi. Nonlinear identification and control of a heat exchanger: A neural network approach. *Journal of the Franklin Institute*, 334(1):135 – 153, 1997.

[13] B. Bond, Z. Mahmood, Y. Li, R. Sredojevic, A. Megretski, V. Stojanovi, Y. Avniel, and L. Daniel. Compact modeling of nonlinear analog circuits using system identification via semidefinite programming and incremental stability certification. *Computer-Aided Design of Integrated Circuits and Systems, IEEE Transactions on*, 29(8):1149 –1162, Aug. 2010.

[14] A. Böttcher and S. M. Grudsky. *Spectral Properties of Banded Toeplitz Matrices*. Society for Industrial and Applied Mathematics, Philadelphia, 2005.

[15] S. Boyd and L. O. Chua. Fading memory and the problem of approximating nonlinear operators with volterra series. *Circuits and Systems, IEEE Transactions on*, 32(11):1150–1171, Nov. 1985.

[16] M. Branicky, M. Curtiss, J. Levine, and S. Morgan. RRTs for nonlinear, discrete, and hybrid planning and control. In *Decision and Control, 2003. Proceedings. 42nd IEEE Conference on*, volume 1, pages 657–663 Vol.1, 2003.

[17] R. R. Burridge, A. A. Rizzi, and D. E. Koditschek. Sequential composition of dynamically dexterous robot behaviors. *International Journal of Robotics Research*, 18(6):534–555, June 1999.

[18] P. Caines. Stationary linear and nonlinear system identification and predictor set completeness. *Automatic Control, IEEE Transactions on*, 23(4):583–594, 1978.

[19] P. E. Caines. *Linear Stochastic Systems*. John Wiley, New York, 1988.

[20] A. Caldern. A note on biquadratic forms. *Linear Algebra and its Applications*, 7(2):175 – 177, 1973.

[21] G. Casella and R. L. Berger, editors. *Statistical Inference*. Duxbury, Pacific Grove, CA., 2nd edition, 2002.

[22] V. Cerone, D. Piga, and D. Regruto. Enforcing stability constraints in set-membership identification of linear dynamic systems. *Automatica*, 47(11):2488 – 2494, 2011.

[23] V. Cerone, D. Piga, and D. Regruto. Set-membership error-in-variables identification through convex relaxation techniques. *Automatic Control, IEEE Transactions on*, 57(2):517 –522, Feb. 2012.

[24] V. Cerone, D. Piga, and D. Regruto. Computational load reduction in bounded error identification of Hammerstein systems. *Automatic Control, IEEE Transactions on*, 58(5):1317–1322, 2013.

[25] J. Chen and G. Gu, editors. *Control-Oriented System Identification: An H-Infinity Approach*. Wiley-Interscience, New York, 1st edition, 2000.

[26] J. Chen, C. Nett, and M. K. H. Fan. Worst case system identification in H-Infinity: Validation of a priori information, essentially optimal algorithms, and error bounds. *Automatic Control, IEEE Transactions on*, 40(7):1260–1265, 1995.

[27] G. Chesi. Estimating the domain of attraction for non-polynomial systems via LMI optimizations. *Automatica*, 45(6):1536 – 1541, 2009.

[28] A. Chottera and G. Jullien. A linear programming approach to recursive digital filter design with linear phase. *Circuits and Systems, IEEE Transactions on*, 29(3):139–149, 1982.

[29] S. H. Collins, A. Ruina, R. Tedrake, and M. Wisse. Efficient bipedal robots based on passive-dynamic walkers. *Science*, 307:1082–1085, Feb. 2005.

[30] M. A. Dahleh, E. D. Sontag, D. N. Tse, and J. N. Tsitsiklis. Worst-case identification of nonlinear fading memory systems. *Automatica*, 31(3):503 – 508, 1995.

[31] DaISy: Database for the Identification of Systems. `http://homes.esat.kuleuven.be/~smc/daisy/`, 2013. Retrieved 2013-13-12. Used dataset: Liquid-saturated steam heat exchanger, section: Process Industry Systems, code: 97-002.

[32] C. A. Desoer and M. Vidyasagar. *Feedback Systems: Input-Output Properties*. Academic Press, Inc., New York, 1st edition, 1975.

[33] P. dos Santos, J. Ramos, and J. de Carvalho. Identification of bilinear systems with white noise inputs: An iterative deterministic-stochastic subspace approach. *Control Systems Technology, IEEE Transactions on*, 17(5):1145–1153, 2009.

[34] P. L. dos Santos, J. A. Ramos, and J. M. de Carvalho. Identification of a benchmark Wiener-Hammerstein: A bilinear and Hammerstein-Bilinear model approach. *Control Engineering Practice*, 20(11):1156 – 1164, 2012. Special Section: Wiener-Hammerstein System Identification Benchmark.

[35] F. J. Doyle III, R. K. Pearson, and B. A. Ogunnaike. *Identification and Control Using Volterra Models*. Springer-Verlag, London., 1st edition, 2002.

[36] B. Dumitrescu and R. Niemisto. Multistage IIR filter design using convex stability domains defined by positive realness. *Signal Processing, IEEE Transactions on*, 52(4):962–974, 2004.

[37] D. Eckhard, A. S. Bazanella, C. R. Rojas, and H. Hjalmarsson. Input design as a tool to improve the convergence of PEM. *Automatica*, 49(11):3282 – 3291, 2013.

[38] M. Farina and L. Piroddi. An iterative algorithm for simulation error based identification of polynomial input-output models using multi-step prediction. *International Journal of Control*, 83(7):1442–1456, 2010.

[39] W. Favoreel, B. De Moor, and P. Van Overschee. Subspace identification of bilinear systems subject to white inputs. *Automatic Control, IEEE Transactions on*, 44(6):1157–1165, 1999.

[40] M. Franz and B. Schölkopf. A unifying view of Wiener and Volterra theory and polynomial kernel regression. *Neural computation*, 18(12):3097 3118, 2006.

[41] E. Frazzoli, M. Dahleh, and E. Feron. Maneuver-based motion planning for nonlinear systems with symmetries. *Robotics, IEEE Transactions on*, 21(6):1077–1091, 2005.

[42] V. Fromion, S. Monaco, and D. Normand-Cyrot. Asymptotic properties of incrementally stable systems. *Automatic Control, IEEE Transactions on*, 41(5):721–723, 1996.

[43] V. Fromion and G. Scorletti. The behaviour of incrementally stable discrete time systems. In *American Control Conference, 1999. Proceedings of the 1999*, volume 6, pages 4563 –4567 vol.6, 1999.

[44] Z. Ghahramani and S. T. Roweis. Learning nonlinear dynamical systems using an EM algorithm. In *Advances in neural information processing systems*, volume 11, pages 431–437, 1999.

[45] A. Girard. Reachability of uncertain linear systems using zonotopes. In M. Morari, L. Thiele, and F. Rossi, editors, *Hybrid Systems: Computation and Control*, volume 3414 of *Lecture Notes in Computer Science*, pages 291–305, Berlin, 2005. Springer.

[46] I. Goethals, K. Pelckmans, J. A. K. Suykens, and B. De Moor. Subspace identification of Hammerstein systems using least squares support vector machines. *Automatic Control, IEEE Transactions on*, 50(10):1509–1519, 2005.

[47] M. Green and D. J. N. Limebeer, editors. *Linear Robust Control*. Prentice-Hall, Upper Saddle River, New Jersey, 1st edition, 1995.

[48] J. K. Hale. *Ordinary Differential Equations*. Robert E. Krieger Publishing Company, New York, 1980.

[49] Y. Han and R. A. de Callafon. Identification of Wiener-Hammerstein benchmark model via rank minimization. *Control Engineering Practice*, 20(11):1149 – 1155, 2012. Special Section: Wiener-Hammerstein System Identification Benchmark.

[50] J. A. Hausman, W. K. Newey, H. Ichimura, and J. L. Powell. Identification and estimation of polynomial errors-in-variables models. *Journal of Econometrics*, 50(3):273 – 295, 1991.

[51] D. Henrion and A. Garulli, editors. *Control Applications of Sum of Squares Programming*, volume 312 of *Lecture Notes in Control and Information Sciences*. Springer Berlin / Heidelberg, 2005.

[52] D. Henrion, M. Sebek, and V. Kucera. Positive polynomials and robust stabilization with fixed-order controllers. *Automatic Control, IEEE Transactions on*, 48(7):1178–1186, 2003.

[53] M. Henson and D. Seborg, editors. *Nonlinear Process Control*. Prentice-Hall, Upper Saddle River, NJ, 1st edition, 1996.

[54] B. L. Ho and R. E. Kalman. Effective construction of linear state-variable models from input/output functions. *Regelungstechnik*, 14(12):545–548, 1966.

[55] J. Hoagg, S. Lacy, R. Erwin, and D. Bernstein. First-order-hold sampling of positive real systems and subspace identification of positive real models. In *American Control Conference, 2004. Proceedings of the 2004*, volume 1, pages 861–866 vol.1, 2004.

[56] C. Hsu. *Cell-to-Cell Mapping: A Method of Global Analysis for Nonlinear Systems.* Springer-Verlag, New York, 1st edition, 1987.

[57] K. W. Iliff. Parameter estimation for flight vehicles. *Journal of Guidance, Control, and Dynamics*, 12:609–622, 1989.

[58] E. M. Izhikevich. *Dynamical Systems in Neuronscience: The Geometry of Excitability and Bursting.* MIT Press, Cambridge, Massachusetts, 1st edition, 2007.

[59] Z. Jarvis-Wloszek, R. Feeley, W. Tan, K. Sun, and A. Packard. Control applications of sum of squares programming. In D. Henrion and A. Garulli, editors, *Positive Polynomials in Control*, volume 312 of *Lecture Notes in Control and Information Sciences*, pages 3–22. Springer Berlin / Heidelberg, 2005.

[60] A. Julius and G. Pappas. Probabilistic testing for stochastic hybrid systems. In *Decision and Control, 2008. CDC 2008. 47th IEEE Conference on*, pages 4030–4035, 2008.

[61] A. A. Julius and G. J. Pappas. Trajectory based verification using local finite-time invariance. In R. Majumdar and P. Tabuada, editors, *Hybrid Systems: Computation and Control*, volume 5469 of *Lecture Notes in Computer Science*, pages 223–236. Springer Berlin Heidelberg, 2009.

[62] S. Karaman and E. Frazzoli. Sampling-based algorithms for optimal motion planning. *International Journal of Robotics Research*, 30(7):846–894, 2011.

[63] H. K. Khalil. *Nonlinear Systems.* Prentice Hall, Upper Saddle River, 2001.

[64] W. Khalil and E. Dombre. Chapter 12 - Identification of the dynamic parameters. In W. Khalil and E. Dombre, editors, *Modeling, Identification and Control of Robots*, pages 291 – 311. Butterworth-Heinemann, Oxford, 2004.

[65] E. Kostousova. Control synthesis via parallelotopes: Optimization and parallel computations. *Optimization Methods and Software*, 14(4):267–310, 2001.

[66] N. Krasovski and A. Subbotin. *Positional Differential Games.* Springer-Verlag, New York, 1st edition, 1988.

[67] S. Kulkarni and S. Posner. Nonparametric output prediction for nonlinear fading memory systems. *Automatic Control, IEEE Transactions on*, 44(1):29 –37, Jan. 1999.

[68] A. Kurzhanski and P. Varaiya. On ellipsoidal techniques for reachability analysis. *Optimization Methods and Software*, 17:177–237, 2000.

[69] A. A. Kurzhanskiy and P. Varaiya. Computation of reach sets for dynamical systems. In W. S. Levine, editor, *The Control Handbook*, 2010.

[70] S. Lacy and D. Bernstein. Subspace identification with guaranteed stability using constrained optimization. In *American Control Conference, 2002. Proceedings of the 2002*, volume 4, pages 3307 – 3312 vol.4, 2002.

[71] G. Lafferriere, G. J. Pappas, and S. Yovine. Symbolic reachability computation for families of linear vector fields. *Symbolic Computation, Journal of*, 32:231–253, 2001.

[72] S. LaValle and J. Kuffner, J.J. Randomized kinodynamic planning. In *Robotics and Automation, 1999. Proceedings. 1999 IEEE International Conference on*, volume 1, pages 473–479 vol.1, 1999.

[73] G. Liu. *Nonlinear Identification and Control: A Neural Network Approach.* Springer-Verlag, London., 1st edition, 2001.

[74] L. Ljung. Convergence analysis of parametric identification methods. *Automatic Control, IEEE Transactions on*, 23(5):770–783, 1978.

[75] L. Ljung. *System Identification: Theory for the User.* Prentice Hall, Englewood Cliffs, New Jersey, USA, 3rd edition, 1999.

[76] L. Ljung. Perspectives on system identification. *Annual Reviews in Control*, 34(1):1 – 12, 2010.

[77] L. Ljung. Comments on model validation as set membership identification. In *Robustness in Identification and Control*, volume 245 of *Lecture Notes in Control and Information Sciences*, pages 7–16, 2011.

[78] L. Ljung. System Identification Toolbox: Getting Started Guide. `http://www.mathworks.com/help/pdf_doc/ident/ident_gs.pdf`, 2013. Retrieved 2013-09-12.

[79] L. Ljung and P. Caines. Asymptotic normality of prediction error estimators for approximate system models. *Stochastics*, 3:29–46, 1979.

[80] W. Lohmiller and J.-J. E. Slotine. On contraction analysis for non-linear systems. *Automatica*, 34(6):683 – 696, 1998.

[81] G. G. Lorentz. *Approximation of Functions*. Holt, Rinehart, and Winston, New York, 1966.

[82] H.-J. Lüthi. On the solution of variational inequalities by the ellipsoid method. *Mathematics of Operations Research*, 10(3):512–522, Aug 1985.

[83] J. Lygeros, C. Tomlin, and S. Sastry. Controllers for reachability specifications for hybrid systems. *Automatica*, 35:349–370, 1999.

[84] A. Majumdar, A. Ahmadi, and R. Tedrake. Control design along trajectories with sums of squares programming. In *Robotics and Automation (ICRA), 2013 IEEE International Conference on*, pages 4054–4061, 2013.

[85] I. Manchester, M. Tobenkin, M. Levashov, and R. Tedrake. Regions of attraction for hybrid limit cycles of walking robots. In *18th IFAC World Congress*, volume 18, pages 5801–5806, 2011.

[86] I. Manchester, M. Tobenkin, and J. Wang. Identification of nonlinear systems with stable oscillations. In *Decision and Control and European Control Conference (CDC-ECC), 2011 50th IEEE Conference on*, pages 5792–5797, 2011.

[87] A. Marconato, J. Sjöberg, and J. Schoukens. Initialization of nonlinear state-space models applied to the Wiener-Hammerstein benchmark. *Control Engineering Practice*, 20(11):1126 – 1132, 2012. Special Section: Wiener-Hammerstein System Identification Benchmark.

[88] A. Megretski. Convex optimization in robust identification of nonlinear feedback. In *Decision and Control, 2008. CDC 2008. 47th IEEE Conference on*, pages 1370 –1374, Dec. 2008.

[89] M. Milanese and C. Novara. Model quality in identification of nonlinear systems. *Automatic Control, IEEE Transactions on*, 50(10):1606–1611, 2005.

[90] M. Milanese and R. Tempo. Optimal algorithms theory for robust estimation and prediction. *Automatic Control, IEEE Transactions on*, 30(8):730–738, 1985.

[91] I. Mitchell and C. Tomlin. Level set methods for computation in hybrid systems. In N. Lynch and B. Krogh, editors, *Hybrid Systems: Computation and Control*, volume 1790 of *Lecture Notes in Computer Science*, pages 21–31, Berlin, 2000. Springer.

[92] I. M. Mitchell and C. J. Tomlin. Overapproximating reachable sets by Hamilton-Jacobi projections. *Journal of Scientific Computing*, 19(1-3):323–346, 2003.

[93] J. Moore and R. Tedrake. Control synthesis and verification for a perching UAV using LQR-trees. In *Decision and Control (CDC), 2012 IEEE 51st Annual Conference on*, pages 3707–3714, 2012.

[94] R. M. Murray, Z. Li, and S. S. Sastry. *A Mathematical Introduction to Robotic Manipulation*. CRC Press LLC, Boca Raton, 1st edition, 1994.

[95] U. Nallasivam, B. Srinivasan, V. Kuppuraj, M. Karim, and R. Rengaswamy. Computationally efficient identification of global ARX parameters with guaranteed stability. *Automatic Control, IEEE Transactions on*, 56(6):1406–1411, 2011.

[96] O. Nelles. *Nonlinear System Identification: From Classical Approaches to Neural Networks and Fuzzy Models*. Springer-Verlag, Berlin., 1st edition, 2001.

[97] D. J. Newman. Rational approximation to $|x|$. *Michigan Mathematics Journal*, 11(1):11–14, 1964.

[98] P. V. Overschee and B. D. Moor. N4SID: Subspace algorithms for the identification of combined deterministic-stochastic systems. *Automatica*, 30(1):75 – 93, 1994.

[99] J. Paduart, L. Lauwers, R. Pintelon, and J. Schoukens. Identification of a Wiener−Hammerstein system using the polynomial nonlinear state space approach. *Control Engineering Practice*, 20(11):1133 – 1139, 2012. Special Section: Wiener-Hammerstein System Identification Benchmark.

[100] G. Pappas and S. Simic. Consistent abstractions of affine control systems. *Automatic Control, IEEE Transactions on*, 47(5):745–756, 2002.

[101] P. A. Parrilo. Semidefinite programming relaxations for semialgebraic problems. *Mathematical Programming*, 96:293–320, 2003. 10.1007/s10107-003-0387-5.

[102] L. Piroddi, M. Farina, and M. Lovera. Black box model identification of nonlinear input-output models: A Wiener−Hammerstein benchmark. *Control Engineering Practice*, 20(11):1109 – 1118, 2012. Special Section: Wiener-Hammerstein System Identification Benchmark.

[103] A. S. Poznyak. *Advanced Mathematical Tools for Automatic Control Engineers Volume 1: Deterministic Techniques*. Elsevier, Amsterdam, The Netherlands, 2008.

[104] S. Prajna. Barrier certificates for nonlinear model validation. In *Decision and Control, 2003. Proceedings. 42nd IEEE Conference on*, volume 3, pages 2884–2889 Vol.3, 2003.

[105] S. Prajna, A. Jadbabaie, and G. Pappas. A framework for worst-case and stochastic safety verification using barrier certificates. *Automatic Control, IEEE Transactions on*, 52(8):1415–1428, 2007.

[106] S. Prajna and A. Rantzer. Convex programs for temporal verification of nonlinear dynamical systems. *SIAM Journal on Control and Optimization*, 46(3):999–1021, 2007.

[107] R. Raich, G. Zhou, and M. Viberg. Subspace based approaches for Wiener system identification. *Automatic Control, IEEE Transactions on*, 50(10):1629–1634, 2005.

[108] A. Rantzer. On the Kalman-Yakubovich-Popov lemma. *Systems and Control Letters*, (28):7–10, Nov. 1996.

[109] P. Regalia. An unbiased equation error identifier and reduced-order approximations. *Signal Processing, IEEE Transactions on*, 42(6):1397 –1412, Jun. 1994.

[110] P. Regalia and P. Stoica. Stability of multivariable least-squares models. *Signal Processing Letters, IEEE*, 2(10):195 –196, Oct. 1995.

[111] T. Reis and M. Heinkenschloss. Model reduction with a-priori error bounds for a class of nonlinear electrical circuits. In *Decision and Control, 2009 held jointly with the 2009 28th Chinese Control Conference. CDC/CCC 2009. Proceedings of the 48th IEEE Conference on*, pages 5376–5383, 2009.

[112] G. Reissig. Computing abstractions of nonlinear systems. *Automatic Control, IEEE Transactions on*, 56(11):2583–2598, 2011.

[113] C. Rohde. Generalized inverses of partitioned matrices. *Journal of the Society for Industrial and Applied Mathematics*, 13(4):1033–1035, 1965.

[114] J. Roll, A. Nazin, and L. Ljung. Nonlinear system identification via direct weight optimization. *Automatica*, 41(3):475 – 490, 2005.

[115] W. H. A. Schilders. The need for novel model order reduction techniques in the electronics industry. In P. Benner, M. Hinze, and E. J. W. ter Maten, editors, *Model Reduction for Circuit Simulation*, volume 74, pages 3–23, 2011.

[116] T. B. Schön, A. Wills, and B. Ninness. System identification of nonlinear state-space models. *Automatica*, 47(1):39 – 49, 2011.

[117] J. Schoukens, J. Suykens, and L. Ljung. Wiener-Hammerstein benchmark. In *System Identification, 15th IFAC Symposium on*, volume 15, Jul. 2009.

[118] J. Sjöberg, L. Lauwers, and J. Schoukens. Identification of Wiener-Hammerstein models: Two algorithms based on the best split of a linear model applied to the SYSID'09 benchmark problem. *Control Engineering Practice*, 20(11):1119 – 1125, 2012. Special Section: Wiener-Hammerstein System Identification Benchmark.

[119] J. Sjöberg, Q. Zhang, L. Ljung, A. Benveniste, B. Delyon, P.-Y. Glorennec, H. Hjalmarsson, and A. Juditsky. Nonlinear black-box modeling in system identification: a unified overview. *Automatica*, 31(12):1691 – 1724, 1995.

[120] T. Soderstrom and P. Stoica. On the stability of dynamic models obtained by least-squares identification. *Automatic Control, IEEE Transactions on*, 26(2):575–577, 1981.

[121] T. Söderström and P. Stoica. Some properties of the output error method. *Automatica*, 18(1):93 – 99, 1982.

[122] E. Sontag. Contractive systems with inputs. In J. Willems, S. Hara, Y. Ohta, and H. Fujioka, editors, *Perspectives in Mathematical System Theory, Control, and Signal Processing*, volume 398 of *Lecture Notes in Control and Information Sciences*, pages 217–228. Springer Berlin / Heidelberg, 2010.

[123] A. Sootla. Semidefinite hankel-type model reduction based on frequency response matching. *Automatic Control, IEEE Transactions on*, 58(4):1057–1062, 2013.

[124] M. Spivak, editor. *Calculus on Manifolds*. Westview Press, 1971.

[125] M. Stolle and C. Atkeson. Policies based on trajectory libraries. In *Robotics and Automation, 2006. ICRA 2006. Proceedings 2006 IEEE International Conference on*, pages 3344–3349, 2006.

[126] J. F. Sturm. Using SeDuMi 1.02, a Matlab toolbox for optimization over symmetric cones. *Optimization Methods and Software*, 11(1-4):625 – 653, 1999.

[127] M. Sznaier. Computational complexity analysis of set membership identification of Hammerstein and Wiener systems. *Automatica*, 45(3):701 – 705, 2009.

[128] Y. Tazaki and J. Imura. Discrete abstractions of nonlinear systems based on error propagation analysis. *Automatic Control, IEEE Transactions on*, 57(3):550–564, 2012.

[129] R. Tedrake. LQR-trees: Feedback motion planning on sparse randomized trees. In *Robotics: Science and Systems (RSS), Proceedings of*, Jun. 2009.

[130] R. Tedrake, I. Manchester, M. Tobenkin, and J. Roberts. LQR-trees: Feedback motion planning via sums-of-squares verification. *The International Journal of Robotics Research,*, 29(8):1038–1052, 2010.

[131] M. Tobenkin, I. Manchester, and R. Tedrake. Invariant funnels around trajectories using sum-of-squares programming. In *18th IFAC World Congress*, volume 18, 2011.

[132] M. Tobenkin, I. Manchester, J. Wang, A. Megretski, and R. Tedrake. Convex optimization in identification of stable non-linear state space models. In *Decision and Control (CDC), 2010 49th IEEE Conference on*, pages 7232 –7237, Dec. 2010.

[133] U. Topcu, A. Packard, and P. Seiler. Local stability analysis using simulations and sum-of-squares programming. *Automatica*, 44(10):2669 – 2675, 2008.

[134] N. Truong and L. Wang. Benchmark nonlinear system identification using wavelet based SDP models. In *System Identification, 15th IFAC Symposium on*, volume 15, pages 844–849, Jul. 2009.

[135] J. Tugnait and C. Tontiruttananon. Identification of linear systems via spectral analysis given time-domain data: consistency, reduced-order approximation, and performance analysis. *Automatic Control, IEEE Transactions on*, 43(10):1354 –1373, Oct. 1998.

[136] T. Van Gestel, J. Suykens, P. Van Dooren, and B. De Moor. Identification of stable models in subspace identification by using regularization. *Automatic Control, IEEE Transactions on*, 46(9):1416 –1420, Sep. 2001.

[137] E. Walter and L. Pronzato. *Identification of Parametric Models from Experimental Data*. Springer-Masson, Paris, 1st edition, 1997.

[138] E. Whitman and C. Atkeson. Control of a walking biped using a combination of simple policies. In *Humanoid Robots, 2009. Humanoids 2009. 9th IEEE-RAS International Conference on*, pages 520–527, 2009.

[139] J. Willems. Dissipative dynamical systems, part I: General theory. *Archive for Rationale mechanics Analysis*, 45:321–393, 1972.

[140] A. Wills, T. B. Schön, L. Ljung, and B. Ninness. Identification of Hammerstein-Wiener models. *Automatica*, 49(1):70 – 81, 2013.

[141] B. Yordanov and C. Belta. Formal analysis of discrete-time piecewise affine systems. *Automatic Control, IEEE Transactions on*, 55(12):2834–2840, 2010.

[142] G. Zang and P. A. Iglesias. Fading memory and stability. *Journal of the Franklin Institute*, 340(67):489 – 502, 2003.

[143] K. Zhou, J. C. Doyle, and K. Glover. *Robust and Optimal Control*. Prentice Hall, Upper Saddle River, New Jersey, 1996.